

PREPARATION AND CHARACTERIZATION OF POLYMERIC COMPOSITE MATERIAL



By

KHAISTA GUL

*A dissertation submitted to the University of Peshawar in
Partial fulfillment of the requirements for the degree of*

DOCTOR OF PHILOSOPHY
IN
PHYSICAL CHEMISTRY

**NATIONAL CENTRE OF EXCELLENCE IN PHYSICAL CHEMISTRY
UNIVERSITY OF PESHAWAR KHYBER PAKHTUN KHWA, PAKISTAN
March 2013**

**NATIONAL CENTRE OF EXCELLENCE IN PHYSICAL
CHEMISTRY UNIVERSITY OF PESHAWAR**

It is recommended that the dissertation prepared by

Mr. Khaista Gul

Entitled “**PREPARATION AND CHARACTERIZATION OF
POLYMERIC COMPOSITE MATERIAL**” be accepted as fulfilling this
part of the requirements for the degree of

DOCTOR OF PHILOSOPHY

APPROVED BY

(Prof. Dr. Mohammad Saleem Khan)

RESEARCH SUPERVISOR

(Prof. Dr. Mohammad Saleem Khan)

DIRECTOR

**EXAMINATION SATISFACTORY
COMMITTEE OF THE FINAL EXAMINATION**

INTERNAL EXAMINER

EXTERNAL EXAMINER

*DEDICATED
TO
MY PARENTS AND FAMILY MEMBERS*

CONTENTS

TITLE	Page
Acknowledgements-----	ix
Abstract-----	xi
Chapter -1	
Introduction-----	1
1.1 Aim and objectives-----	15
Chapter- 2	
Literature Review-----	16
Chapter -3	
Experimental-----	38
3.1 Preparation of plain polymer film -----	39
3.2 Preparation of polymer composite -----	40
3.1.1 Instrumentation -----	40
Chapter- 4	
Results and Discussion-----	47
4.1. PMMA+ Na ₂ SO ₄ composite -----	48
4.2. PMMA+ clay composite-----	64
4.3. PMMA+ activated carbon composite-----	72
4.4. PMMA+ CaCO ₃ composite-----	81
4.5. PMMA+ SiO ₂ composite-----	88
4.6. PMMA+ ceramics composite-----	97
4.7. PMMA+ glass composite-----	106
Comparison of the studied composites system-----	114
Conclusions-----	123
References-----	125

LIST OF FIGURES

- Figure 1: Scanning electron micrograph of Plain PMMA
- Figure 2: Scanning electron micrograph of PMMA+ Na₂SO₄ composite
- Figure 3: EDX study of PMMA + Na₂SO₄ composite
- Figure 4: FTIR spectra of plain PMMA
- Figure 5: FTIR spectra of PMMA + Na₂SO₄ composite
- Figure 6: TGA traces for pristine PMMA
- Figure 7: DSC study of plain PMMA
- Figure 8: TGA traces for PMMA + Na₂SO₄ composite
- Figure 9: DSC study of plain PMMA+ Na₂SO₄ composite
- Figure 10: Tensile strength of plain PMMA
- Figure 11: Tensile strength of plain PMMA+ Na₂SO₄ composite
- Figure 12: Scanning electron micrograph of PMMA+ clay composite
- Figure 13: FTIR spectra of PMMA + clay composite
- Figure 14: TGA traces for pristine PMMA + clay composite

- Figure 15: DSC study of plain PMMA+ clay composite.
- Figure 16: Tensile Strength of PMMA+ clay composite
- Figure 17: Scanning electron micrograph of PMMA+ activated carbon composite
- Figure 18: EDX study of PMMA + activated carbon composite
- Figure 19: FTIR spectra of PMMA + activated carbon composite
- Figure 20: TGA traces for PMMA + activated carbon composite
- Figure 21: DSC study of plain PMMA+ activated carbon composite.
- Figure 22: Tensile Strength of PMMA+ activated carbon composite
- Figure 23: Scanning electron micrograph of PMMA+ CaCO₃ composite
- Figure 24: FTIR spectra of PMMA + CaCO₃ composite
- Figure 25: TGA traces for PMMA+ CaCO₃
- Figure 26: DSC study of plain PMMA+ CaCO₃
- Figure 27: Tensile Strength of PMMA+ CaCO₃ Composite
- Figure 28: Scanning electron micrograph of PMMA+ SiO₂ composite
- Figure 29: EDX study of PMMA + SiO₂ composite
- Figure 30: FTIR spectra of PMMA + SiO₂ composite

- Figure 31: TGA traces for PMMA+SiO₂ composite
- Figure 32: DSC study of plain PMMA+ SiO₂
- Figure 33: Tensile strength of PMMA+ SiO₂ composite
- Figure 34: Scanning electron micrograph of PMMA+ ceramics composite
- Figure 35: FTIR spectra of PMMA + ceramics composite
- Figure 36: TGA traces for PMMA+ ceramics composite
- Figure 37: DSC study of plain PMMA+ composite
- Figure 38: Tensile Strength of PMMA+ ceramics Composite
- Figure 39: Scanning electron micrograph of PMMA+ glass composite
- Figure 40: FTIR spectra of PMMA + glass composite
- Figure 41: TGA traces for PMMA+ glass composite
- Figure 42: DSC study of plain PMMA+ glass composite
- Figure 43: Tensile Strength of PMMA+ glass Composite
- Figure 44: Comparison of thermal stability of various composites system
- Figure 45: Comparison of tensile strength of various composites system
- Figure 46: Comparison of elongation of various composites system

LIST OF TABLES

- Table 1: System studied
- Table 2: Comparison of thermal stability of various composite systems
- Table 3: Comparison of tensile strength of various composite systems
- Table 4: Comparison of elongation of various composite systems

ACKNOWLEDGEMENTS

All praises be to Almighty Allah who guides us in darkness and helps us in difficulties and all respects for his Holy Prophet Muhammad (Peace be upon him) who enabled us to recognize our Creator.

I owe a special debt of gratitude to my learned supervisor Professor Dr. Muhammad Saleem Khan M.Sc.(Pesh), Ph.D (Pesh), D.C.C.E.(Japan), Director, National Centre of Excellence in Physical Chemistry, University of Peshawar, for his proper guidance, long discussions, devotion of time, invaluable suggestions, sympathetic attitude and constant encouragement during the course of this work.

My thanks, needless to say, are also due to Professor Dr. Hasan Mahmood Khan Ex Director, National Centre of Excellence in Physical Chemistry, University of Peshawar for providing research facilities.

Heart felt gratitude to my father Mr. Hazrat Said (May he long live) for his continuous encouragement, sympathetic attitude and financial support. Thanks are also due to my mother, wife, and siblings for their moral support.

Thanks are also due to my Lab. mates, Mr. Dr. Najeeb-ur-Rehman, Mr. Dr. Gulfam Nasar, Mr. Dr. Arshad Hussain, Mr. Dr. Rehmat Gul, Mr. Dr. Humayoon, Ms. Dr. Sabiha Sultana and Ms. Dr. Uzma Khalil for their cooperation.

Again special thanks are due to Mr. Dr. Syed Salman, Mr. Rashid Hussain and Mr. Mohammad Amin Khan for their good wishes.

I extend my thanks to Mr. Ikhtiar Gul, Lab. supervisor and Mr. Misal Khan, Lab. Attendant for their cooperation.

Khaista Gul.

ABSTRACT

Composite materials are superior to other known structural materials in specific strength and stiffness, high temperature strength, fatigue strength and other properties. The present study was carried out to prepare such types of polymer composites which possess the better properties than the pure polymer. In this study we prepared seven different types of composites of PMMA with clay, Na₂SO₄, CaCO₃, activated carbon, SiO₂, ceramics and glass, PMMA was used as Matrix. The films were prepared by solvent cast method, using benzene as solvent. The structure and properties of these composites were investigated by SEM, EDX, DSC, UTM, TG/DTA and FTIR techniques. SEM of pure PMMA showed uniform surface while the morphology changed by the addition of various fillers. Clay, glass and Na₂SO₄ were uniform and well dispersed in PMMA matrix while CaCO₃ show somewhat spherical structure, SiO₂ and ceramics seemed to be embedded in between cavities. The size of the particles varied with the system. EDX studies on all these composites showed that the particles were incorporated in the PMMA matrix and have sufficient amount in the matrix. FTIR studies revealed that there was interaction between the polymer molecule and the various fillers added to them. The peak at 1729 cm⁻¹ in PMMA was assigned to be due to C=O group. This is strong electron donor group so the cations tend to make complexes with this group. It was shown that the cations of Na⁺, Ca⁺⁺ and Si⁺⁺ interact with this and shift toward lower wave number. In the case of clay, the silicates present in the clay tend to interact and shift it again toward lower wave number. The thermal properties of all these composites were studied. These TGA showed that the added

materials in to polymer matrix increased the thermal stability .The order of increasing thermal stability of various composites was:

PMMA < PMMA-activated carbon < PMMA-SiO₂ < PMMA-Na₂SO₄ < PMMA – CaCO₃ < PMMA- clay < PMMA-ceramics < PMMA-glass

The glass composite showed maximum thermal stability among all the studied composites. The mechanical studies of these composites were investigated by universal testing machine .It was shown that the tensile strength of the tested composites were much better than the pure PMMA. The order of increasing tensile strength of various composites was:

PMMA < PMMA-Na₂SO₄ < PMMA-glass < PMMA- clay < PMMA-ceramics < PMMA -CaCO₃ < PMMA-SiO₂ < PMMA-activated carbon

The activated carbon composite showed maximum tensile strength among all the studied composites. The elongation at break was another parameter showing strength of material and the values of elongation at break for the composites was found to be higher than the pure polymer. The order of increasing elongation at break of various composites was:

PMMA < PMMA-Na₂SO₄ < PMMA-activated carbon < PMMA- clay < PMMA-ceramics < PMMA-glass < PMMA -CaCO₃ ≤ PMMA-SiO₂

Finally, the present study has shown that various composites of PMMA have been successfully prepared showing incorporation of filler. The interaction of cations of the compositing materials with the polymer has also been shown. The composite materials showed improved thermal and mechanical stability.

Chapter -I:
INTRODUCTION

Composite is a material made up of two or more components. Plastics, metals, and ceramics are the main classes categorized by the researchers. Metals being hard used mainly for their stiffness and strength, plastics are light and inexpensive to manufacture and ceramics are hard, resistive to heat and corrosion also having good electrical insulation at ambient temperature but super conductivity at low temperature. All composites commonly have one thing in regular, a matrix or binder combined with a reinforcing material. Matrix material of a composite is apparently dispersed within one or more phases of another material. Material is termed an advanced composite, if the fibers are directionally leaning and continuous. The combined mechanical characteristics of composites are better to those of either of the constituent phases. Some common varieties of composites include glass fibers, reinforced concrete, fiber-resin, fiber-ceramic, carbon-metal, metal concrete, clay, metal resin and wood plastic.

Advanced fiber reinforced polymer composite is made up of fiber, resin, fillers and additives. The fibers provide increased stiffness and tensile capacity. The resin offers high compressive strength and binds the fibers into a firm matrix. The fillers give out to reduce cost and shrinkage. Additive not only serves to improve the mechanical and physical properties of the composites but also workability.

A resin being very expensive is not a gainful choice to fill up the voids in a composite matrix. Fillers are incorporated to the resin matrix for controlling material cost and improving its mechanical and chemical properties. Some composites that are rich in resins can be subjected to high shrinkage, slink and low tensile strength. Although these properties may be undesirable for structural applications, there may be a place for their uses.

Composite materials are advanced to all other known structural materials in terms of specific strength and stiffness, high temperature and fatigue strength and other characteristics. The desired combination of properties can be adapted in advance and be realized in the manufacture of a particular material. Moreover the material can be shaped in this process as close as possible to the form of final products or even structural units.

Composite materials are multipart materials whose components differ strongly from each other in properties which are jointly insoluble or only faintly soluble and divided by discrete limitations. The principle of manufacturing a composite has been rented from nature. Examples of natural composites are Trunks, stems of plants, bones man and animals. In wood, cellulose fibers are bonded by plastic lignin, in bones, thin and strong fibers of phosphates are bonded by plastic collagen.

The binding and shaping component in composites is basically the matrix. Its properties determine to a large extent the process conditions for the manufacturing of composite materials and the important operating characteristics, e.g., working temperature, fatigue strength, resistance to environmental effects, density and specific strength. Some composites have a mutual matrix, consisting of alternating layers (two or more) of different composition.

Fillers on the other hand called reinforcing components. This is a broader term than 'strengthened, it does not specify the particular strengthening role of filler which may be used for improving other properties of a composite. Filler's shape (geometry), size, concentration and division (reinforcement pattern) determine the properties of a composite material. Fillers of different shape may be used for obtaining a wider complex of properties or enhancing a particular property of composite material. For example the

modulus of elasticity of composite materials with a polymer matrix reinforced by glass fibers can be increased by additional reinforcement with boron fibers. Complex-reinforced composites contain two-or more different fillers.

Hybrid composites are obtained by using two or more different kinds of fibers in a single matrix. Hybrid composites have overall better combination of properties than composites containing only a single fiber type. Even though a variety of fiber combinations and matrix materials are used but in the most common system both carbon and glass fibers are incorporated into a polymeric resin. The carbon fibers are costly but they are strong and fairly rigid and afford low density reinforcement. Glass fibers are deficient in the stiffness of carbon but they are inexpensive. In addition to strength and toughness the glass-carbon hybrid may be produced at a lower cost than either of the analogous all-carbon or all-glass reinforced plastics.

The mechanical properties of composites depend on many variables such as orientations, fiber's types and construction. The fiber architecture defines the preformed textile configurations by weaving, braiding or knitting. Composites materials show different strength in different direction. Their stress-strain curves are linearly elastic to the point of failure by rupture. The polymeric resin in a composite material which consists of viscous fluid and elastic solids responds viscoelastically to applied loads. Although the viscoelastic material will creep and relax under a sustained load, it can be designed to perform satisfactorily. Composites have many excellent structural qualities. Some examples are high strength, material toughness, fatigue endurance, and light weight. Other highly desirable qualities are high resistance to elevated temperature, abrasion, corrosion and chemical attack.

Some of the disadvantages in the use of composites in bridges are high first cost, creep, and shrinkage. The design and construction require highly trained specialists from many engineering and material science disciplines. The composites have a potential for environmental degradation, for examples, alkalis' attack and ultraviolet radiation exposure. There are very little or nonexistent design guidance and/or standards. There is a lack of joining and/or fastening technology. Because of the use of thin sections there are concerns in global and local buckling. Although the light weight feature may be an advantage in the response to earthquake loading, it could render the structure aerodynamically unstable. In manufacturing with the hand layup process there is a concern about the consistency of the material properties.

Many researches dealing with the construction of polymer microspheres and microcapsules for a wide number of prospective applications have been carried out over the past decade. Mainly microspheres with hollow interiors have drawn a number of interactions due to their applications including stationary phases for separation sciences, biomedical devices, coating additive, controlled release reservoirs and a small container for micro-encapsulation. Recently great attention has been directed towards the functionality of these hollow microspheres. Various approaches have been proposed to prepare the composite microspheres to obtain the desired properties and promising applications in frequent fields including optics, membranes, electronics, protective coating, mechanics, catalysis, biology, sensors and others. Among these composites, many efforts have been focused on the combination of organic conjugated polymer and inorganic nano-crystals in order to yield new functional materials that may combine the advantages of each component.

Composites are combinations of materials which have different properties belonging to different class either same are better in properties from their parent one. This idea is very old. This old idea of composite was formulated by Israelites in Egypt for making bricks from clay and straw.

In 1918 Griffith a renowned scientist revealed that thin glass fibers are very strong but can easily be broken by any surface scratch. Ultimately inventors came to know to protect the strong fibers with various techniques like coatings that made them to be used like common textile fibers. Later on it was discovered that the fibers were essential constituents of the composite. The fiberglass composite which is made from glass fiber and resin famous for the construction of automobile bodies and boats. These materials are light, prevent corrosion of plastic and increase the durability of glass fibers. Composites of carbon fiber and resin are equivalent to the toughness and strength of steel but have four times low weight in comparison to steel. These properties make it more specialized for fishing rods and aircraft construction. In 1963 this type of carbon fiber was first fashioned. In 1970s the use of graphite (composites of carbon fiber and epoxy) were reduced to three-quarters of the jet fighter aircraft mass.

It is well known that the addition of fillers to polymers can influence their thermal stability .This play important role for processing because the initial properties of the material should not change due to degradation or cross linking. Therefore industrial processing steps at elevated temperature have to be kept short in time and usually last not more than a few minutes. In contrasts for polymer research long time tests at high temperature are of great interest. Some rheological tests for instance last for hours which raise the necessity to know whether the material stays stable during the required

measuring time. The thermal stability of polymer composite is mostly tested by means thermo gravimetric analysis.

Automobile and aerospace industries need stronger, less expensive, lighter and more versatile polymeric composites to meet their demands. Polymer composites such as carbon or glass fibers reinforced thermoplastic and thermosets are very common. In addition to glass fibers, many other organic and inorganic materials both synthetic and natural are commonly used. Talc and other platy materials add rigidity, increase the heat deflection temperature and reduce the thermal expansion of the polymer. Important factor in the effectiveness of reinforcing material is how well the filler is dispersed in the polymer matrix.

PMC (Polymer Matrix Composites) or FRP (Fiber Reinforced Polymers) are commonly used materials in which polymer act as matrix reinforced by variety of fibers like aramid, glass and carbon.

Composite material is made up of at least two elements combine together to fabricate new materials which have different properties of the parent elements. Commonly composites consist of matrix (bulk material) and a reinforcement of some kind usually in the form of fiber which increase strength and stiffness of the matrix. Organic and inorganic components mixed together to form a unique composite material possess combined properties which is new challenge in the field of nanotechnology. In the earlier period many kinds of composites have been considered as pioneering advanced materials and hopeful applications have been predicted in many fields like sensors, optics, ionics, electronics, mechanics, membranes, protective coating, biology, catalysis, etc.

Mini emulsion polymerization, intercalative polymerization, emulsion polymerization, hybrid latex polymerization methods have been used to produce polymer composite materials. Conversely more multitalented synthetic approaches are desired to find an effective solution to the advantage of dispersing of inorganic particles in polymer matrix. A strong interface adhesion between the matrix and nanofillers are encouraged for the preparation of functional composite microspheres.

PLSN (polymer layered –silicate nanocomposite) is the polymer –based nanocomposite having industrial and academic interest. Natural or synthetic clay is used as reinforcing materials in the class of hybrid films both of which are composite of regular stacking of silicate layers around with weak interatomic force depending on physical properties of the matrix. As a result three different types of composites are formed namely intercalated nanocomposite, microphase –separated conventional composite and an exfoliated composite. The morphology, crystal nucleation rate and crystallization rate depend on the final physical properties of filled polymer composites which are useful from both academic and industrial perspectives.

Since 1887 nylon-6-montmorillonite nanocomposite prepared by Toyota research group. The results proved that incorporation of inorganic particles in polymeric matrix improve the basic properties of composite like mechanical properties, reduced flammability ,better barrier properties and higher heat alteration temperatures.

Lithium salt-based electrolytes have been the focus of several basic research oriented studies during the past decade. Li^+ based polymer electrolytes have one drawback, that of low ionic conductivity at ambient temperature. To overcome this problem polymer electrolyte nanocomposite can be produced which have high

conductivity and maintains enough performance. Due to its small particle size and high intercalating property, intercalating polymer formed in layered inorganic hosts. Numerous studies show that additives like ceramic powder and clays which have high surface area render polymers matrix crystallinity. The polymer chains are most flexible in the system due to high amorphous area.

It is suggested that the presence of finally dispersed inorganic particles in polymer matrix improve the membrane performance. To improve the mechanical and thermal properties of inorganic ones with flexibility and ductility of organic polymers new type of organic/inorganic hybrid materials are prepared which has the potential to combine the desired properties on inorganic and organic system. Sol-gel process is used to prepare such hybrid materials which show better results over other techniques. Various parameters were applied like pH, concentration, temperature, pressure, water-to-alkoxide ratio, type of catalyst and solvent to control the micro and macrostructure of a hybrid composite. Poly methyl methacrylate hybrid composite as an organic matrix has been of special interest for its exceptional thermal and mechanical properties which has been applied for all types of industries.

Polymeric composite are applicable in various aspects of life such as construction, transportation and consumer products. The dimension of microstructure of the dispersed phase strongly influences properties of particle reinforced polymer composite. Nanocomposites are new class of material in which filler are dispersed in nano scale in polymer matrix. The size of nano particles should be in range of 1-100 nm which gives improved properties when compared to macro and micro composites.

Semtic clay such as montomorillonite are valuable minerals and widely used in many industrial applications because of their high aspect ratio, plate morphology, natural abundance and low cost. These are expandable layer silicates and can be intercalated and /or exfoliated into nanocomposites.

CPC (Composite polymer particles) have been used in a variety of applications such as impact coatings, adhesives and modification. The performance of composite polymer particles greatly depends on their morphology. Extensive researches have been designed to control particle morphology resulting in the production of submicron-sized composite particles. For example PMMA/graphite composite is commonly used for the improvement of electrical devices, conducting devices, aerospace engineering and electrochemistry.

Nano ZnO as one of the multifunctional inorganic particles has shown increasing attention in recent years due to its prominent physical and chemical properties such as chemical stability low dielectric constant, high luminous, transmittance, high catalysis activity, effective antibacterial and bactericide behavior. Moreover the incorporation of nano-ZnO particles to polymer matrix could improve the optical and chemical properties of the polymer matrix.

Filler plays an important role in the preparation of polymeric composite materials. Filler gives the economical benefits vis-à-vis improvement of the thermal, mechanical, electrical and optical properties of the polymeric composites. Metallic fillers also improve the thermal and electrical conductivity of polymers materials. Metallic fillers are especially used as anti-fouling compounds, corrosion resistant paints, repair and maintenance products for example cold poured steel and tooling.

During the past decade considerable efforts have been devoted to the development of solid polymer electrolytes with high ionic conductivity at room temperature. PEO based polymeric electrolytes are still among the most extensively studied polymeric ionic conductors due to the beneficial structure i.e supporting fast ionic transport. Unfortunately a high crystalline phase concentration limits the conductivity of PEO based electrolytes. Clay mineral is inorganic filler with intercalation property. Intercalating polymer as PEO in layered clay host can produce polymer electrolyte nanocomposite with huge interfacial area. The higher interfacial area not only reduces the crystallinity of PEO chains resulting in higher ionic conductivity but also sustains the mechanical property of this semi-crystalline PEO based electrolyte.

Typically nanocomposites embrace the organically modified clay and the virgin polymer. Montmorillonite is the most commonly used clay which have aluminosilicate mineral with sodium counterions between the layers. The space between these layers is called the clay gallery. To formulate this inorganic clay well-suited with organic polymers sodium counter ions are usually ion-exchanged with an organic phosphonium or ammonium salt to adapt the material into hydrophobic ammonium- or phosphonium-treated clays. Mostly nanocomposites prepared either by situ polymerization process or blending process in the presence of the naturally modified clay.

The intercalations of organic alkylammonium cation in to montmorillonite (MMT) clay have been reported in literature. Mostly low-molecular-weight alkylammonium salts, diamine salts and amino acids have been intercalated. Naturally intercalation results in expansion of the clay basal spacing to within the range 19 - 40 Å^o which link linearly with the molecular size of the intercalating agent. These intercalated

semitic clays are exfoliated with polymer to form nanocomposites materials. It is conformed from literature that nanoclay-filled polymeric composites shows important improvements in their thermal and tensile properties, resistance to flammability, heat distortion temperature, reduced solvent uptake and reduced permeability to small molecules. It is concluded from these studies that the dispersion of the clay layers in the polymeric matrix improves the desire properties.

Keeping all their own unique set of properties such as strength, toughness, stiffness, cost, heat resistance, production rate etc the Resins, Fibres and Cores are selected. The final properties of a composite part produced from these various materials is not only a function of the individual properties of the resin matrix and fibre plus the function of the way in which the materials themselves are shaped into the part and also the way in which they are formulated.

The basic definition of composite is, that material which is composed of at least two elements working together to manufacture material properties that are different to the properties of those virgin elements. Mostly composite materials consist of a bulk material which is called matrix and reinforcing materials added primarily to improve the stiffness and strength of the matrix. Fibers are usually reinforcing materials.

In the research area of polymer-nanoscale filler composites the primary goal is to enhance thermal and mechanical properties of the polymers such as stiffness, toughness and heat resistance by using molecular or nanoscale reinforcement. Various nanoscale filler including aluminium oxide, silica and calcium carbonate has usually been reported. Due to nanoscale effects polymer/silica nanocomposites can often exhibit dramatic improvements in heat resistance, tensile strength and modulus [1].

During the last two decades aluminum pigments have been widely used in automotive coatings, printing inks, roof coating and plastic materials for their protective decorative function [2-4]

Fixation of the major of prostheses in the past has been performed using poly (methyl methacrylate) (PMMA) bone cement. However an unresolved problem with using PMMA as bone cement is a thickening of the intervening fibrous tissue layer which leads to aseptic loosening of the cement in some cases [5, 6]

To provide new functionalities such as high thermal stability, high transparency, gas-barrier, shock resistance, etc Polymer/silica nano-composites have been synthesized and widely studied [7-12]

Combining properties of organic and inorganic components in a unique composite material is a new challenge in the field of nanotechnology. In the past decade different types of composites have been considered as pioneering advanced materials and hopeful applications have been expected in many fields, including optics, electronics, biology, ionics, mechanics, membranes, protective coatings, catalysis, sensors and so many [13-19] To show controllable properties such as thermal, optoelectronic, electrical, optical and mechanical behaviors, polymer–inorganic hybrid composites had been widely investigated because such hybrids prepared via various techniques might combine the features of organic and inorganic functions [20, 21].

TGA and DSC of the PMMA-silica composite shows that this system is thermally stable up to 405 C⁰. The resultant CPEs (composite polymer electrolytes) showed high room temperature conductivity with silica addition [22]. PMMA-SiO₂ hybrid membranes were also prepared by solvent casting method and from TGA analysis it was found that

the hybrid membranes have high thermal stability compare to pristine PMMA while the type of solvents used play important in their degradation behavior [23]. Most sulfate systems such as LiSO_4 and LiNaSO_4 are fast ionic conductors. The ionic conductivity of Na_2SO_4 is much better than any other sulfate system. For example the ionic conductivity of Na_2SO_4 at 250 C^0 is approximately 30-40 times larger than that of normal state LiSO_4 at the same temperature [24]. It will also be interesting to use these as fillers in polymer matrix to see the conductance behavior of the polymer electrolytes

Through functionality of organic materials would be disturbed by silica that existed in organic domains when organic materials were hybridized with silica while the thermal stability of the organic materials was improved. By doping guest ions it is recommended that, it lower the transition temperature phase near room temperature [25, 26].

The synthesis of nanocomposites based on polymers as hosts and inorganic layered materials as guests has shown a very competent future due to improved thermal stability[27-29], corrosion protection [30-32], mechanical performance[33,34], flame retardance [35,36],gas barrier[37] and electrorheology [38,39] properties even with small loading of layered inorganic compound.

The polymer composite with different additives has not been given attention in detail in literature. It will be very interesting to prepare these composites and study their properties, so we have attempted to prepare and study various polymers composite systems which are very interesting in properties enhancement

1.1. Aims and objectives

In view of the continued and increasing importance of polymer composites, their uses in various fields and their significance as means of economically developing new materials with desirable properties the current work is aimed at the following:

- To prepare different types of polymer composites of PMMA with Na₂SO₄, clay, CaCO₃, activated carbon, ceramics, glass and SiO₂.
- To find the size and existence of nano particles in polymer matrix using SEM and EDX techniques.
- To investigate thermal stability of the prepared composites by analytical techniques like TG/DTA and DSC.
- To test the tensile strength of the prepared composites using UTM.
- To find out the chemical nature of the prepared composite using FTIR.

Chapter -2

LITERATURE REVIEW

There are large numbers of literature reports available on polymer composites. Scientists throughout the world have done work and are doing work on various polymer composite systems. In this literature review, we are presenting mostly the literature regarding PMMA as matrix because our work is also on the same polymer.

Thermal stability of PMMA filled with SiO₂ particles was investigated by Katsikis and co workers. It was suggested that the thermal stability of the composites depend on the melting temperature, SiO₂ particles size and volume fraction of the fillers. It was further suggested that an increasing modulus of filled composites with time, chemical reaction between silanol groups on the SiO₂ particles surface and Poly (methyl methacrylate) as cross linking reaction. Furthermore silicon particles had no influence on the thermal stability of polystyrene [40].

Then film of PMMA and PMMA-CNT composites were deposited onto heated substrates using matrix assisted pulsed laser evaporation (MAPLE) to understand the effect of substrate temperature on the surface roughness of the deposited films. With increase in temperature the surface roughness was shown to decrease. DSC analysis confirmed that MAPLE deposited PMMA possessed a lower T_g than the as-received PMMA. Gel permeation chromatography (GPC) analysis showed an overall decrease in the molecular weight of MAPLE deposited PMMA relative to the as-received PMMA. SEM analysis showed that the final roughnesses of the composite films were significantly greater than those of the pure polymer films [41].

Yuen and co worker successfully prepared Si-MWCNT/PMMA composites. SEM and TEM micrographs show that the Si-MWCNTs were dispersed completely in the polymer matrix. Thermal conductivity increases with MWCNT content [42].

Polymer composite blend films of poly (methyl methacrylate)-poly (ethylene oxide) blends-ceramics filler composite were prepared by Shanmukaraj and Co workers. XRD pattern revealed the homogenous nature of the polymer films. The addition of Al₂O₃ fillers resulted in a peak shift toward the lower angle which was due to the swelling of the polymer matrix. Conductance of the films was shown to depend on Al₂O₃ concentration. The authors suggested that these films would have widespread application in electrochemical devices [43].

Ye Xiaoyun and Co workers synthesized PMMA/Ag composite via an ultrasonic wave method. Emulsion process, structure and thermal properties were measured with TEM, UV-Vis, FTIR and TG/DTA. Results showed that the interfacial interactions such as hydrogen bond greatly affected on emissivity of the composite. The interfacial interactions could be employed to explain the decrease of the emissivity value [44].

Ding and coworkers synthesized PMMA/ MgFe (DS)-LDH nanocomposites via in situ polymerization technique. Due to molecular level dispersion of inorganic nanolayer and small inorganic loading in polymer matrix all composites had excellent transparency. TGA of these nanocomposites showed better thermal stability on the whole temperature region. The participation of Fe³⁺ ion was found to play significant role in the enhancement of thermal stability of the nanocomposites [45].

The effect of Fe-OMT based on electrospun PA6 nanocomposite fibers were investigated by Cai and coworkers. The thermal stability, structure and morphology of these composite were characterized by TGA, HREM and SEM respectively. It was found from the SEM image that the nanofibers were randomly distributed to form the fibrous web. It was also found from HREM observations that the silicate clay layers were well

dispersed within the nanocomposites fibers. The TGA analysis revealed that the incorporation of Fe-OMT led to the crosslinking of the PA6 promoted the catalytic graphitization and charred residue yield [46].

Fuan et al prepared Poly (vinylidene fluoride) (PVDF)/graphite composites via solution precipitation method. Dynamic mechanical analysis (DMA), Differential scanning calorimetry (DSC) and ac impedance analyzer were used for mechanical, thermal and dielectric properties. The results demonstrated that graphite had important effect on the crystallization behavior of the Poly (vinylidene fluoride).The dielectric constant and the storage modulus of the composites improved linearly with concentration of graphite [47].

Yanfeng and coworkers prepared PMMA-kaolinite intercalation composites via in-situ polymerization technique. These composites were characterized by XRD XPS, ATR-FTIR, SEM, UV and TGA. The Incorporation of nanoparticles with polymer matrix resulted in an increase in mechanical strength vis-a-vis thermal stability. When kaolinite content was increased the intercalated composites revealed UV transparency and stronger resistance property for UV spectra [48].

Raeve et al [49] showed that the handling of PVA fibers as well as the machining of PVA and cellulose fiber containing cement products in the fiber-cement factories has a low potential to release fibers with critical fibrous dimensions.

Nelson and Yang found an enhancement in the thermal stability of PMMA by accumulation nano-silica and by using silane coupling agents prior to polymerization by PMMA on the pretreated silica [50].

Goyal et al showed that nanocomposites of poly (ether ether ketone) (PEEK) containing nano- Al_2O_3 filler up to 30% had more thermal stability, crystallization and Coefficient of thermal expansion [51].

To improve the dispersibility of Silica, polymer/Silica nanocomposite particules were prepared through mini-emulsion polymerization by using methyl methacrylate / butylacrylate mixture containing the well dispersed nano-sized silica particules treated with 3-Trimethoxy silyl Propylmethacrylate (PMS)[52].

Aiping et al prepared PMMA - SiO_2 composite with suspension -dispersion polymerization the result showed that PMMA covering the surface of SiO_2 nanoparticles improve the spreading of nano silica dispersion, increase heat resistance, tensile strength and elongation at break [53].

Carrado proposed that in the research area of the polymer -nano scale filler composite the primary goal is to improve thermal and mechanical properties of the polymers, e.g stiffness, toughness and heat resistance by using nanoscale or molecular reinforcement [54].

Reynaud et al demonstrated that due to the effects of nanoscale, Polymer Silica nanocomposite can often reveal impressive improvement in modulus, strength, heat resistance and gas permeability barrier properties [55].

Nanodispersed coreshell SiO_2 /Polymer spheres in submicrometer size were successfully synthesized by Asher et al via dispersion polymerization, and were used as the building units for the fabrication of photonic crystals [56].

CaCO_3 /PMMA nanospheres [57] were synthesized by soapless emulsion polymerization techniques. Results showed that this method was effective to enhance the

loading of CaCO_3 in composite which in turn enhanced the thermal stability of Poly (methyl methacrylate) and the acid-resistant of CaCO_3 nanoparticulates in composites.

Meneghetti and Qutubuddin synthesized PMMA/Clay nanocomposites via emulsion and insitu polymerization techniques. DSC results showed that the Tg of these composites were 10 - 8 $^{\circ}\text{C}$ higher than pure PMMA. Mechanical and thermal properties of these composites were also better than pure PMMA [58].

Khan and coworkers found out the ionic conductivity of PPO and PEO in pure solution form, individually complexed with salts of Na^+ and Li^+ , with and without plasticizer. It was shown that the addition of salts in pure PEO increased conductivity many times. The plasticizer showed the same effect. It was also shown that the blending of PEO and PPO gives enhanced conductivity as compared to pure PEO [59].

By understanding and controlling the swelling of montmorillonite clay material, the expanding nature of MMT was used by Nehal Salahuddin and Mohamed Shehata to counteract polymerization shrinkage and the resultant residual stress development in PMMA polymer. Polymerization Shrinkage of PMMA and linear dimensional changes of PMMA greatly decreased and found to be controlled in PMMA-MMT composite [60].

Poly (methyl methacrylate) silica hybrid thin films were successfully synthesized by Song et al .TGA results showed the enhancement of thermal stability of hybrid thin film. SEM results showed that the silica particles were well dispersed and had strong interaction between Poly (methyl methacrylate) and inorganic particles .In short the Poly (methyl methacrylate) silica hybrid thin films synthesized by non-hydrolytic sol gel route had enhanced thermal and other basic properties judged against to samples prepared by sol gel technique [61].

PMMA, PEO blends with ceramic filler were prepared by D. Shanmukakaraj et al. The results reveal that these composites show high (maximum) conductivity at 21 °C along with their improved electrochemical stability and suggested that these blends would have widespread application in electrochemical devices [62].

Harrup et al prepared novel polymer/silicate nanocomposites and studied their structure and mechanical properties using Scanning Electron Microscopy (SEM) and Dynamic Mechanical Analyzer (DMA). It was concluded from the results that the novel nanocomposites could be used in the solid electrode polymer, in separation membranes and other selective barriers, as subsurface permeable reactive barriers and other such industrial applications [63]

Ma and co workers prepared water-soluble gold nanoparticles/ polyaniline nanocomposite using organic amine 3- APBA as reductive and protective agent. PVA played an important role in the preparation of this nanocomposite and the size of nanoparticles could be adjusted by the concentration of PVA. To characterize the nanoparticles, UV–vis (ultra violet visible) absorbance spectroscopy and transmission electron spectroscopy were used. [64]

Zhang et al studied the soluble functionalized carbon nanotube/poly (vinyl alcohol) (PVA) nanocomposite as the electrode for glucose sensing. In their study polymeric nanocomposites from carbon nanotubes and PVA were prepared and characterized. Parallel to PVA, the functionalized carbon nanotube/ poly (vinyl alcohol) nanocomposite samples were soluble in highly polar solvents like water and DMSO (Dimethyl sulfoxide). Furthermore, it improved the processibility of carbon nanotube-based materials. These nanocomposites showed high electrical conductivity [65].

Tsai and Huang investigated a simple and versatile protocol for the noncovalent solubilization of MWNTs (Multi-Walled Nanotubes) in aqueous solution. The results showed that the MWNTs could be suspended homogeneously in PVA aqueous solution which was prepared by a freeze–thawing process to avoid the toxicity and leaching problem of chemical cross-linking agents [66].

Wu and co workers prepared novel dendritic nanostructures; self-assemblies of nanoparticles of PVA coated Ag or Cu₂O. They realized the controlled synthesis of well-defined dendritic nanostructures. They were really selfassemblies of PVA colloidal particles with embedded Ag or Cu₂O nanocrystals. It was one-step in situ reduction of Ag⁺ and Cu²⁺ in an aqueous solution of amphiphilic poly (vinylacetone) under γ -ray radiation using the low hydrolysis rate of the poly (vinylacetone) in dilute acidic solution[67].

Ishimori and Senna [68] conducted a study on Control of microstructure and disintegration properties of silica granules from PVA. The microstructure of spray-dried model granules comprising silica microspheres and poly (vinyl alcohol), granules were characterized by a shear method for granular beds, and by a compression test for single granules. The internal structure changed significantly with the pH of the slurry from which the granules were spray-dried.

Zvonimir et al [69] synthesized PS-PMMA/LDH-B nanocomposites by situ bulk multistep polymerization. X-ray diffraction (XRD) and Fourier transform infrared (FTIR) results pointed to the incorporation of the LDH-B within polymer matrix. A TGA and DSC result showed high thermal stability than net PS-PMMA copolymer.

Qian and coworkers [70] prepared Polymer-inorganic nanocomposites of PVA with calcium sulphide (CdS) by hydrothermal method. It was found that, to prepare poly (vinyl alcohol) (PVA) /zinc sulphide (ZnS) and PVA/cadmium sulphide (CdS) nanocomposites through the hydrothermal process by the situ reaction of zinc chloride ($ZnCl_2$) or cadmium chloride ($CdCl_2$) with carbon disulphide (CS_2) at $120 \pm C^\circ$ for 8 hours.

Nanocomposites of polypropylene (PP) and organophilic montmorillonites were prepared by Cora et al [71]. The XRD, SEM and rheological results presented in this study confirmed that for given composition and processing conditions, the microstructure and flow behavior of PP/OMMT strongly depended upon the nature of the intercalant used in organophilic montmorillonites

Kutsenko and coworkers [72] studied the third-order nonlinear optical response of a new PVA composite with lead sulphide (PbS) nanocrystals showing that high third-order NLO (Non Linear Optics) susceptibility values in the visible spectral region could be achieved in polymer composites with nanocrystals of narrow-gap semiconductors with large dielectric constant and exciton diameter.

Avella et al [73] studied the thermal, mechanical and barrier properties of poly (vinyl alcohol) (PVA)/poly (tetrafluoroethylene) (PTFE) nanocomposites and explained that the presence of nanoparticles strongly influences the water permeability. The unique and unexpected properties of polymer based nanocomposites were strictly correlated to the enormous specific surface of the nanoparticles and consequently to the large potential interfacial region.

Mirmohsenia and Wallace [74] worked on the preparation and characterization of processable electroactive polyaniline–poly (vinyl alcohol) composite. They prepared a series of polyaniline–poly (vinylalcohol) dispersions with different polyaniline contents. Films prepared from these dispersions had excellent mechanical properties. They were flexible (as verified by modulus values) and could be stretched up to 190%. A tensile strength value as high as 40 MPa was obtained. The electrical conductivity of the composite was improved with increasing amount of polyaniline and reached a high value of 2.5 S cm^{-1} at room temperature.

Dense, microporous and macroporous hydroxyapatite special granules for medical application were prepared by Descamps and coworkers [75]. During this study, a new process for fabrication of drug delivery system combining an osteoconductive material and a bioactive agent was developed. Macroporous beads with porous volume of 70% were also obtained by adapting the method to commence microporosity.

Calcium Phosphate nanoparicles were prepared by Thomas et al and characterized with TEM and XRD [76].The particles sizes were found to be around 10 nm. The Glass transition temperature showed a positive shift demonstrating better reinforcement in polymer matrix. The specific heat capacity of this system showed extreme reduction which indicates good filler matrix interaction.

Iwaseya et al [77] conducted a study on PVA / CH_3COONa / Na_2SO_4 composites and studied the relationship between the structure of the composite and strength. Generally, higher the degree of crystallization, lower the draw ratio for crystalline polymers. In this study the results obtained were shown to be reverse. These results could be understood by considering that suitable networks which had the drawability to a

higher extent are made after separation of Na_2SO_4 and CH_3COONa . The crystallites increased with an increase in Na_2SO_4 and CH_3COONa concentrations which leads to increase the density. As the method shown in this paper was new for making polymer materials so it named the salt ions-induced crystallization method.

Experiments testing absorbance change of UV–vis spectrum was conducted on the phase transition process of $\text{PMMA-SiO}_2@$ paraffin microcapsules with copper-chelating as the ion probe. The phase transition process had successfully measured that there was little change in absorbance of UV–vis spectrum which should be caused by the heat absorbance of the phase change materials. After the phase change was completed, the spectrum of absorbance of microcapsules had a sudden drop. The special UV–vis spectrum of $\text{PMMA-SiO}_2@$ paraffin microcapsules should be caused by the changes of charge distribution or molecular interaction of ion probe Cu (II) chelating in microcapsules [78].

Nanocomposites of poly(methyl methacrylate) (PMMA) containing various multi-walled carbon nanotubes (MWCNT) contents were prepared using melt mixing by Logakis and co workers[79]. Several techniques were employed to study the influence of the MWCNT addition on the thermal, mechanical, electrical and dielectric properties of the PMMA matrix. The electrical percolation threshold (p_c) was found to be 0.5 vol.% by performing AC and DC conductivity measurements. Significantly high conductivity levels (σ_{dc}) were achieved: σ_{dc} exceeds 10^{-2} S/cm already at 1.1 vol.%, the criterion for EMI shielding ($\sigma_{dc} > 10^{-1}$ S/cm) was fulfilled at 2.9 vol.%, and the highest loaded sample (5.2 vol.%) gave a maximum value of 0.5 S/cm. Dielectric relaxation spectroscopy measurements in broad frequency (10^{-1} – 10^6 Hz) and temperature ranges (-150 to 170 °C)

indicated weak polymer-filler interactions, in consistency with differential scanning calorimetry and dynamic mechanical analysis findings. Weak polymer-filler interactions and absence of crystallinity facilitated the achievement of high conductivity levels in the nanocomposites.

The morphology and thermomechanical properties of composites of poly(methyl methacrylate) (PMMA) and chemically modified graphene (CMG) fillers were investigated by Jeffrey et al[80]. For composites made by *in situ* polymerization, large shifts in the glass transition temperature were observed with loadings as low as 0.05 wt% for both chemically-reduced graphene oxide (RG-O) and graphene oxide (G-O)-filled composites. The elastic modulus of the composites improved by as much as 28% at just 1 wt% loading. Wide angle X-ray scattering suggested an exfoliated morphology of both types of CMG fillers dispersed in the PMMA matrix, while transmission electron microscopy revealed that the platelets adopt a wrinkled morphology when dispersed in the matrix. Both techniques suggested similar exfoliation and dispersion of both types of CMG filler. Structural characterization of the resulting composites using gel permeation chromatography and solid state nuclear magnetic resonance showed no change in the polymer structure with increased loading of CMG filler.

Jun et al [81] synthesized long and highly dispersible multi-walled carbon nanotube (MWCNT) bundles in large quantity by catalytic chemical vapor deposition, and its structural and electrical properties were characterized. It was found that the MWCNTs could be synthesized with either bundled (long-aligned) or short-entangled structure depending on the catalyst system. The aligned MWCNTs were found to be more conductive and more dispersible than the entangled ones. The MWCNT/poly (methyl

methacrylate) composites were prepared using both entangled and aligned MWCNTs. The aligned MWCNTs were found to give the composite higher electrical conductivity which might be attributed to long length and high dispersibility. It was further found that the longer the MWCNT bundle, the higher electrical conductivity of the composite.

PMMA–mesoporous silica nanocomposites were prepared for the first time through *in situ* batch emulsion polymerization [82]. For composites containing 5.0 wt % silica, the onset decomposition temperature and the temperature at 10% weight loss for the nanocomposite increased 41 °C and 50 C⁰, respectively, in comparison to pure PMMA. The glass transition temperature of the nanocomposite increased 9.3 C⁰, as determined by differential scanning calorimetry. In addition, the storage modulus determined by dynamic mechanical analysis increased 17% and 80% at 50 C⁰ and 100 C⁰, respectively. Substantial improvements in tensile strength (+50%) and modulus (+72%), were achieved at 10 wt % nanoparticle loading. Composites made by compression molding of physical mixtures of PMMA and MSU-F silica powders provided less improvement in thermal stability, glass transition temperature and mechanical properties in comparison to the composites made through *in situ* batch emulsion polymerization.

Charles et al [83] prepared a series of aluminum-containing layered double hydroxides (LDHs), containing Mg, Ca, Co, Ni, Cu and Zn as the divalent metals by the co-precipitation method and used to prepare nanocomposites of PMMA by *in situ* bulk polymerization. The additives were characterized by Fourier transform infrared spectroscopy, X-ray diffraction spectroscopy (XRD) and thermogravimetric analysis while the polymer composites were characterized by XRD, transmission electron

microscopy, differential scanning calorimetry and cone calorimetry. Polymerization of methyl methacrylate in the presence of these undecenoate LDHs resulted in composites with enhanced thermal stability. The glass transition temperatures of the composites and the pristine polymers were found to be around 110 °C. This suggested that the presence of additives have little effect on the polymer. It was found that the additive composition and the dispersion state of LDHs agglomerates in the polymer matrix influence the fire properties of composites as measured by cone calorimetry.

Poly (methyl methacrylate) (PMMA) matrix, propylene carbonate (PC), LiClO₄ and OREC (Rectorite modified with dodecyl benzyl dimethyl ammonium chloride) were prepared by Yun and co workers [84]. The interaction between components was quantitatively determined. Characterization of interaction of C=O in PC and PMMA with Li⁺ and OH group on OREC surface had been thoroughly examined using FTIR respectively. The quantitative analysis of FTIR showed that the absorptivity coefficient of PMMA/LiClO₄, PC/LiClO₄, PC/OREC and PMMA/OREC was 0.902, 0.113, 0.430 and 0.753, respectively, which meant that the Li⁺ or OH bonded C=O was more sensitive than the free C=O in FTIR spectra. The limit value of bonded C=O equivalent fraction of PMMA/LiClO₄, PC/LiClO₄, PC/OREC and PMMA/OREC was 17%, 94%, 57% and 20%, respectively, which showed that all the interaction within the components were reversible and the intensity of interaction was ordered as PC/LiClO₄, PC/OREC, PMMA/OREC and PMMA/LiClO₄.

The electroless coating of Ag on PMMA sphere pre-coated with polyaniline (PANI) was investigated by Yejin Lee et al [85]. Situ chemical polymerization was used for Pre-coating. The extent of silver coating on PMMA and PMMA/PANI particles was

studied by measuring the remaining content of Ag using thermo gravimetric analysis, in terms of the number of pretreatment steps, the particle size, AgNO₃ concentration and PANI content. The results signified that the deposition of PANI on the polymethylmethacrylate surface induced high efficiency of the silver plating due to the activation effect. The resistivity of PMMA/Ag and PMMA/PANI/Ag composites varied between 10¹⁴ and 10⁻¹ Ω cm and between 10⁸ and 10⁻⁴ Ω cm, respectively. Such increase in resistivity, along with the relatively compact and continuous silver layer on PMMA/PANI/Ag composite particles explained that this method was effectively applicable on the improvement of conductive materials.

Pattern transfer of silicon dioxide, nanoparticles–poly (methylmethacrylate) nanocomposite was studied using two soft lithographic techniques, micro molding in capillaries (MIMIC) and micro transfer molding (μTM) using an elastomeric stamp in Poly (dimethyl siloxane) (PDMS). Nanocomposite periodic arrays of 20 μm wide and 10 μm deep lines with 10 μm spacing were obtained over approximately 1 cm² area on silicon substrates by μTM and MIMIC using a 3 wt.% monodisperse silica nanoparticles (~338 ± 2 nm) in poly (methyl methacrylate) solution. In addition, free standing nanocomposite self-standing films of centimeter size were also manufactured by μTM. Using MIMIC with a lower concentration of silica NPs (0.25 wt.%) in PMMA obtained single line of nanocomposite [86].

Mara et al [87] prepared a porous hybrid structure by blending molecularly imprinted polymeric particles with PMMA, using a supercritical carbon dioxide (scCO₂)-assisted method. Membranes were characterized in terms of mechanical performance, morphology and transport properties. The capacity of the polymers and hybrid

membranes to adsorb bisphenol was tested in aqueous medium and fitted to a linearized Langmuir equation, which showed that the adsorption took place at homogeneous affinity binding sites within the imprinted surface.

Yuan et al [88] successfully grafted multiwalled carbon nanotubes (MWCNTs) with maleic anhydride (Mah-g-MWCNTs) via Friedel–Crafts acylation with the aluminum chloride catalyst (AlCl_3). It was investigated by Raman and TGA analysis. The covalent bonds and carboxylic groups of maleic anhydride provided additional active species, improving adhesion between the MWCNTs and poly(methyl methacrylate) (PMMA). This research also studied the morphology and dynamic mechanical properties of pristine MWCNTs (P-MWCNTs) and modified MWCNTs (Mah-g-MWCNTs) reinforced with poly(methyl methacrylate). Results showed a homogeneous distribution of MWCNTs throughout the matrix for Mah-g-MWCNTs/PMMA composites revealed by transmission electron microscope (TEM). The addition of both MWCNTs influenced the molecular arrangement of the PMMA matrix and also increased the dynamic mechanical properties of MWCNTs/PMMA composites. Glass transition temperature (T_g) and storage moduli (E') of the Mah-g-MWCNTs/PMMA composites increased significantly comparing with P-MWCNTs/PMMA composites which were attributed to improved interfacial adhesion between the reinforcement and the matrix. DMA studies revealed that adding 4.76 wt% Mah-g-MWCNTs into PMMA generated a 184% enhancement in the storage modulus and a 19 $^{\circ}\text{C}$ increase in T_g . However adding 4.76 wt% P-MWCNTs into PMMA only generated 108% enhancement in the storage modulus and a 14 $^{\circ}\text{C}$ increase in T_g .

Fiber glass-reinforced polymer composites were investigated by Eduard et al [89] for potential use as structural dielectrics in multifunctional capacitors that require simultaneous excellent mechanical properties and good energy storage characteristics. These composites were fabricated using poly (methyl methacrylate), PMMA, as the structural matrix. Barium titanate (BaTiO_3) nanopowder was added to the composites for its high room temperature dielectric constant, fiberglass was added to confer high stiffness. A conductive polymer blend of poly (3,4-ethylenedioxythiophene) and polystyrene sulfonate (PEDOT:PSS) was used to coat the BaTiO_3 nanoparticles with the purpose of further elevating the dielectric constant of the resultant PMMA-composites. FTIR spectroscopy, TGA and SEM measurements were conducted to prove the successful coating of BaTiO_3 nanoparticles with the PEDOT:PSS blend. TEM results showed a good dispersion of coated nanoparticles throughout the PMMA matrix. The fiberglass-reinforced-PMMA composites containing neat and coated BaTiO_3 were found to exhibit excellent stiffness. In addition, the use of PEDOT:PSS in conjunction with BaTiO_3 was observed to improve the dielectric constant of the composites.

Gas permeabilities and selectivities of some gases like He, O_2 , N_2 and CO_2 were evaluated in inorganic-organic membranes based on 6FDA-6FpDA and 6FDA-6FpDA:DABA and PMMA-g-silica. PMMA was grafted onto the silica to make it miscible with 6FDA-based polyimide after surface treatment with γ -MPS. The PMMA-g-silica showed better dispersion than did the pure silica particles in the polymer matrix. The two types of polyimide polymer had same trends with respect to gas transport properties. The increase in permeation was endorsed to changes in the free volume distribution up to 1 wt% silica. Above 1 wt%, the permeabilities decreased as a result of

reduced effective area for gas transport. The selectivities decreased when PMMA-g-silica content increased. However due to strong interaction between PMMA and polar gas the selectivity of CO₂ in 6FDA–6FpDA was found greater [90].

Silica/PMMA nanocomposites with different silica quantities were prepared by M.L. Saladino et al [91] Applying melt compounding method. Transmission electron microscopy (TEM), dynamic mechanical analysis (DMA), X-ray diffractometry (XRD), thermogravimetric analyses (TGA), Fourier-transform infrared spectroscopy (FTIR) were used to investigate the morphology, mechanical properties and thermal degradation of the composite. Results showed that silica nanoparticles were well dispersed in the polymeric matrix whose structure remained amorphous. The degradation of the PMMA occurred at higher temperature in the presence of silica because of the interaction between the two components.

Poly (methyl methacrylate) (PMMA)/organically modified montmorillonite (O-MMT) composite microfibers were firstly prepared by emulsion polymerization combined with electrospinning, and then coated by nanosize titanium dioxide (TiO₂) using RF magnetron sputter technique. The modified surfaces of PMMA/O-MMT composite microfibers were characterized by scanning electron microscope (SEM), Fourier transform infrared spectroscopy (FTIR), transmission electron microscope (TEM), UV–vis spectroscopy, X-ray diffraction (XRD), and drop shape analyzer. The experimental results showed that anatase-TiO₂ and rutile-TiO₂ nanoparticles were well spread and physically deposited on the surface of PMMA/O-MMT microfibers, and the wettability of the PMMA/O-MMT composite microfibers was better after surface modification by sputter coating [92].

Poly (methyl methacrylate) (PMMA)/ Carbon nanofiber (CNF) nanocomposites were prepared via melt-compounding, solvent casting and in situ polymerization by Varela-Rizo et al [93]. Mechanical properties, electrical resistivity and rheological behavior were investigated in specimens with varying CNF loadings. The three processing techniques were compared. Improved properties were obtained in the solvent process and in situ polymerized composites. No changes were found in melt-compounding, even by the addition of 10 wt% of CNFs. The rheological and electrical percolation of these nanocomposites appeared in the same concentration set (between 1 and 5 wt %). Electrical resistivity of the samples prepared by solvent casting was measured before and after pressing in the hot plate press. It is significant that in the non-pressed samples the CNFs formed an efficient 3-D conductive network, yielding composites with percolation thresholds even six orders of magnitude lower than after pressing, where this 3-D network was destroyed.

Telma Nogueira et al [94] investigated in situ bulk polymerization of methyl methacrylate (MMA) in the presence of LDH intercalated with the stearate anion. In situ polymerization was evaluated in order to obtain a more uniform LDH dispersion in the PMMA matrix for improving thermal and mechanical properties of nanocomposite.

Yang Zhao and co workers [95] used rice straw fiber (RSF) to improve the compatibility of poly (lactic acid) (PLA). Methyl methacrylate (MMA) was selected as the monomer in the admicellar polymerization for the RSF treatment because RSF coated with poly (methyl methacrylate) (PMMA) thin film would have better compatibility with the PLA matrix according to a preliminary estimated using Hansen solubility parameters. The extensively improved mechanical properties were attributed to the interfacial adhesion

improvement between TRSF and PLA which was investigated by scanning electron microscope (SEM). The thermal properties of (T)RSF-PLA were investigated by thermogravimetric analysis (TGA), and the TGA results confirmed that the thermal stability of TRSF-PLA was enhanced compared with RSF-PLA composite.

Thermoplastic polymer with high ceramic content composite was developed by Kristina Brandt et al [96] using a radical emulsion polymerization reaction in an aqueous suspension. TiO₂ is encapsulated by a thin layer of PMMA. Consequently the coated particles are compacted by applying high pressure at a temperature above the glass transition temperature of the PMMA. SEM study confirmed successful coating of TiO₂ particles by PMMA. Thermogravimetric measurements estimated the compositions of the matrix. Vickers micro hardness as well as flexural strength and elastic modulus were used for characterizing mechanical properties. This composite exhibited a 10-fold increase in micro hardness with respect to pure PMMA. For ceramic polymer composites these moduli are among the highest found in literature.

To improve the process of encapsulation of inorganic nanoparticles into polymer matrix the intensified processes based on the ultrasonic irradiations were used by B.A. Bhanvase and co workers [97]. The result showed that the use of ultrasonic irradiations increased the dispersion of functional nano-inorganic particles into the monomer during polymerization process. The model system was based on the nanocomposite of PMMA/CaCO₃) which had been synthesized by this technique. To improve the compatibility of the monomer with the inorganic particles, CaCO₃ nanoparticles were pretreated with myristic acid. TEM image of PMMA/CaCO₃ composite particles with well-defined core-shell structure give direct evidence of encapsulation.

Thermogravimetric analysis showed that this composite has better thermal stability as compared to the plain PMMA.

TiO₂ nanoparticles and poly (methyl methacrylate) (PMMA) mixture were used by Mengjin Yang and co workers [98] to produce very hydrophobic surface. To make very hydrophobic the volume ratio of the mixture of two hydrophilic materials, TiO₂ to PMMA was between 35 vol. % and 50 vol. %. IR spectroscopy showed that this strong hydrophobicity was due to the preferential orientation and attachment of a carbonyl group of a polymer molecule to the surface of TiO₂ nanoparticles. By exposing this composite to UV light, PMMA on the surface of the mixture film decomposed through a photocatalytic reaction and hydrophobic surface turned to the superhydrophilic one. The superhydrophilic property of UV-irradiated composite lasted for long time. This long lasting superhydrophilicity was credited to the porous structure which provides high roughness and strong capillary interaction.

Aligned chemical vapor deposition (CVD)-grown graphite nanofibers (GNFs) were used as a conductive filler in a poly(methyl methacrylate) (PMMA) system to investigate the effect of GNF content on the thermo-mechanical properties of GNFs/PMMA composites. In the result, an electrical percolation threshold for the composites was found between 1 and 2 wt% GNF contents which depended on high aspect ratio and good electrical conductivity of GNFs enabling them to percolate systems at low volume fraction. All of the composites contained individually dispersed GNFs after initial shear-intensive stirring. Negative surface charges on the GNFs led to charge-stabilized dispersions. Above the melting temperature of PMMA, the GNFs re-aggregated on application of elevated temperatures and/or modest shear forces.

Additionally, the composites exhibited higher thermal and impact properties and lower thermal shrinkage compared with those of the neat PMMA. Consequently, it was demonstrated that GNFs had positive impacts on the thermo-mechanical properties of polymer composites and that they had the potential to be effectively utilized to enhance the structural performance of composites [99].

The holographic recording and grating formation dynamics in SiO₂ nanoparticle-dispersed PQ-PMMA photopolymer are investigated theoretically and experimentally by Hongpeng Liu et al [100]. It has demonstrated a possibility to improve the refractive index modulation by doping inorganic nanoparticles into the polymer matrix. Mutual diffusion dynamics as dark diffusional enhancement mechanism after exposure was analyzed and simulated by mutual diffusion model. The maximum of mutual diffusion coefficient with the order of magnitude 10⁻¹⁶ m²/s was extracted. This study can provide a significant foundation for improving the properties of the polymer using inorganic nanoparticles as dopants.

Chapter -III:
EXPERIMENTAL

Materials

In this study we prepared the following seven composite systems and characterize them

SR. NO.	POLYMER	ADDITIVES
1	PMMA	Na ₂ SO ₄
2	-do-	Clay
3	-do-	Activated carbon
4	-do-	CaCO ₃
5	-do-	SiO ₂
6	-do-	Ceramics
7	-do-	Glass

Table1. Systems studied

Poly (methyl methacrylate) (PMMA), Sodium Sulphate (Na₂SO₄), clay (montmorillonite), CaCO₃, SiO₂ and Benzene were purchased from the Aldrich. These materials were used as received without any purification. Activated carbon, ceramics and glass were mechanically ground to fine powder and then passed through 20 micron mesh. Colorless single crystals of sodium sulfate (Na₂SO₄) were developed from aqueous solution at 50 C⁰ by slow evaporation of the solvent. The sodium Sulfate powder was dried for 24 hours in oven at 150 C⁰

3.1. Preparation of plain polymer film:

02% PMMA solution was prepared in benzene and was continuously stirred with magnetic bar at 80 C⁰ for about 24 hours until homogenous solution was obtained. This was then transferred to Petri dishes of appropriate size and maintained at 50 C⁰ in oven in for additional 24 hours. During this time excess solvent evaporated. Then the remaining

films were kept in desiccators for an additional 3 days. Finally stable films were obtained. These were stored in desiccators.

3.2. Preparation of polymer composites

PMMA solution of 2% was prepared along with appropriate concentrations of additives in benzene and the same procedure was followed as given before.

3.2.1. Instrumentation

The morphologies of PMMA- composites were examined using a JEOL-JSM-6700F field emission Scanning Electron Microscope (SEM).

The samples for SEM measurements were mounted on aluminum stud using adhesive graphite tape and sputter coated gold before analysis.

Fourier transfer infrared (FTIR) spectra were recorded on Avatar 320 FTIR spectrometer, Nicolt instrument corporation, Madison, WI, USA.

EDX (Energy Dispersive X-rays) analysis were performed by EDX spectrometer ICCA 200, Oxford instruments UIC.

Perkin Elmer DSC Diamond and Perkin Elmer TG/DTA Diamond instruments were used for thermal studies. The sample chamber was purged with cleaned Nitrogen and Argon at every time. Measurements were carried out at a heating rate of $5\text{ C}^{\circ} / \text{min}$ from room temperature to 500 C° .

Tensile strength was measured by Testometric Universal Testing Machine (UTM) M350/500 manufactured by Testometric UK at room temperature.

Scanning Electron Microscope (SEM)



Scanning Electron Microscope (SEM)



Energy dispersive X-ray spectroscopy (EDX), INCA200/ Oxford instruments, U.K



FTIR (Fourier Transform Infrared) Spectrophotometer



Thermo Gravimetric and Differential Thermal Analyzer (TG/DTA)



Differential Scanning Calorimetry (DSC)



Universal Testing Machine (UTM), Testometric Inc. UK,

Chapter -IV:
RESULTS AND DISCUSSION

4.1. PMMA+ Na₂SO₄ composite system

Morphology

The scanning electron microscopy (SEM) of PMMA and PMMA/Na₂SO₄ are shown in figure 1 and figure 2 respectively. As one can see, from figure 1 that the surface of PMMA is plain and smooth. There is no pellet shape in plain PMMA, furthermore, it conform complete amorphous nature of pure PMMA. There is no crystalline behavior occurring in virgin Poly (methyl methacrylate). Figure 2 demonstrates the surface of PMMA /Na₂SO₄ composite which is rougher due to Na₂SO₄ visible particles. From the morphology of the polymeric composite it is apparent that the size of the Na₂SO₄ particles in polymer matrix ranges from 2.5 micrometer to nanometer and fully but randomly dispersed in polymer matrix. EDX study also confirm the existence of Na₂SO₄ particles in polymer matrix which is shown in figure 3

Chemical structure

The FTIR spectra of PMMA were recorded in the frequency range 4000-1000cm⁻¹ shown in figure 4 in transmittance mode. From this figure two distinct bands located at 2994.8 cm⁻¹ and 2950.4cm⁻¹ correspond to asymmetrical and symmetrical stretching. The first of these is the asymmetrical stretching mode in which two C-H bonds of the methyl group are broadening while the 3rd one is contracting ($\nu_{as}CH_3$). The 2nd arise from symmetrical (s) stretching (ν_sCH_3) in which all three of the C-H bonds contract and extend in phase.

According to literature the peak at 1729cm⁻¹ represent the free C=O group of PMMA [101-104]. Our result given in figure 4 also shows the same peaks.

Since the carbonyl group (C=O) is strong electron donor with in the PMMA so cation tends to complex with the oxygen atom of the carbonyl group. FTIR is powerful tool to monitor such ionic interaction. In the composites which we have prepared and being discussed in the coming section, we will focus on this peak especially to see whether interaction with added inorganic substances / ions is shown or not.

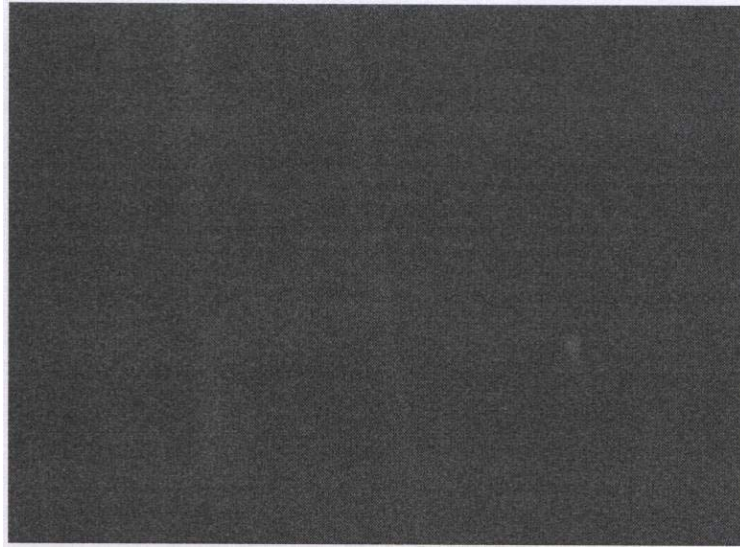


Fig.1. Scanning electron micrograph of plain PMMA

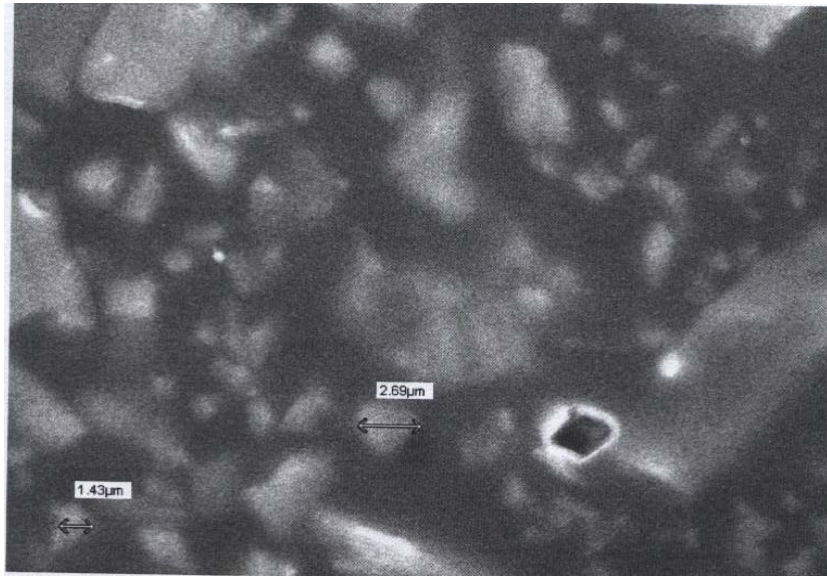


Fig.2. Scanning electron micrograph of PMMA+ Na₂SO₄ composite

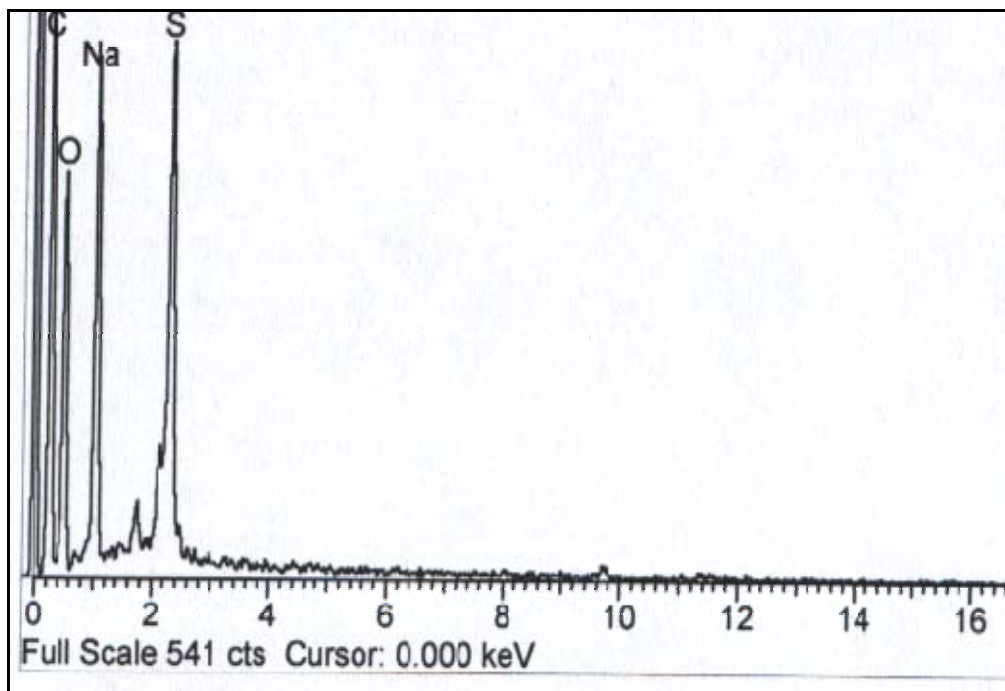


Fig.3. EDX study of PMMA + Na₂SO₄ composite

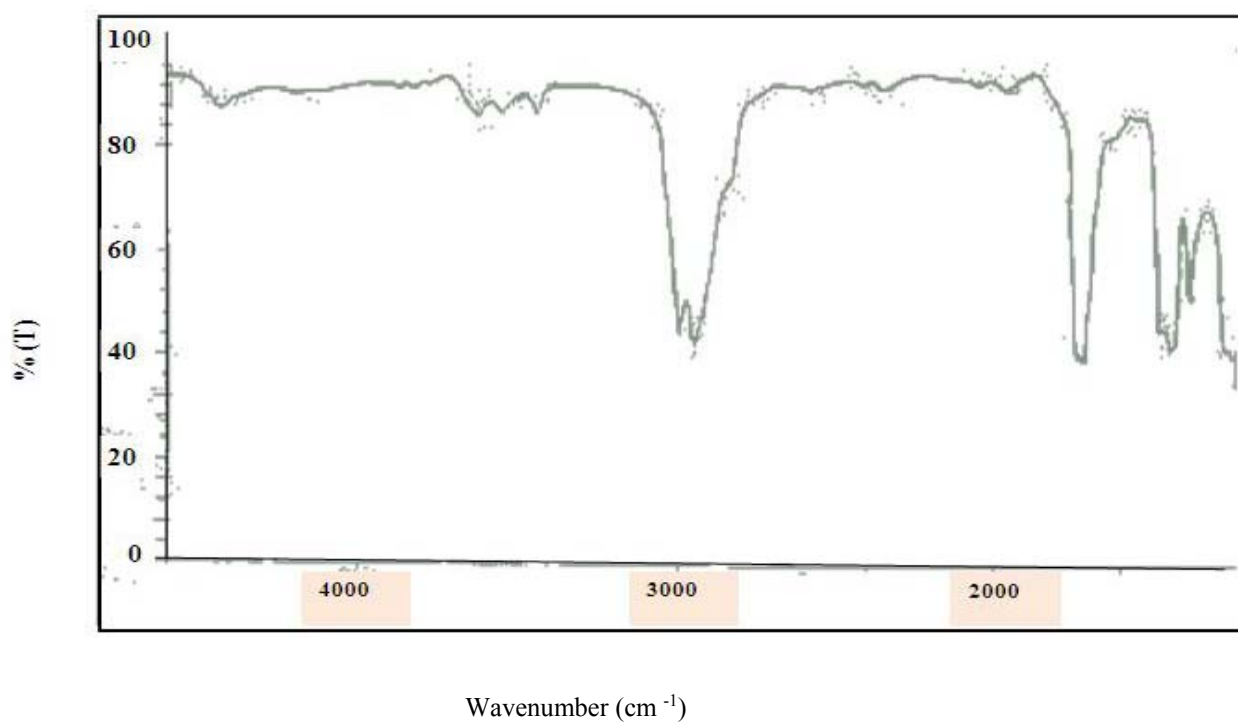


Fig.4. FTIR spectra of plain PMMA

Figure 5 represent FTIR spectra of PMMA/Na₂SO₄ composite .In this it can be seen that the peak position of C=O stretching shifts towards low wave number i.e from 1729.5 cm⁻¹ to 1724.7 cm⁻¹, indicating interaction between Na⁺ with carbonyl group of PMMA. It indicate the interaction between C=O of PMMA and Na⁺ of Na₂SO₄ particles. The Na⁺ particle bearing +ve is attracted by oxygen of C=O, Oxygen bearing electronegative, attracts Na⁺ and a kind of attractive forces are produced .So the position of the peaks is shifted. The addition of Zn particles (in the ZnO form) to PMMA has also shown to shift the peak toward lower wave length [105].This confirms our results are in agreement with earlier similar reports.

Thermal properties

Figure 6 illustrates TGA traces for pristine PMMA. The TGA curve indicates first smooth weight loss in the range 125 C⁰ to 270 C⁰ .This mean that PMMA is stable up to 125 C⁰, then the evaporation of solvent starts which goes up to 270 C⁰. After that continuous weight loss from 337 C⁰ to 400 is seen while no weight loss was observed after 400 C⁰ - 600 C⁰.It means that the PMMA was fully destroyed beyond 400 C⁰.

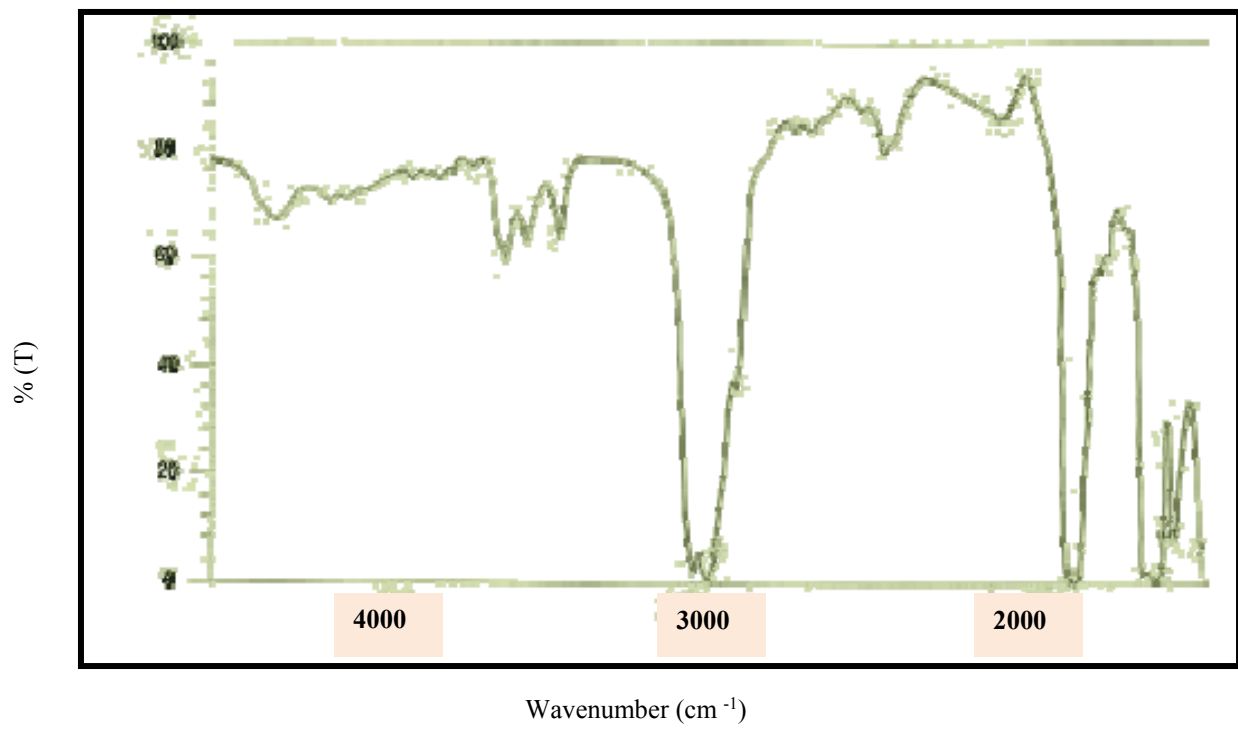


Fig.5. FTIR spectra of PMMA + Na₂SO₄ Composite

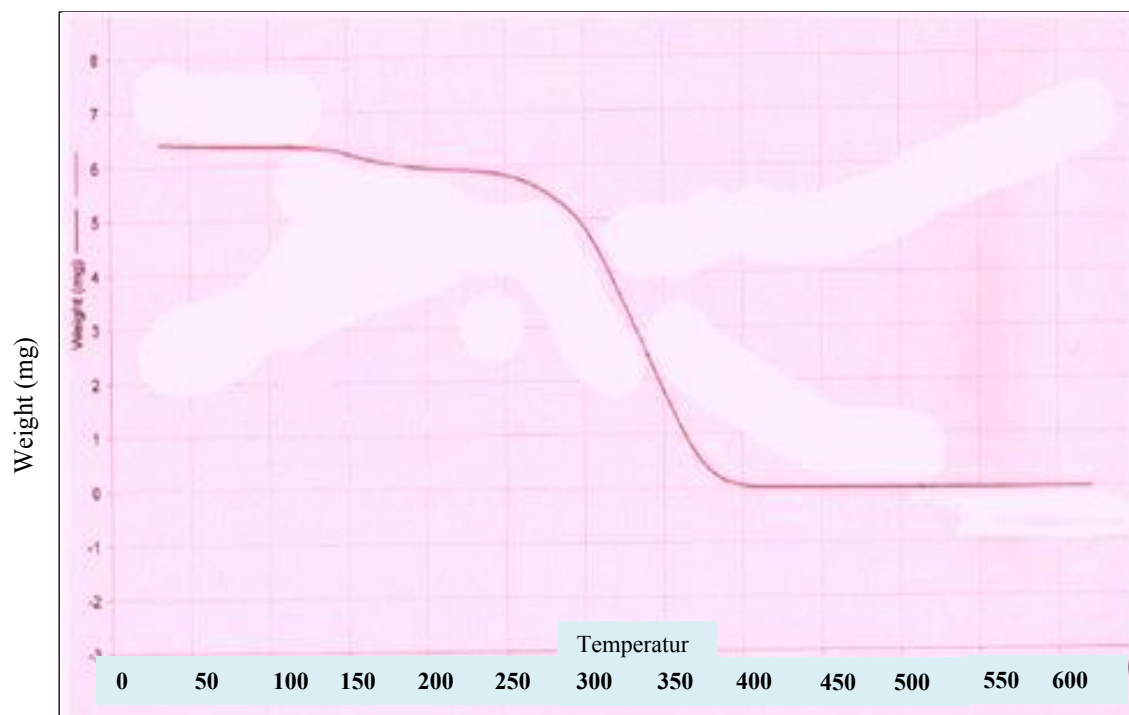


Fig.6. TGA traces for pristine PMMA

DSC traces of pure PMMA are shown in figure 7, two stages are clear from this, one is endothermic peak at 337.49 C⁰ and then the exothermic peak going up at around 397.85 C⁰. The first is due to heat adsorption which can be due to polymer degradation of unsaturated groups. The second is the opposite of first one; it is exothermic which may be due to opening produced by monomer evaporation.

The TGA curve of PMMA/ / Na₂SO₄ composite indicates similar trends in the beginning as that of pure PMMA but continuous weight loss was observed in a little higher range i.e 350 C⁰ to 405 C⁰. Beyond this temperature no weight loss was observed till 600 C⁰, which is illustrated in figure 8. This shows that this composite is more thermally stable with less weight loss. This enhancement of the thermal stability of the composite is induced by the Na₂SO₄ particles in polymer matrix. A protective barrier against thermal degradation is formed due to these particles. Na₂SO₄ particles enhancing the thermal stability of the hybrid more efficiently with smaller size and good dispersion.

DSC study of the above systems shows same thermal stability which are illustrated in figure 9. The major peak appearing in the DSC in figure 9 is at 350.09 C⁰ which is endothermic peak. This peak corresponds to degradation of polymer unsaturated group in pure PMMA. This has now shifted about 20 C⁰ at higher temperature. So the thermal stability has been enhanced. The incorporation of Na₂SO₄ has thus significantly increased the thermal stability. There is small peak at around 260 C⁰ which we attribute to glass transition temperature (T_g). The glass transition temperature is around 125-150 C⁰ according to literature. But now the addition of Na₂SO₄ it has shifted toward 260 C⁰. This again shows that Na₂SO₄ addition has increased thermal stability.

Ash et al prepared alumina/PMMA composites and suggested that variations on the thermal properties due to compatibility between the surface of nanoparticles and the Poly (methyl methacrylate). It was concluded that the ability of the polymer to soaked the particles did not significantly change as the function of the nature of particles surface [106]

Thermal degradation can be observed by TGA. Hirata at al reported two main reaction stages occurs during degradation of Polymethyl methacrylate in Nitrogen atmosphere, the first stage concerned with disintegration of weak head to head linkages impurities in the range $160\text{ C}^0 - 240\text{ C}^0$, and the decomposition of Polymethyl methacrylate chain ends around 290 C^0 , the 2nd stage in range $300\text{ C}^0 - 400\text{ C}^0$ correspond to random Scission of the polymer chain [107]

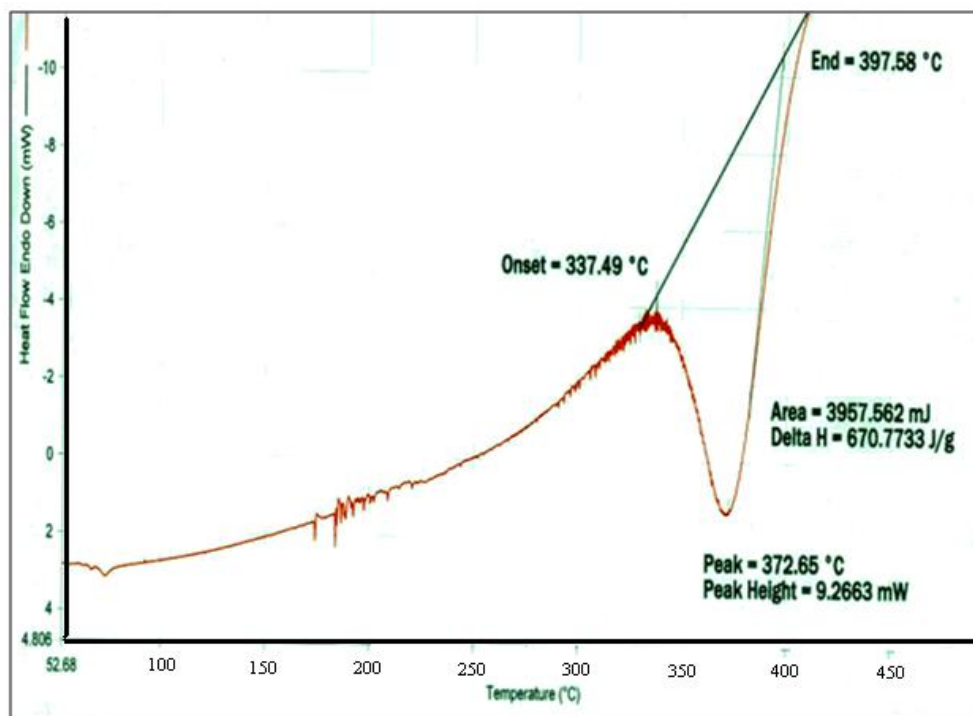


Fig.7. DSC study of plain PMMA

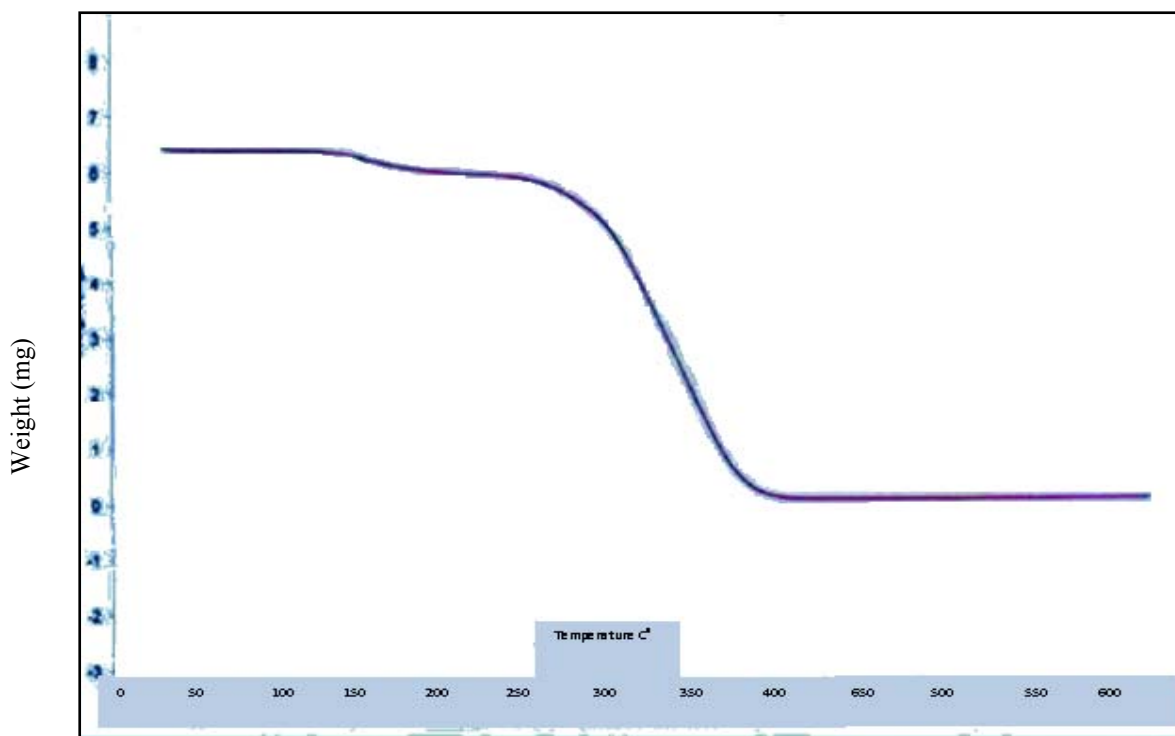


Fig.8. TGA traces for PMMA + Na₂SO₄ composite

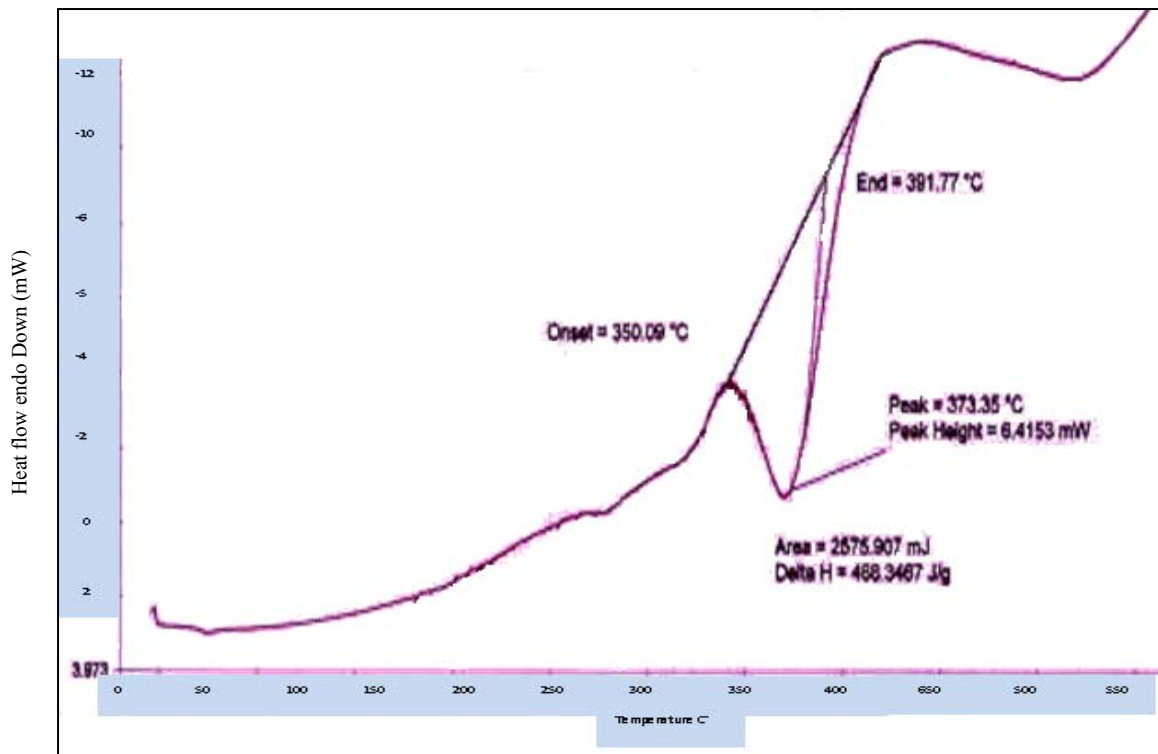


Fig.9. DSC study of PMMA+ Na₂SO₄ composite

Mechanical properties

Tensile strength is the ability of a material to withstand tensile load without rupture when the material is in tension. The young modulus of the composite depends on the volume fraction of the constitutions, the stiffness of the phases and the aspects ratio of the discrete particles. Various publications are found on the theoretical guess of E (Modulus of elasticity) for particles filled composites. It is common that addition of rigid particles like glass beads into a polymer matrix probably increase E, while addition of the soft particles decrease this property [108]

The Tensile properties of pure PMMA and PMMA/Na₂SO₄ composite are shown in figure 10 and figure 11 respectively. From these plots it is clear that PMMA/Na₂SO₄ shows greater tensile strength as compare to neat PMMA. From this plot it can be seen that the composite film can withstand almost double force and its elongation has also increased before rupture. The incensement in tensile strength is due to the development of Na₂SO₄ network and its chemical bonding with Poly (methyl methacrylate) which provides strengthening to the composite [109]

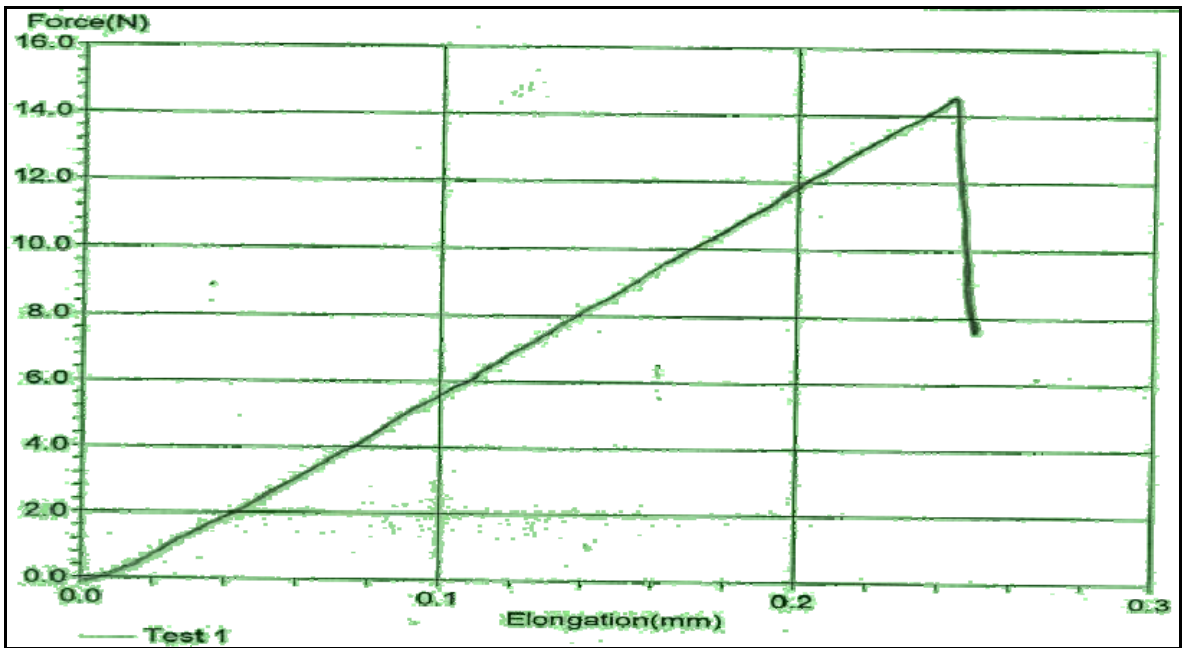


Fig.10. Tensile strength of plain PMMA

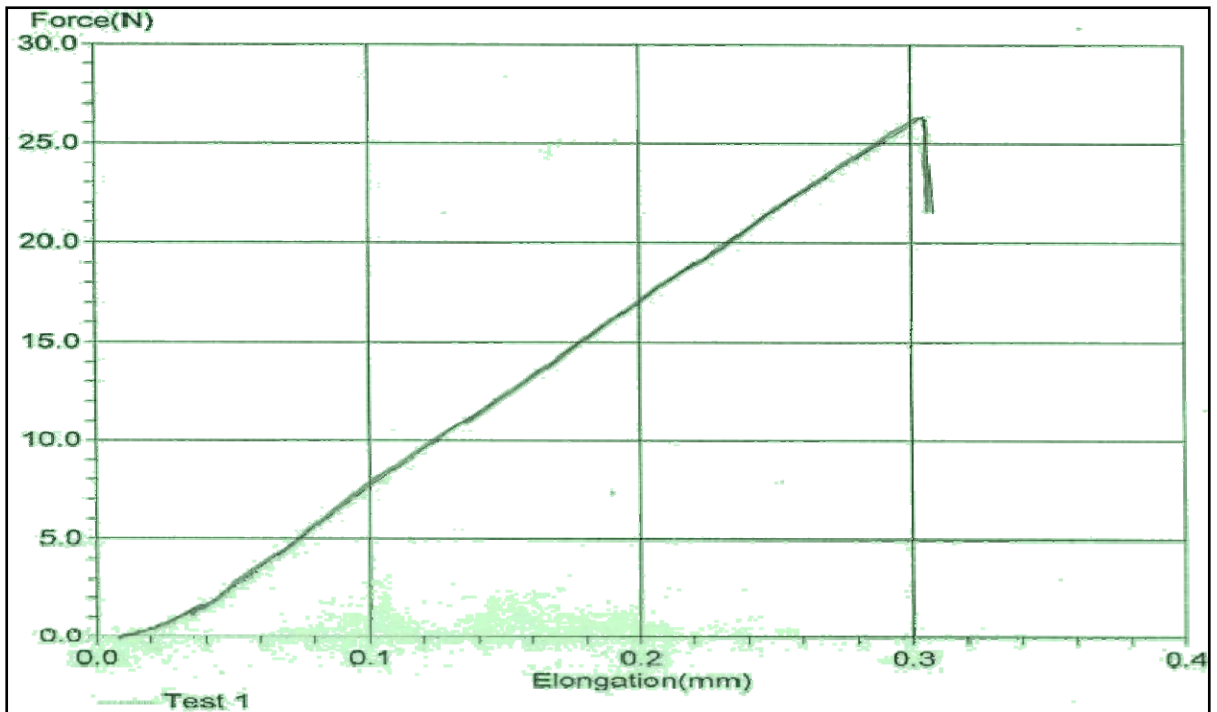


Fig.11. Tensile strength of PMMA+ Na₂SO₄ composite

4.2. PMMA+ clay composite system

Morphology

The morphological images of PMMA+ clay composite were studied by SEM. The SEM image representing the PMMA/clay composite is shown in figure 12. The smooth morphology of pure polymer (PMMA) is shown to be distributed and now the clay particles are visible in it. The particles are of various sizes, some are bigger while some are smaller. The size range from 2.3 micrometer to nanometer. The particles seem to be mixed homogeneously in the polymer matrix.

Chemical structure

Figure 13 shows that, peak on 1729 cm^{-1} for C=O shifts towards lower wave number i.e 1716.00 cm^{-1} which may match to the interaction between the clay particles and carbonyl group of PMMA. This examination confirmed the interaction between the PMMA and clay layer.

As we know the clay may contain various elements but major among these is the silicates and +ve cation (like Na^+ etc). If the clay is layered in structure (as we have used) each layer may contain numerous -ve and +ve charges which may form dipoles. When clay is well dispersed, it means that there are numerous well distribute dipoles in the environment. As in our system clay is well dispersed (shown from SEM in figure 12) this means that the +ve site can interact with C=O group of pure PMMA. So this is why there is shift in C=O peak. There is shift and enhancement in other peaks like 4436, 3628, 3438 also. Other interaction are also responsible apart for C=O which show these peaks are shifted.



Fig.12. Scanning electron micrograph of PMMA+ clay composite

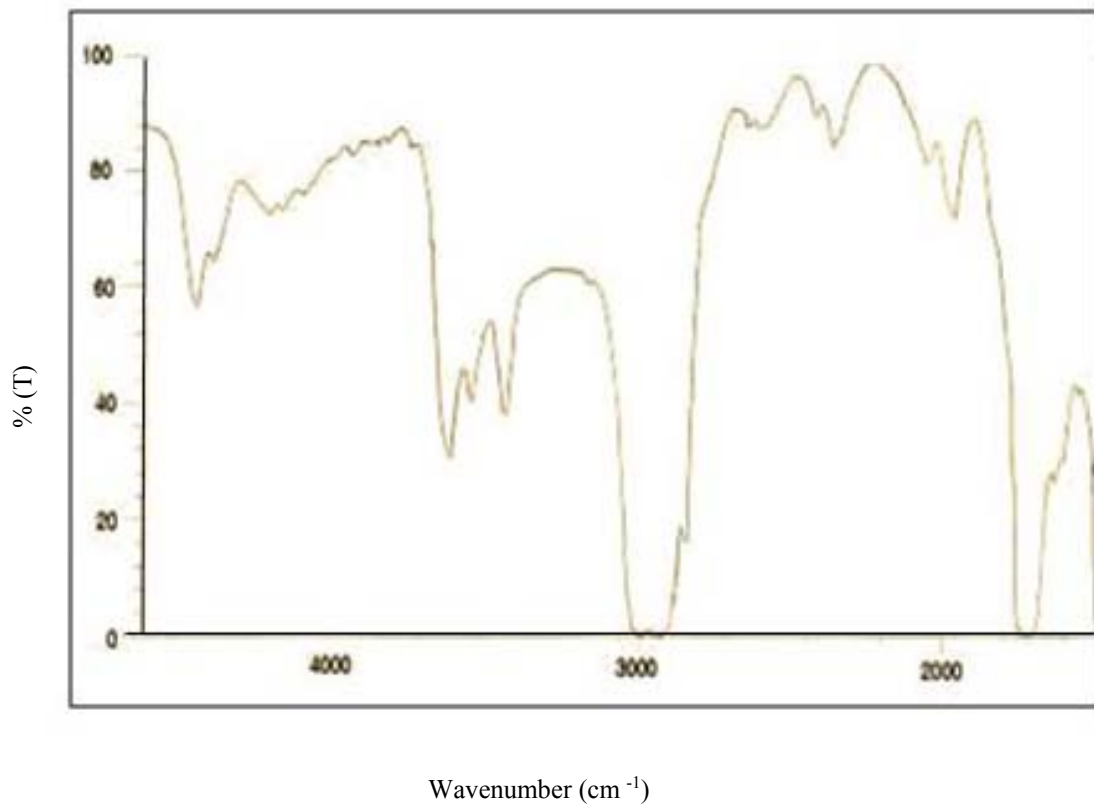


Fig.13. FTIR spectra of PMMA + clay Composite

Thermal properties

Figure 14 shows a distinctive TGA thermogram of weight loss as a function of temperature for Poly (methyl methacrylate) /clay composite. In general, major weight losses were observed in the range 230 C⁰ - 420 C⁰ for these materials, which may be due to the structure disintegration of the polymer composite. Obviously, the thermal disintegration of PMMA/Clay composite shift toward slightly high temperature than that of pure Poly (methyl methacrylate). All above confirm the enhancement of thermal stability of polymer composite. This idea is also supported by literature [110]

After 420 C⁰ the curves become flat and mainly the inorganic residue remained.

Figure 15 shows the DSC traces of PMMA/clay composite, the peak at 378.02 C⁰ shows higher degradation temperature than pristine PMMA. This is due to intercalated of polymer chains within the clay galleries that avoid the segmental motion of the polymer chains [111]

This phenomena can be interpreted as the Lewis acid base type interaction between polymer matrix and clay .Clay is natural minerals with high dielectric constant, so the silicate layer of the clay play the role of Lewis base to complex with polymer maternal. PMMA/Clay composite showed better thermal stability when compared to the pristine PMMA [107]

This result demonstrated that the resistance to thermal degradation is improved for clay content

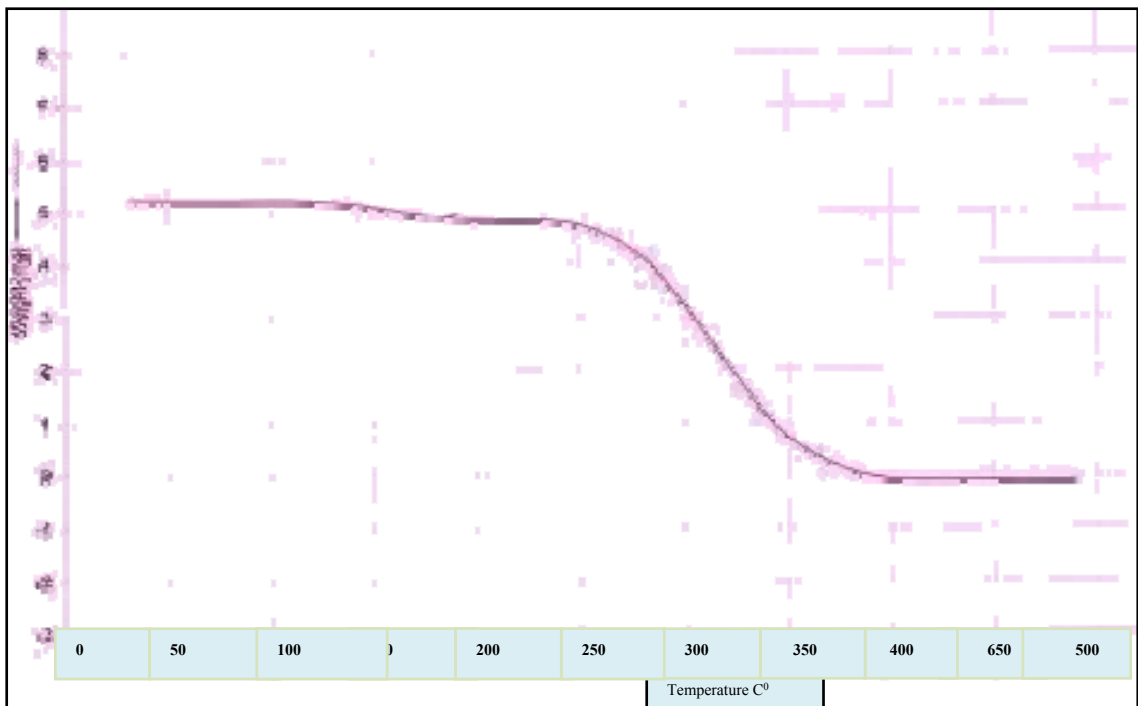


Fig.14. TGA traces for PMMA + clay Composite

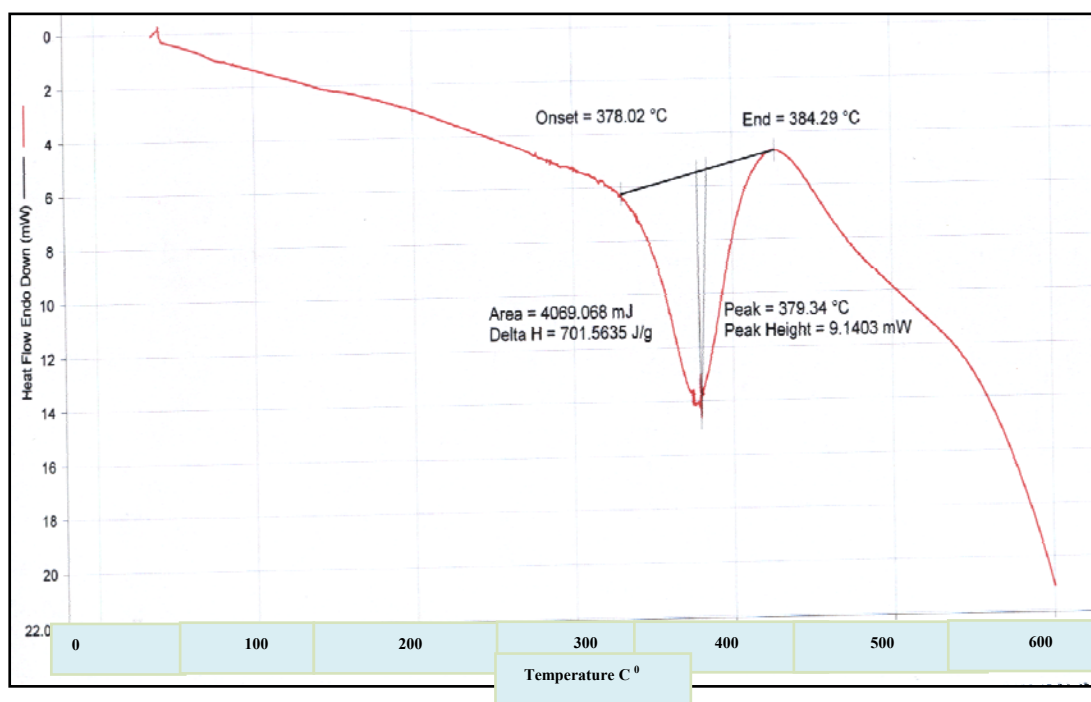


Fig.15. DSC study of PMMA+ clay composite

Mechanical properties

It is clear from the figure 16 that the tensile strength of PMMA/clay is greater than pure PMMA. This shows that the interactions of PMMA with clay network has established and have larger length before break. Because of the reinforcing of the clay particles, more strength exists in composite.

It is also reported in literatures that the young modulus of the polymer composite is found high as compare to plane PMMA [112]

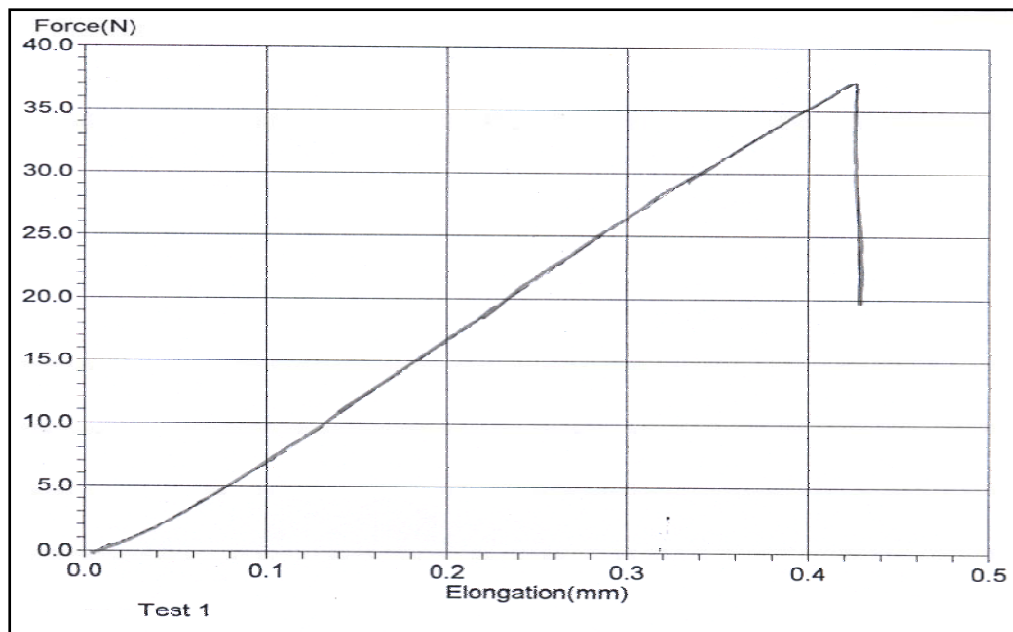


Fig.16. Tensile strength of PMMA+ clay composite

4.3. PMMA+ activated carbon composite system

Morphology

Figure 17 shows the photographs of PMMA/activated carbon composite ,the structure contains multiples pores which have the size roughly 706 nm to 60 nm .The dispersion of the carbon in the polymer matrix is very important .In this study ,we used long time stirring to enhance fine dispersion in the desired composite. The satisfactory adsorption of the Poly (methyl methacrylate) molecular chains into various pores of the carbon was also the possible factor contributing the better dispersion. For viscous solution, it may hinder the polymer chains from entering the minor pores of the carbon and as a result poor dispersion of the carbon flakes in the polymer matrix. In this study carbon particles are well mixed and evenly distributed in the polymer matrix. The presence of carbon particles in the polymer matrix is confirmed by EDX as shown in figure 18. Carbon peak is stronger and sharp in this which means that carbon is incorporated in the polymer.

Chemical structure

Figure 19 shows the FTIR spectra of PMMA/activated carbon composite. The peak at 3628 cm^{-1} could be ascribed to hydroxyl group (-OH) stretching vibration of carbon on PMMA molecule .The peak at 1725 cm^{-1} was deduced to be of C=O stretching vibration of PMMA confirms the interaction of PMMA and carbon particles.

Thermal properties

As clear from the TGA traces (Figure 20) that the thermal stability of PMMA/activated carbon is higher than the plane PMMA .The enhancement in thermal stability correlate to the limited segmental movement upon the addition of the fillers. The

results emerge consistent with the behavior of other filled polymeric composite system [113]

According to DSC curve (Figure 21) the peak at 345.40 C⁰ represent the degradation of PMMA/Activated carbon composite which shows that this composite is more thermally stabile than PMMA. It is suggested that this behavior is due to nucleation effect of the carbon particles on the polymer chain [114]

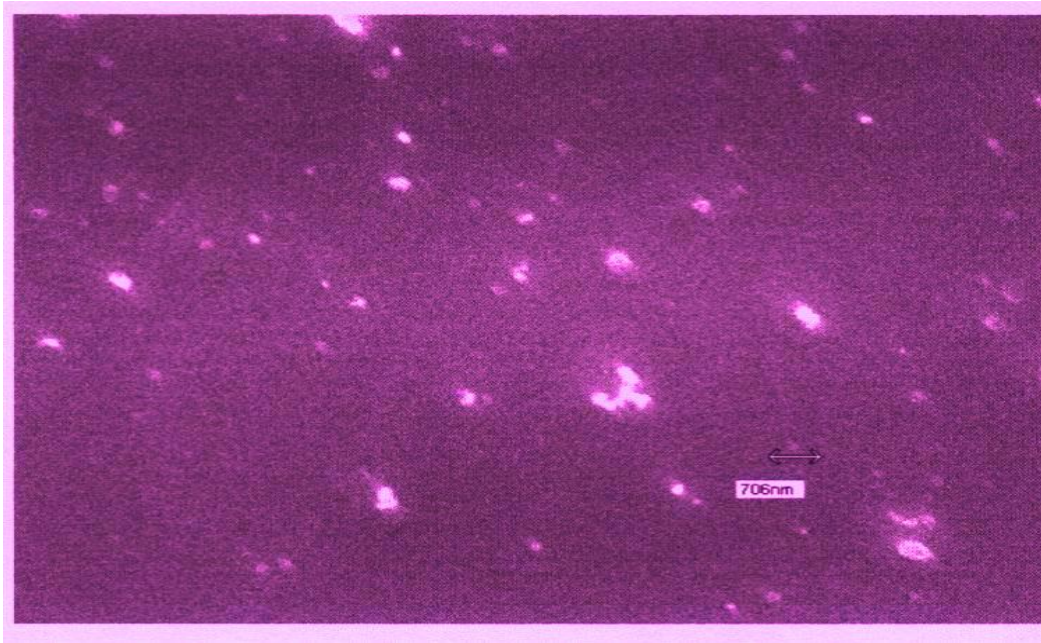


Fig.17. Scanning electron micrograph of PMMA+ activated carbon composite.

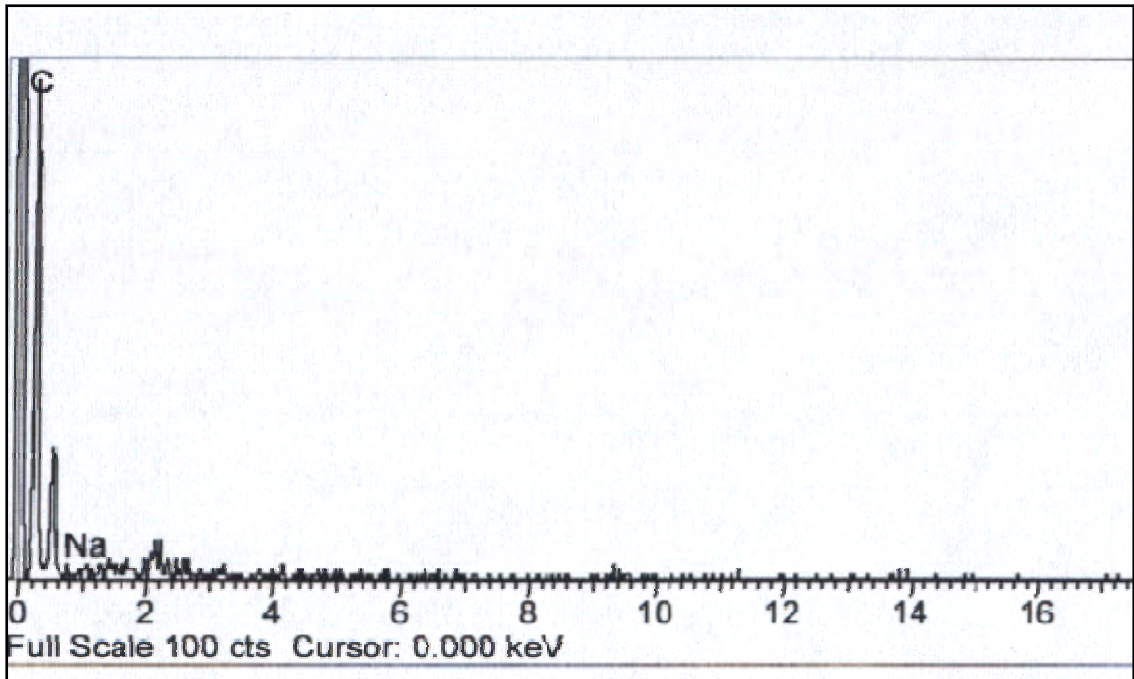


Fig.18. EDX study of PMMA + activated carbon composite

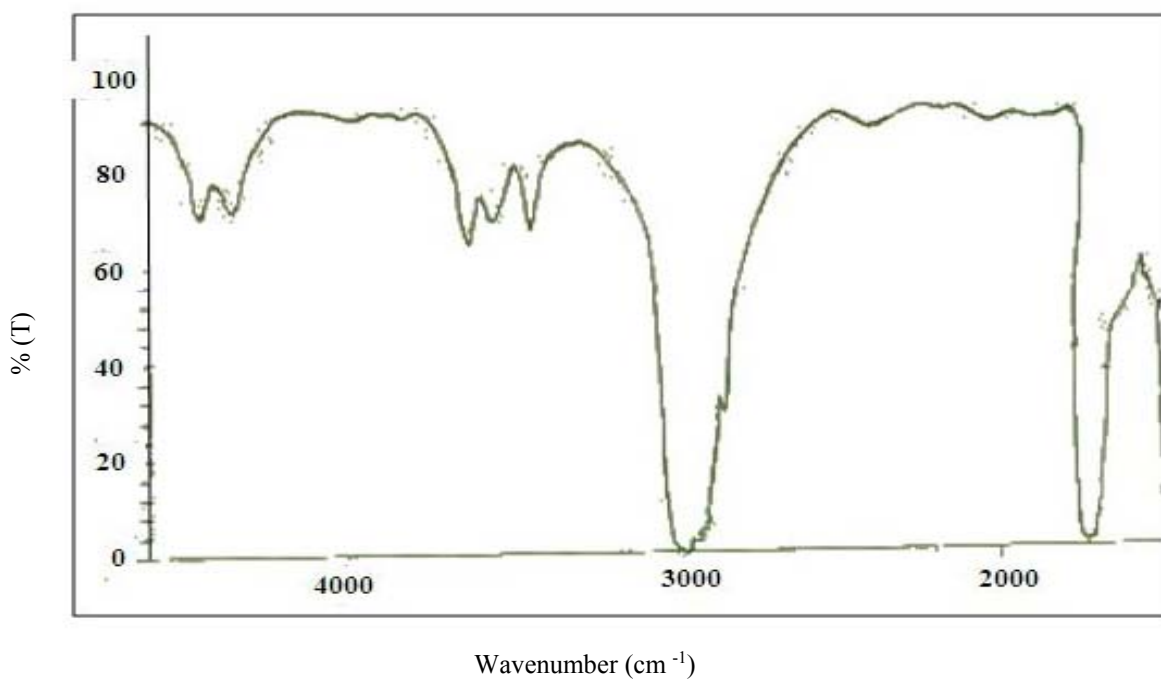


Fig.19. FTIR spectra of PMMA + activated carbon composite

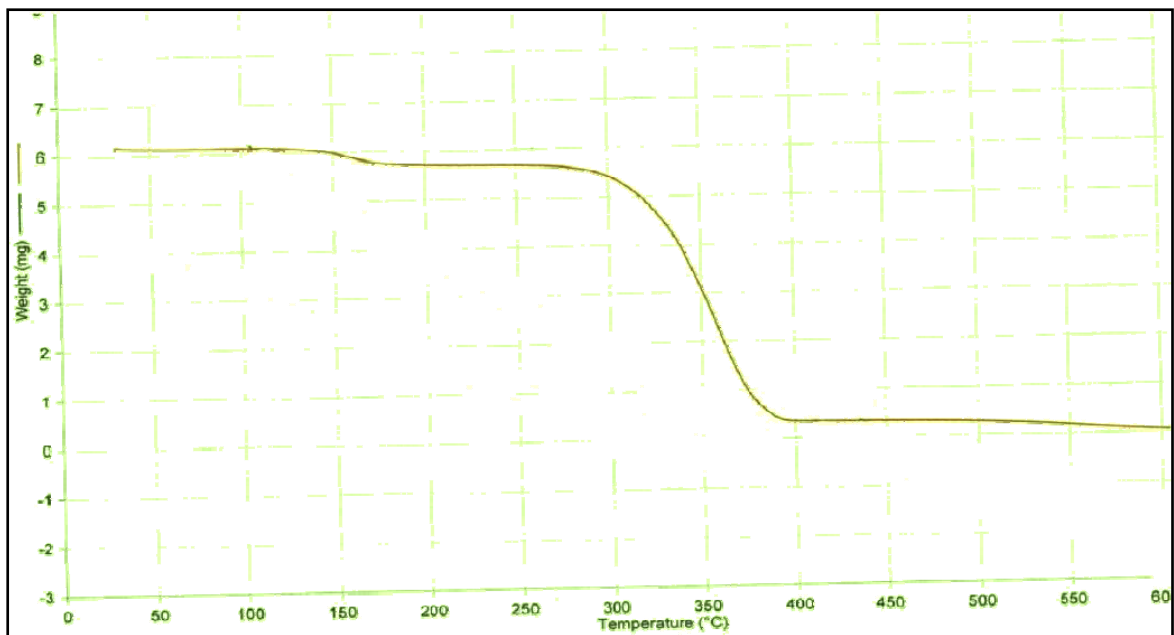


Fig.20. TGA traces for PMMA + activated carbon composite

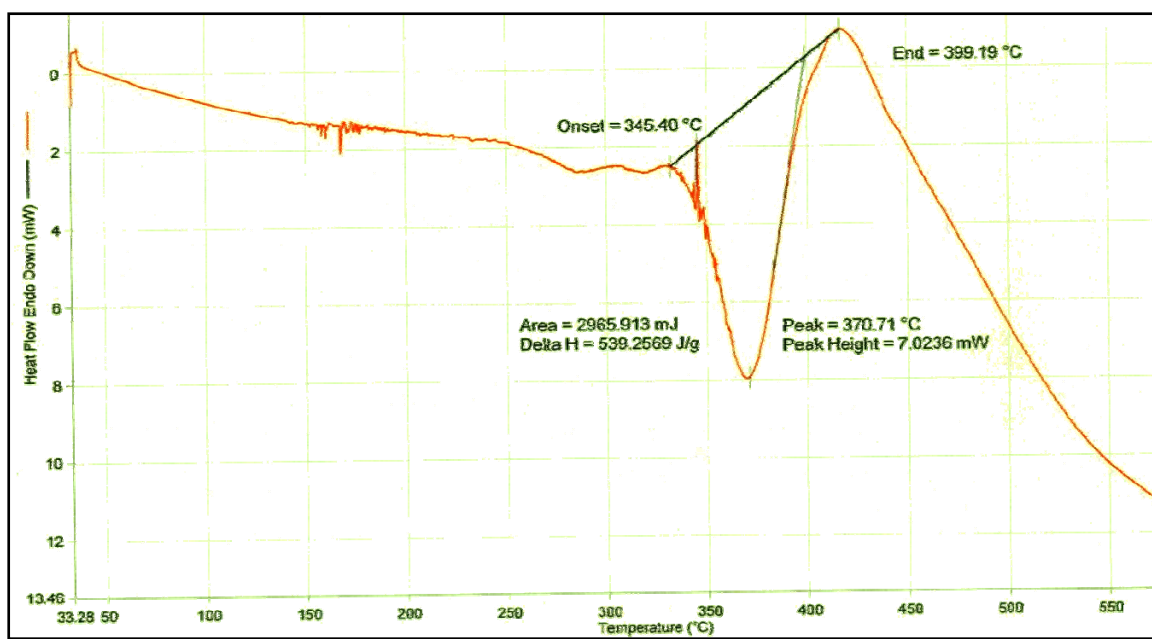


Fig.21. DSC study of PMMA+ activated carbon composite

Mechanical properties

Carbon is the most important organic filler which possesses superior electrical conductivity and elevated modulus [115]. When inorganic fillers are fine dispersed in the polymer matrix the homogenous effect lead and high performance composite were produced [116]. In simple words, for Polymer-inorganic composite, polymer chains can crystallize by themselves (due to self nucleation effect) or crystallize with inorganic fillers as nucleation agent (due to heterogeneous nucleation effect).

Our research data also show that the tensile strength of PMMA/activated carbon composite is better than plane polymer, which is illustrated in figure 22.

This result specifies that the assimilation of carbon particle into PMMA matrix has a superior reinforcing effect, which may initiate from both the rigid carbon particle and carbon-induced enlarge in the degree of crystallinity of PMMA. The composite of PMMA/carbon shows more tensile strength than pure PMMA which is consistent with some other nanocomposite [117]

In broad sense it is clear that the PMMA/carbon exhibits superior mechanical reliability in comparison with the plane PMMA.

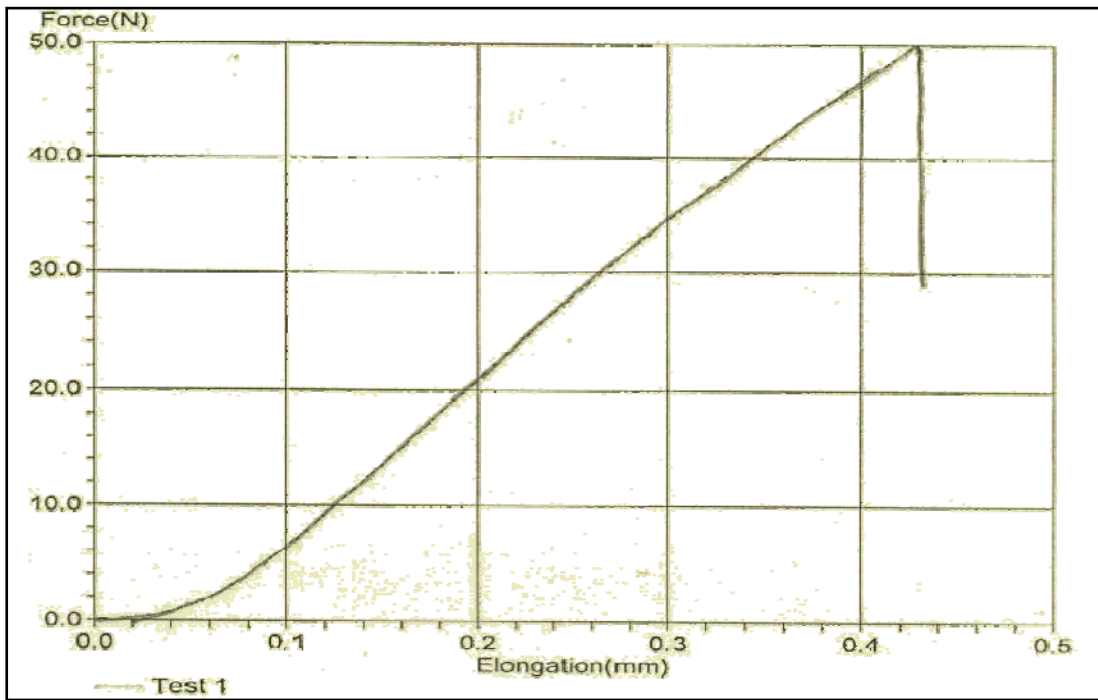


Fig.22. Tensile strength of PMMA+ activated carbon composite

4.4. PMMA+ CaCO₃ composite system

Morphology

Figure 23 shows the micrographs of PMMA/CaCO₃ composite. It can be seen from the figure that CaCO₃ are equally distributed in the polymer matrix. The size of the particles range from 1.38 micrometer to 520 nanometer. The shape of the particles is irregular but most look like some what spherical.

Chemical structure

Figure 24 shows the spectra of PMMA+ CaCO₃ composite, the change in the peak is suggest that the calcium Carbonate particles are grafted in PMMA skeleton. .The peaks at 3000 to 2900 cm⁻¹ are assigned to the stretching vibration of CH₃ of PMMA [118]

It can be seen that the peak position of C=O stretching shifts towards low wave number i.e from 1729.5 cm⁻¹ to 1725.2 cm⁻¹, indicating interaction between Ca⁺ with carbonyl group of PMMA. It indicated that the interaction between C=O of PMMA and Ca⁺ of CaCO₃ particles. The Ca⁺ particle bearing +ve charge is attracted by oxygen of C=O in PMMA skeleton. Due to this attraction the peak position shifts towards lower wave number.

Thermal properties

Figure 25 illustrated thermo gravimetric analysis of PMMA/ CaCO₃ composite. From this traces it is clear that this polymer composite is again thermally stable than pure PMMA. The main weight loss is due to the breakdown of polymer in the composite.

Peak at 360.08 C⁰, as illustrated in figure 26, confirmed the high degradation temperature of PMMA/ CaCO₃ composite than pristine PMMA.

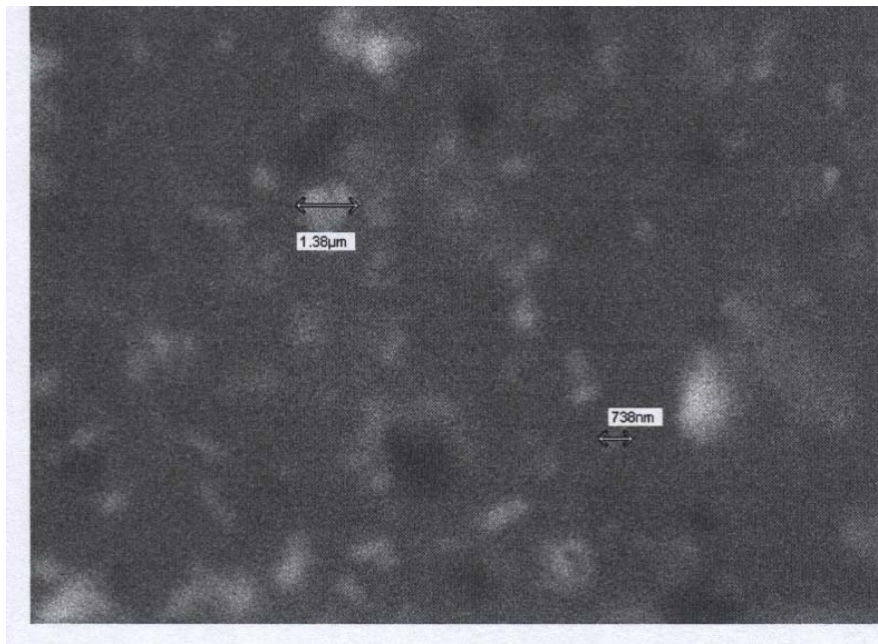


Fig.23. Scanning electron micrograph of PMMA+ CaCO₃ composite

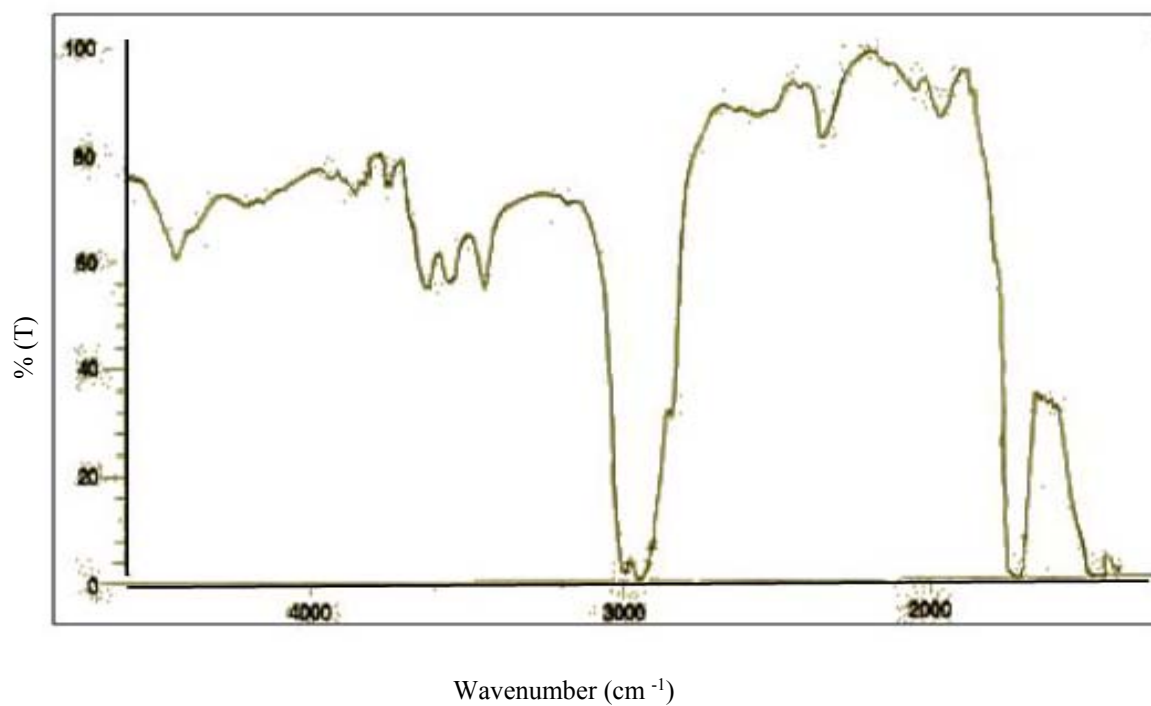


Fig.24. FTIR spectra of PMMA + CaCO₃ composite

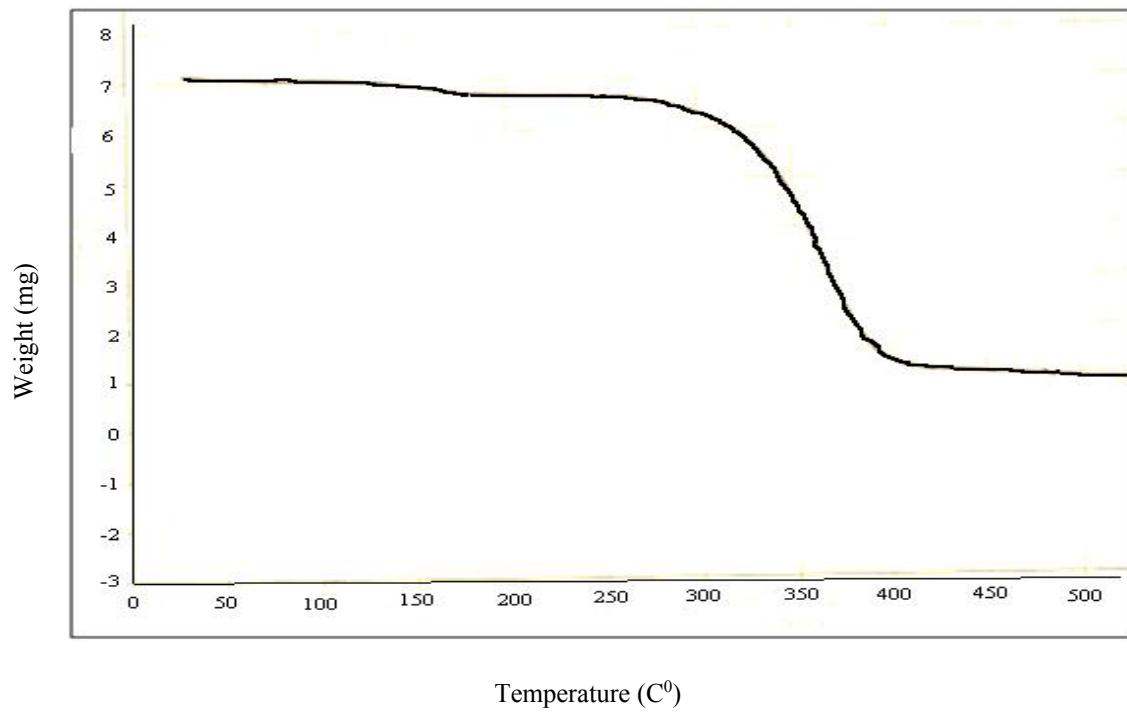


Fig.25. TGA traces for PMMA+ CaCO₃ composite

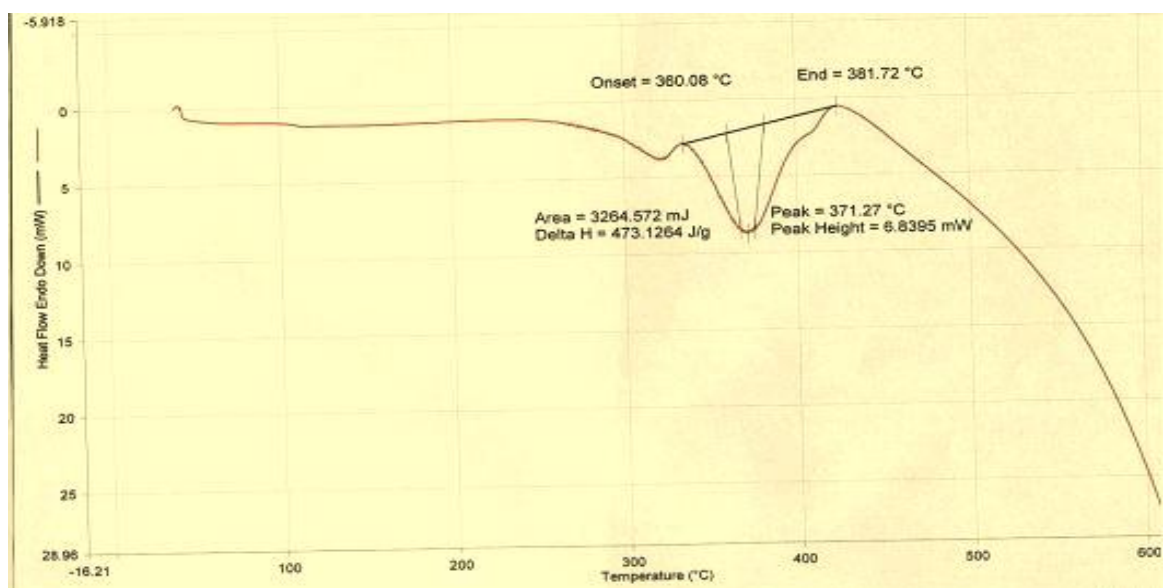


Fig.26. DSC study of PMMA+ CaCO₃ composite

Mechanical properties

Figure 27 shows that the tensile strength of PMMA/CaCO₃ is high than plain PMMA. It is due to chemical bond between carbon atoms of CaCO₃ and PMMA. Calcium carbonate is electrovalent bonded compound. The CO₃²⁻ is covalent radical which contains C=O double bond. The increasing polymer chains react with C=O double bond to generate more stable radicals, which grafted on the surface of calcium carbonate. The remain radicals and monomers chains are adsorbed simply on the surface of CaCO₃, as a result more polymerize and enfold on the surface of CaCO₃.

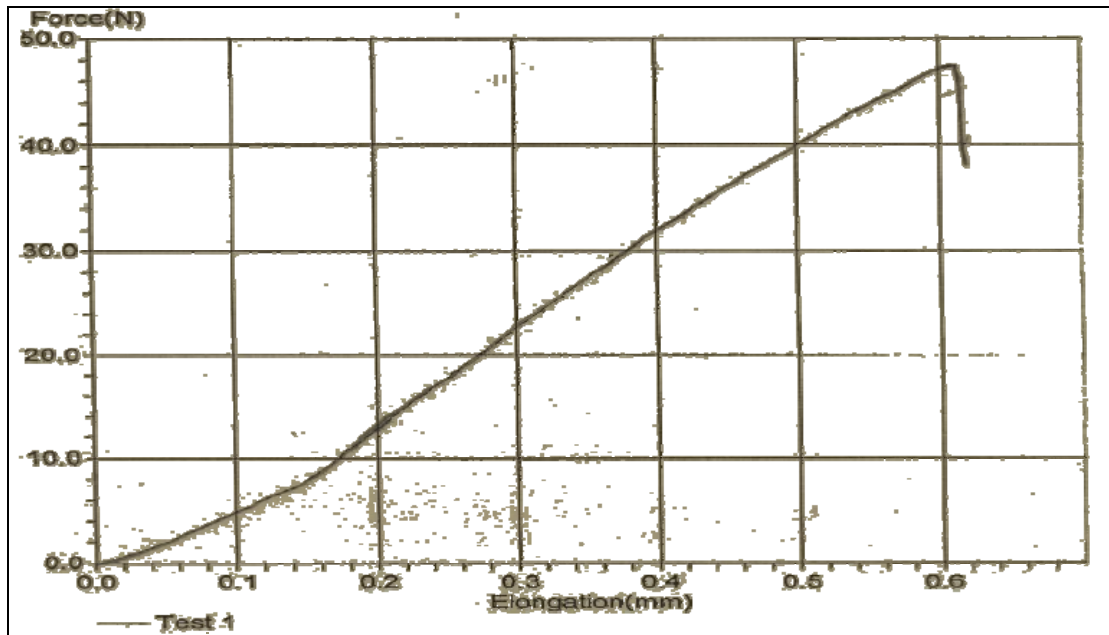


Fig.27. Tensile strength of PMMA+ CaCO₃ composite

4.5. PMMA+ SiO₂ composite system

Morphology

The SiO₂ particles are clearly visible in the figure 28. The micrograph shows cavities and particles. The size of cavities is bigger than particles. The particles are embedded in between the cavities (black in color in micrograph) or we can see that the particles are present in the inter cavities space. The size of SiO₂ particles vary with 738 nm particles of lowest size. The bigger particles of 1.38 micrometer are also visible. The whole picture shows that the dispersion of SiO₂ particles is attained.

EDX spectrum showed the characteristics peaks of oxygen, carbon and silicon which are presented in figure 29.

Chemical structure

FTIR spectra of PMMA/SiO₂ are shown in Figure 30. A small band at 3735 cm⁻¹ is represents the pure silica which is O-H stretching of the hydroxyl groups covering the surface of silica. When the silica is mixed with polymer the maximum of the O-H stretching bands shift to around 3619 cm⁻¹. This specify that hydroxyl group on silica surface are implicated in bond interaction.

The peak position for the C=O stretching was also shifted toward lower wave number i.e from 1729.5 cm⁻¹ to 1725.2 cm⁻¹ again confirming the interaction of silica particles.

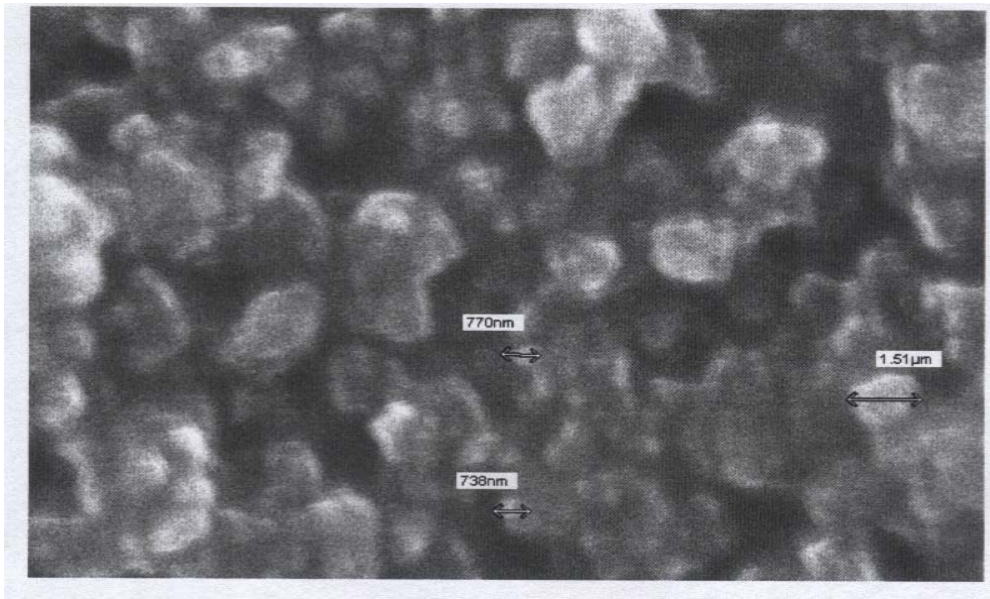


Fig. 28. scanning electron micrograph of PMMA+ SiO₂ composite

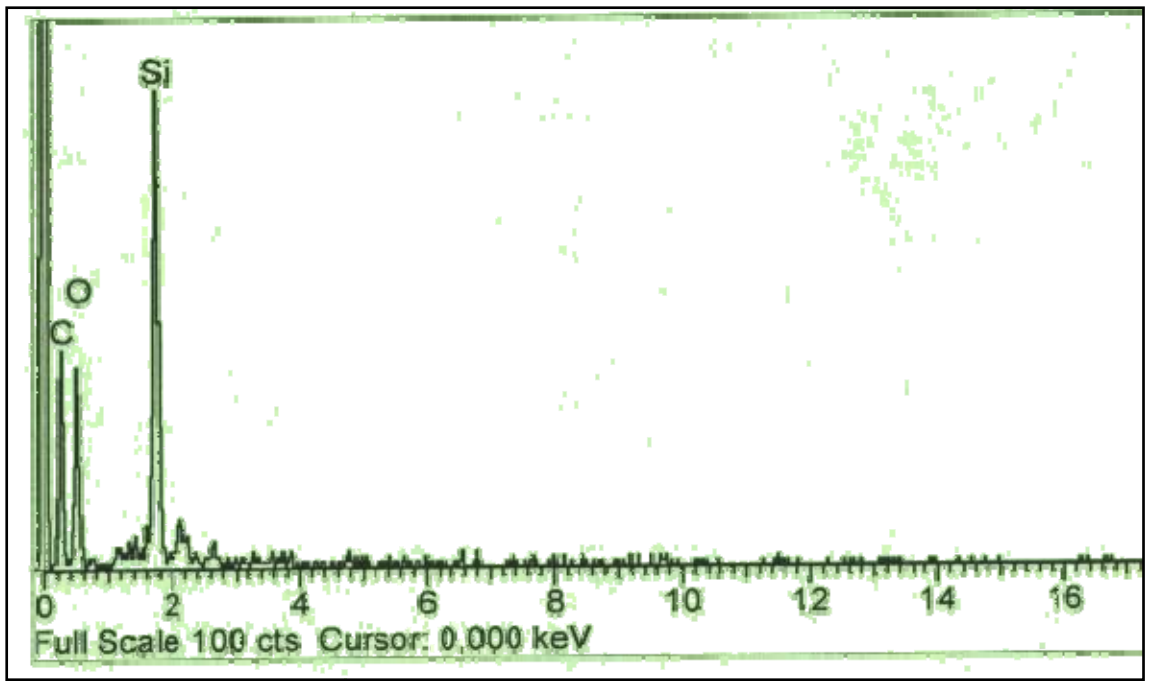


Fig.29. EDX study of PMMA + SiO₂ composite

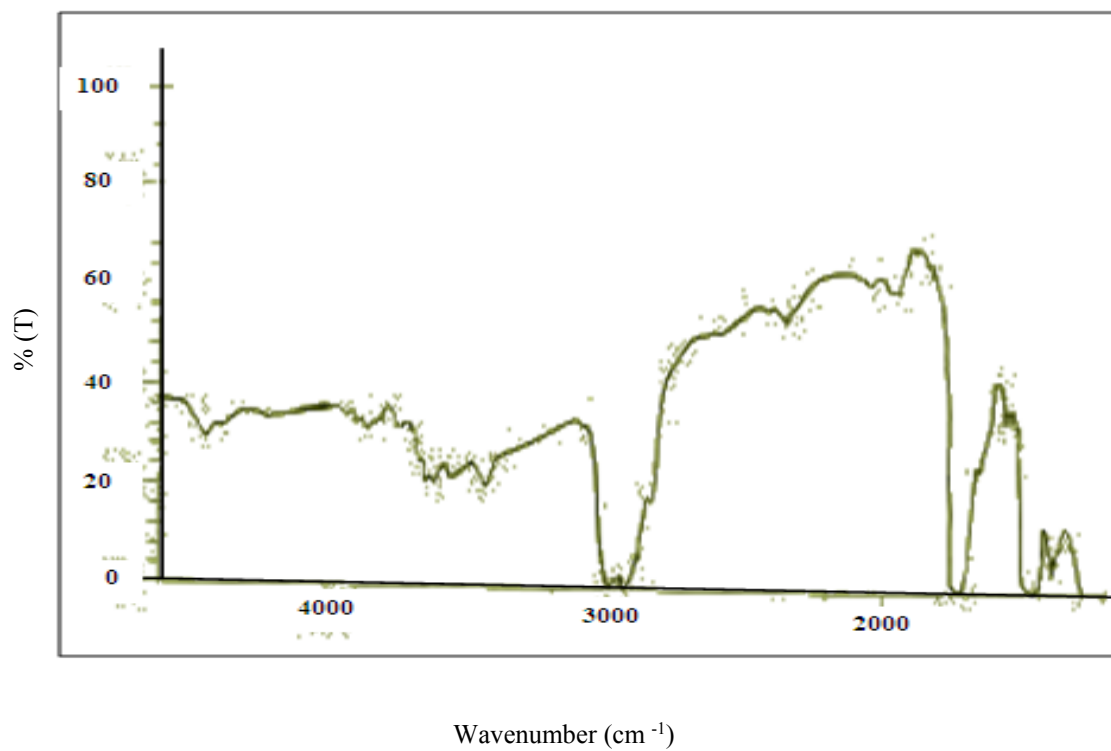


Fig.30. FTIR spectra of PMMA + SiO₂ composite

Thermal properties

Thermo gravimetric analysis PMMA/SiO₂ composite are shown in figure 31, which illustrated that composite is more thermally stable than pristine PMMA. It is suggested that the particles are well soaked by the Poly (methyl methacrylate), representing a very fine adhesion between the fillers and the polymer matrix. This good adhesion lead to important interaction between the Poly (methyl methacrylate) and particles surface which may be interpreted into an intimate contact between the substrate and polymer chains. This result should cause a reduction in the mobility of the PMMA macromolecule near the silica surface and one might consider thermal relaxation due to this explanation [119].

The strong interaction limiting the movements of the polymer chain segments is due to the increased stiff structure of the polymer. Resonance structure in the system can also enhance thermal stability of the system. By increasing inorganic silica content the T_{gs} of hybrid membranes also increased. It is concluded that content of SiO₂ is key factor manipulating the compatibility of the polymer chains and the inorganic Silicon dioxide network.

DSC technique was used for measuring glass transition temperatures of these composites. Figure 32 shows that the endothermic peak at 346.66 C⁰ correspond to the degradation of the composite which is more thermally stable than PMMA, which specify that the thermal properties of the polymer improve by incorporation of minerals. It is due to presences of strong interaction (hydrogen bonding) between the polymer matrix and silicates net work [120]

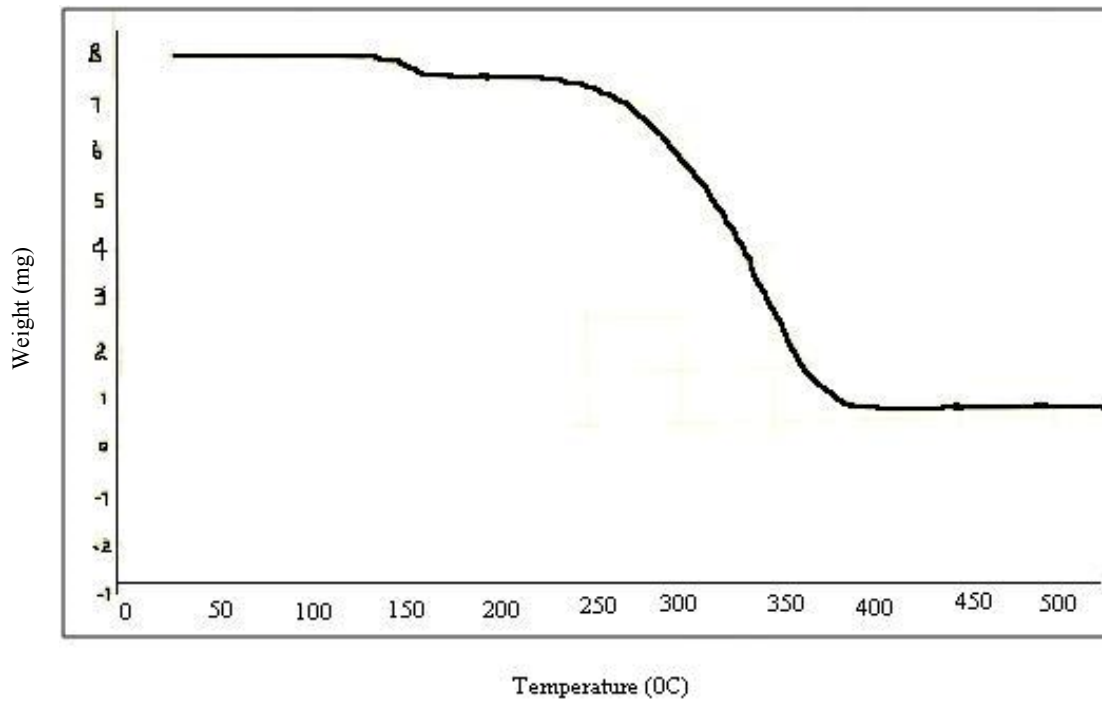
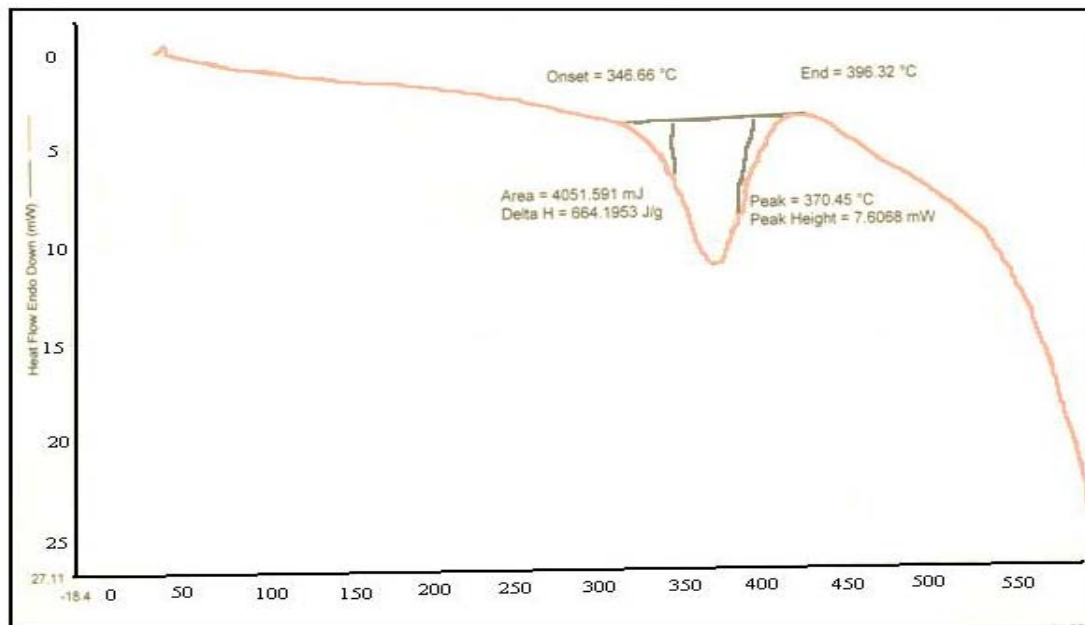


Fig.31. TGA traces for PMMA+SiO₂ composite



Temperature (C°)

Fig.32. DSC study of PMMA+ SiO₂ composite

Mechanical properties

The tensile strength of PMMA/SiO₂ is high as compare to neat PMMA as shown in figure 33, the possible explanation for this is that the adhesion between the polymer and filler is very good .This very good adhesion should ensure an important interaction between Poly (methyl methacrylate) and SiO₂ particles which is a key factor for the better tensile strength.

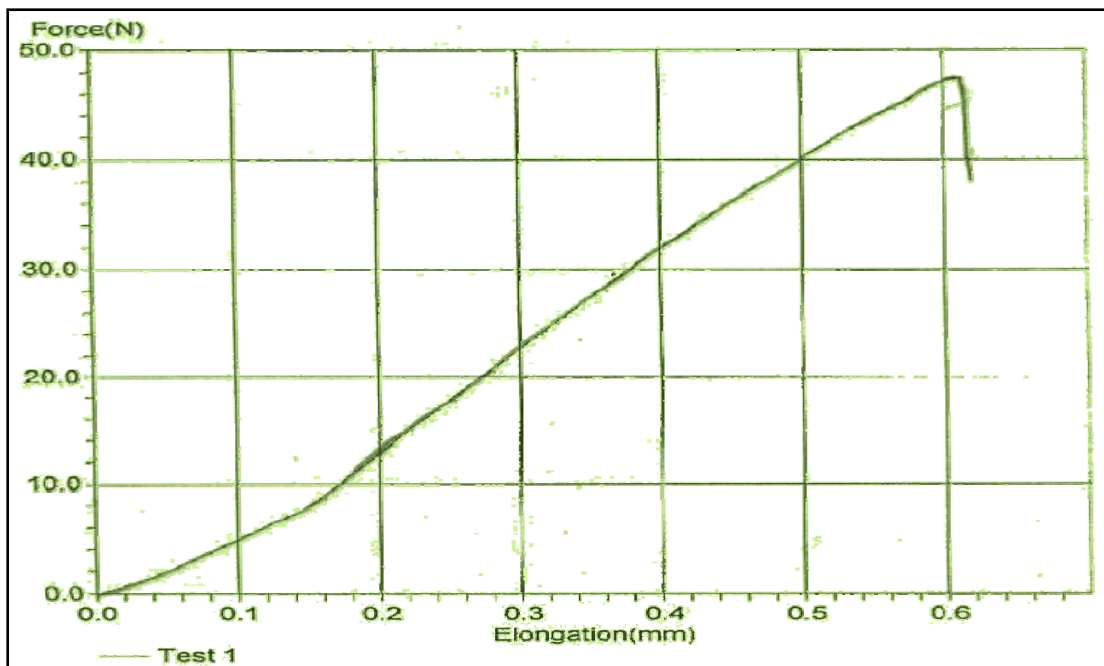


Fig.33. Tensile strength of PMMA+ SiO₂ composite

4.6. PMMA+ ceramics composite system

Morphology

Figure 34 shows SEM morphology of PMMA+ ceramics composite. The SEM image shows that ceramics particles have an average diameter in range of 250 nm to 6.67 μm and uniformly distributed in polymer matrix. The interface between ceramics particles and PMMA matrix is more adhesive. These results indicates that the PMMA covered the surface of ceramics particles enhances the interaction between ceramics particles and PMMA which improve the adhesion and morphologic structure of PMMA/ceramics composite. The particles seem to be mixed homogenously in the polymer matrix.

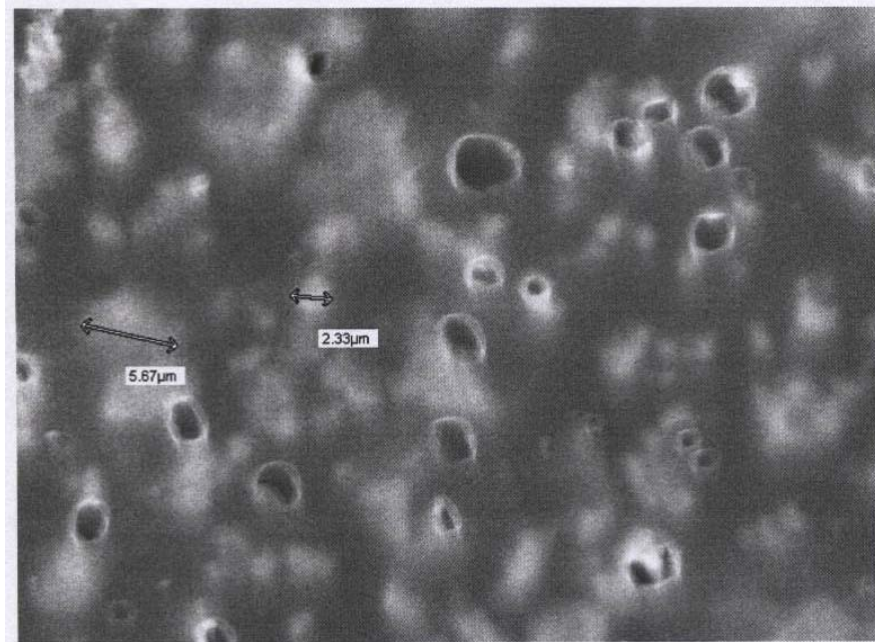


Fig.34. Scanning electron micrograph of PMMA+ ceramics composite

Chemical structure

The FTIR spectrum of the PMMA/ceramics composite is presented in figure 35. The broad peak on 1729 cm^{-1} for C=O shifts towards lower wave number i.e 1725 cm^{-1} indicating the interaction between the ceramics particles and carbonyl group of PMMA. The ceramics as all know may contain various elements but major among these is Al and Ti cations. If the ceramics is layered in structure (as we have used) each layer may contain numerous -ve and +ve charges which may form dipoles. When ceramics is well dispersed, it means that there are numerous well distribute dipoles in the environment. From our SEM photograph ceramics is well dispersed in polymer matrix this means that the +ve site can interact with C=O group of pure PMMA, which results in a red shift to the absorption peak.

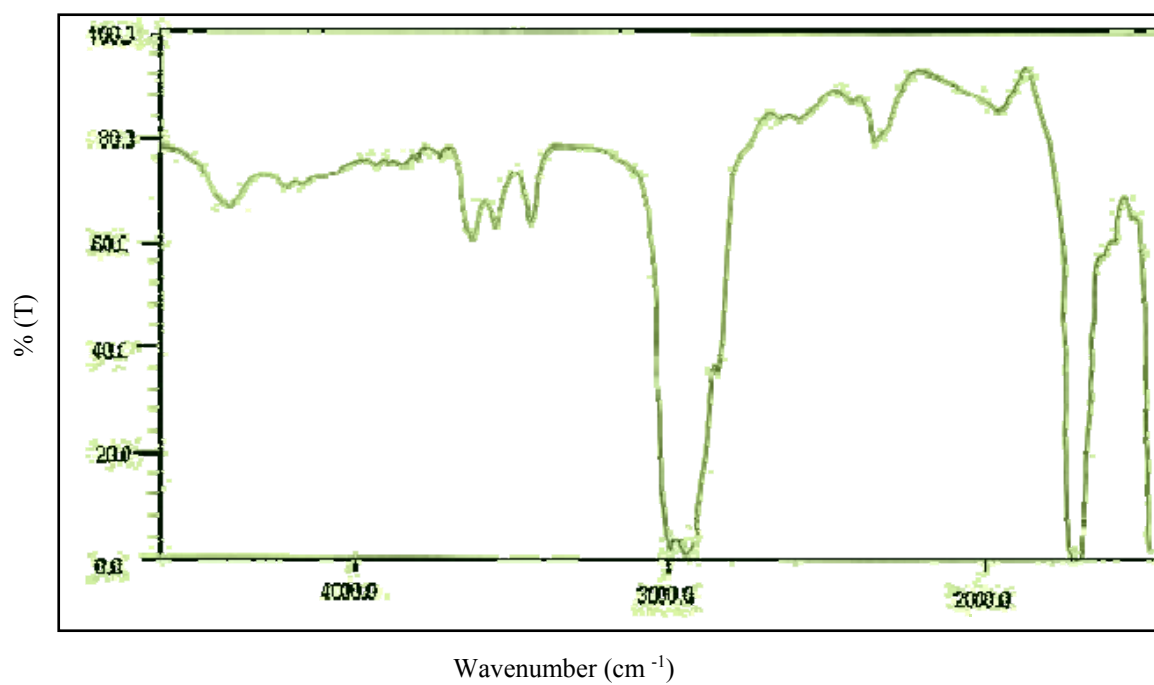


Fig.35. FTIR spectra of PMMA + ceramics composite

Thermal properties

TGA is widely used for the determination of composition of organic/inorganic hybrid particles. Figure 36 shows the thermal analysis (TG) curve of the Poly (methyl methacrylate)/ceramics composite. The TG curve could be divided in two main stages during the weight loss process of the composite. The first stage is due to the pyrolysis of the polymer Poly (methyl methacrylate) in the composite. The second stage is corresponding to the dissociation of the hydroxyl groups from the surface of TiO₂ particles. It is well known that there are two types of surface OH groups, terminal Ti-OH and bridge Ti-OH-Ti. This interaction improved the stability of the final Poly (methyl methacrylate)/ceramics composite. It is also suggested that the improvement of the thermal stability of the composite is interpreted by the ceramics components inducing a protective barrier against thermal degradation for organic species.

DSC study of the above systems shows same thermal stability which are illustrated in figure 37. The major peak appearing in the DSC in figure 37 is at 443.58 C⁰ which is endothermic peak showing higher thermal stability than pure PMA, which indicates that the mobility of the polymer chains are restrained by the addition of ceramics particles. From the DSC analysis it is confirmed that the Poly (methyl methacrylate) /ceramics composite is more thermally stable as compare to plane PMMA.

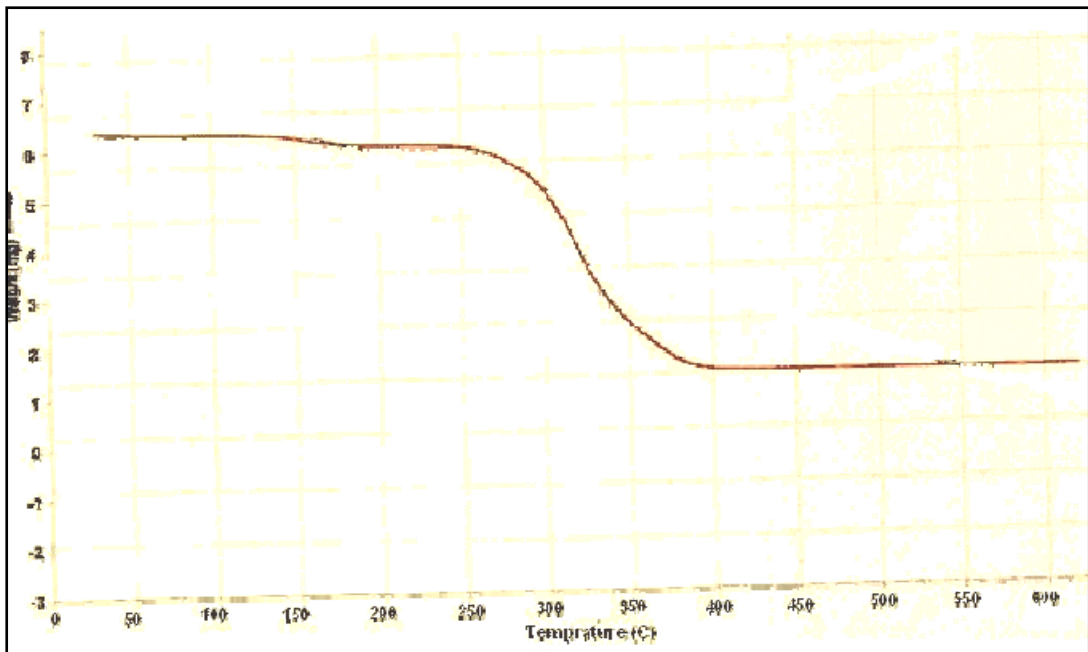


Fig.36. TGA traces for PMMA + ceramics composite

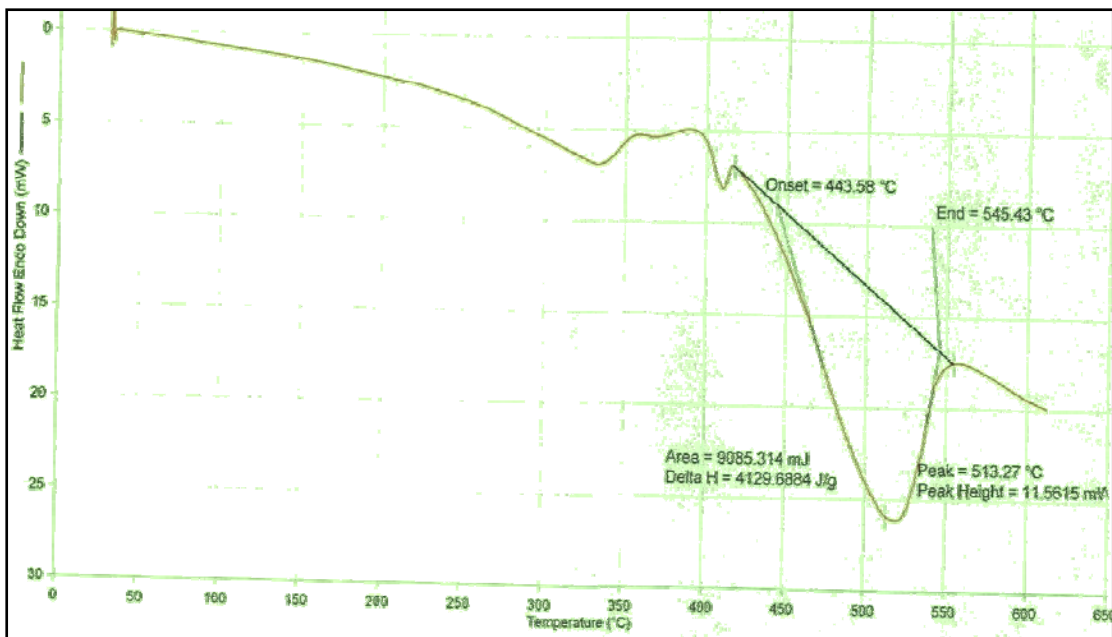


Fig.37. DSC study of PMMA+ ceramics composite

Mechanical properties

The tensile strength and elongation at break for PMMA/ceramics are shown in figure 38. The tensile strength and elongation at break both are enhanced greatly due to ceramics filling. The enhancement of mechanical properties of composite is due to bonding between organic polymer and inorganic ceramics particles and the aggregation of ceramics particles in polymer matrix. Moreover, PMMA can effectively improved the dispersion of ceramics particles in polymer matrix, this factor also lead to increase the tensile strength and elongation at break of composite.

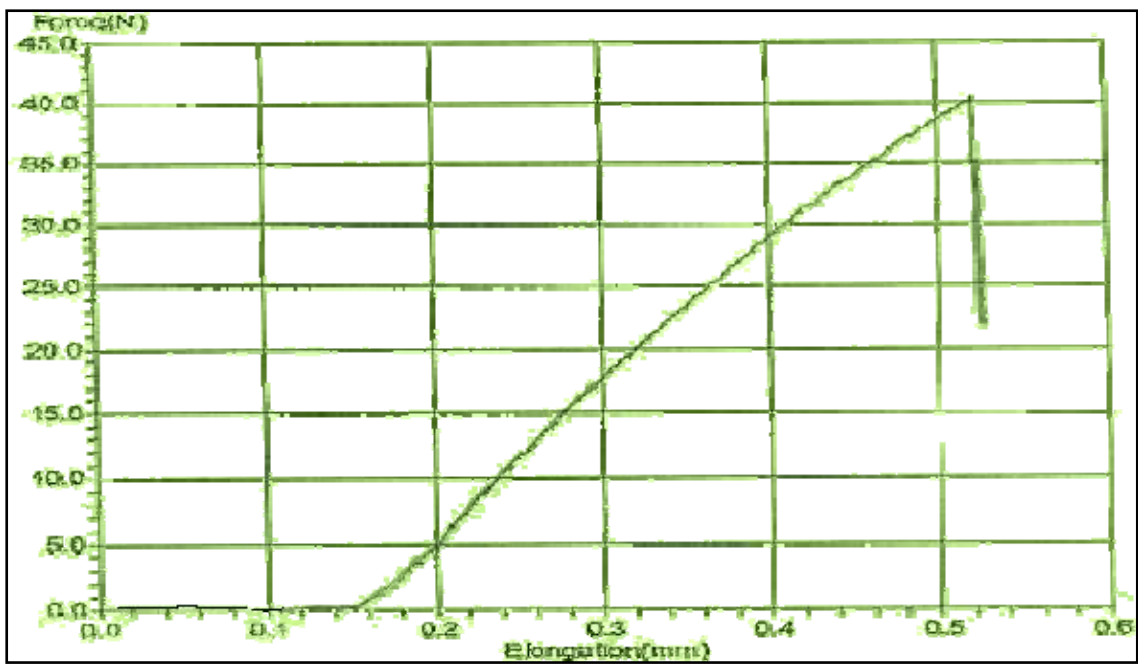


Fig.38. Tensile strength of PMMA+ ceramics composite

4.7. PMMA+ glass composite system

Morphology

Figure 39 demonstrated poly (methyl methacrylate) / glass composite system. From the image the filler particles appears black or dark gray. The white spots present the area where polymer layer is very thin or has holes. It can be seen that the glass particles are fairly well dispersed in the polymer matrix. Figure 39 shows that the average diameters of glass particles are in range of 80 nm to 850 nm. It can be seen from the photograph of PMMA/glass composite that the particles are separated from each other or touch one or two other particles.

Chemical structure

Figure 40 shows the spectra of PMMA- glass composite. It can be seen from the spectra that there is a very pronounced band appearing at 1726 cm^{-1} indicating the interaction of glass particles with C=O group in poly(methyl methacrylate)skeleton. It can be seen that the peak position of C=O stretching shifts towards low wave number i.e from 1729.5 to 1726 cm^{-1} the change in the peak is suggest that the glass particles are grafted in PMMA skeleton. The peaks at 3000 to 2900 cm^{-1} are assigned to the stretching vibration of CH_3 of PMMA. In the spectrum of PMMA-glass there are peaks at 2952 , 1732 , 1439 cm^{-1} , which are assigned to CH, C=O and CH_3 stretching vibration of poly(methyl methacrylate) respectively. These spectra indicate that poly (methyl methacrylate) has been grafted onto the surface of glass particles.

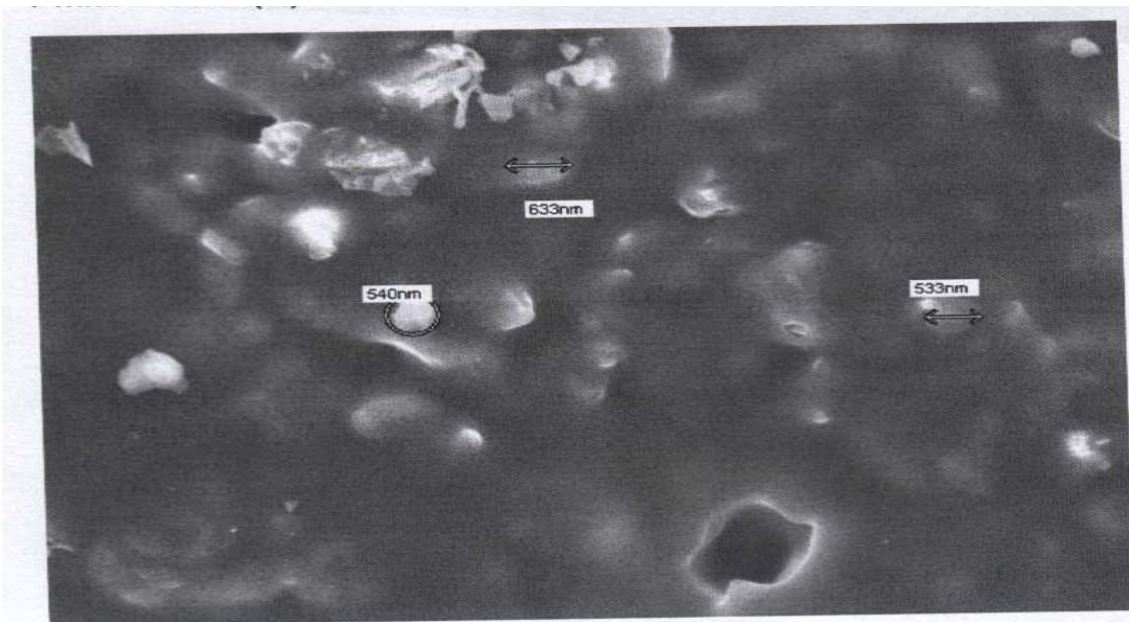


Fig.39. Scanning electron micrograph of PMMA + glass composite

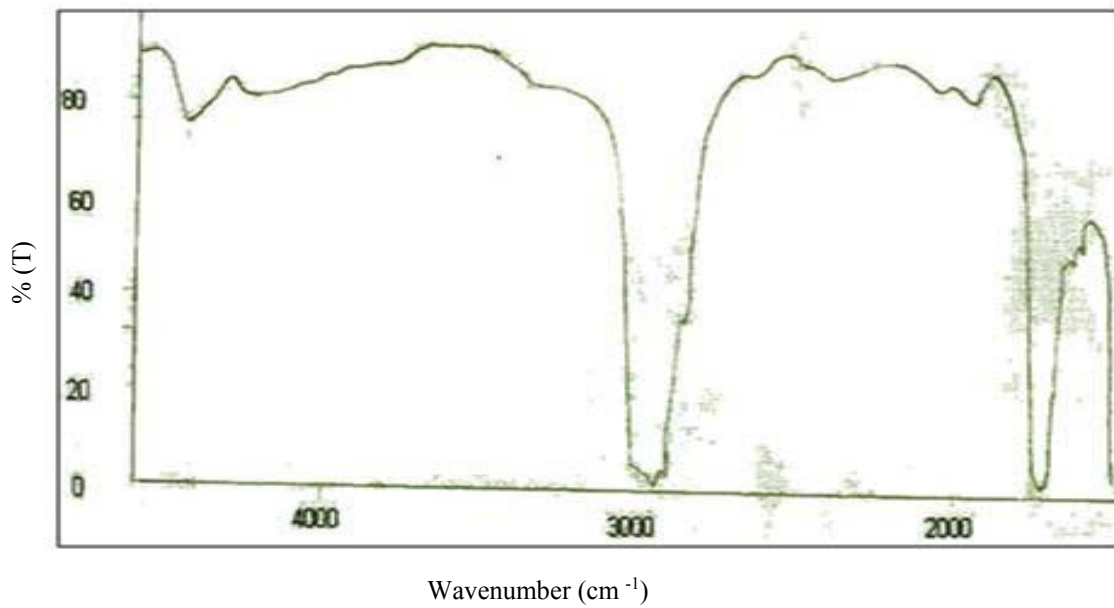


Fig.40. FTIR spectra of PMMA + glass composite

Thermal properties

The thermal stability of PMMA-glass composites were evaluated by thermogravimetric analysis. According to literature, the stability limit in the thermogravimetric analysis (TGA) was set to 10 % weight loss compared to the initial sample weight. According to Figure 41 the PMMA/glass composite showed an increase in the degradation temperature i.e 350 C⁰ to 452 C⁰. This behavior suggests a random scission of the main chains as the prevailing degradation reaction .The reason for the absence of any degradation at lower temperature will be the stabilization of commercial Poly (methyl methacrylate). It can be explained by the interaction between filler and polymer matrix. Hydrogen bonding and grafting of the Poly (methyl methacrylate) molecules onto the surface of the glass particles lead to decrease of the mobility chains and therefore scission of the polymer chains is inhibited .The Si – O – Si functional group may inhibit the thermal degradation of polymer matrix. Stabilization of the degradation products by the glass particles surface is also possible.

The DSC plot shown in figure 42 acquired for PMMA/glass composite. From this data ,it is observed that the peak at 513.27 C⁰ shows high thermal degradation of polymeric composite as compared to pure PMMA(337.49 C⁰). These indicating the mobility of the polymer chains are restrained by the addition of glass particles. It is suggested that the decrease in Tg is due to enhanced motion of the polymer segments. As the temperature increase the density of the film decreases which enhanced the mobility of polymer segments.

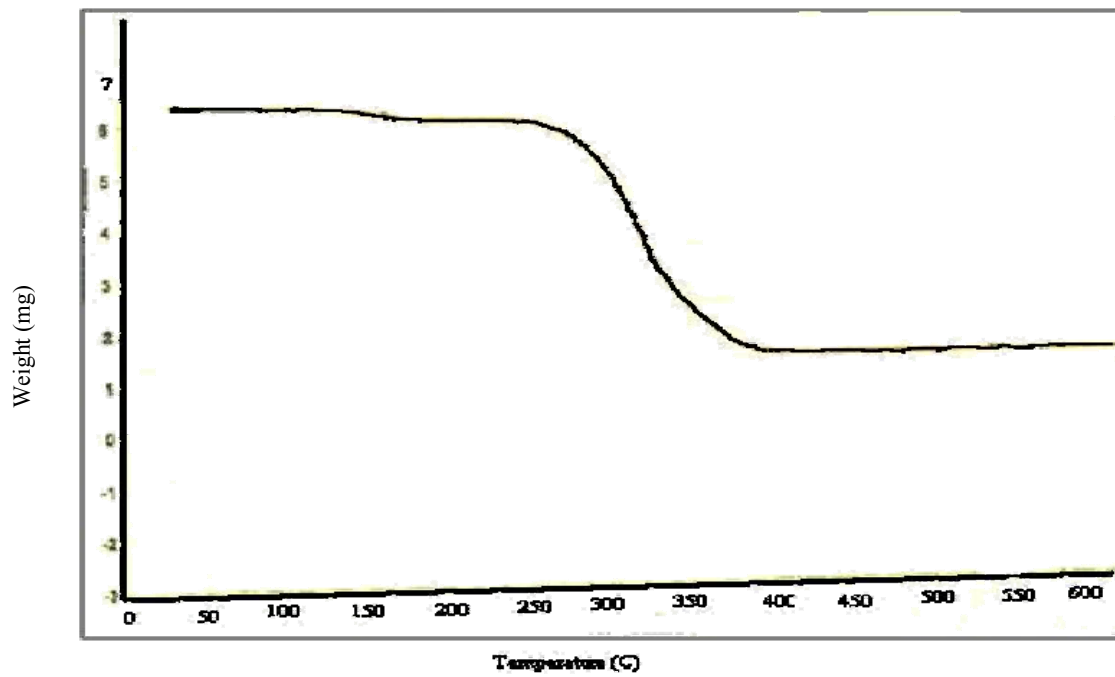


Fig.41. TGA traces for PMMA+ glass composite

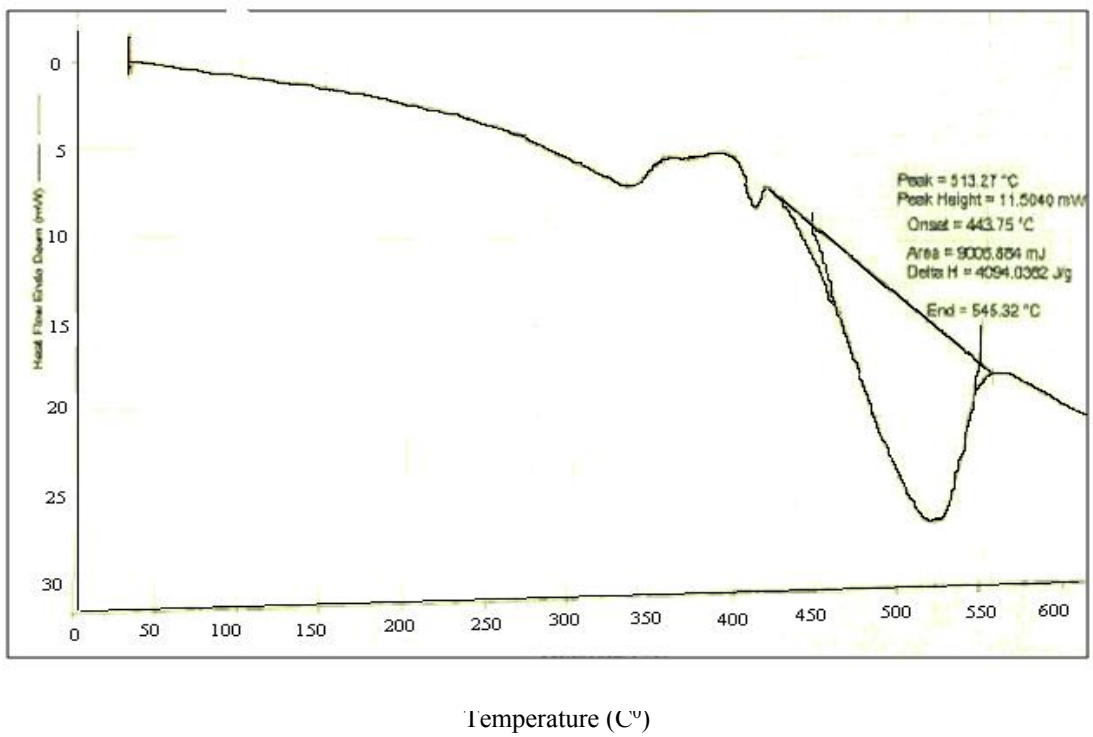


Fig.42. DSC study of PMMA+ glass composite

Mechanical properties

Many aircraft components are made from PMMA or polycarbonates rather than glass because they are lighter. However, the mechanical strength of PMMA and polycarbonates is not sufficient. While glass reinforced composites provide the mechanical properties needed for company requirements. Figure 43 shows that the tensile strength of PMMA/glass is high than plain PMMA. This is due to grafting of the polymer chains to glass particles it is reasonable to assume that an interphase is formed around the glass particles, whereby the segmental motions of the macromolecular chains are restricted. Grafting of PMMA molecule onto the glass particles surface is the most probable mechanism for the increase in tensile strength of the composite.

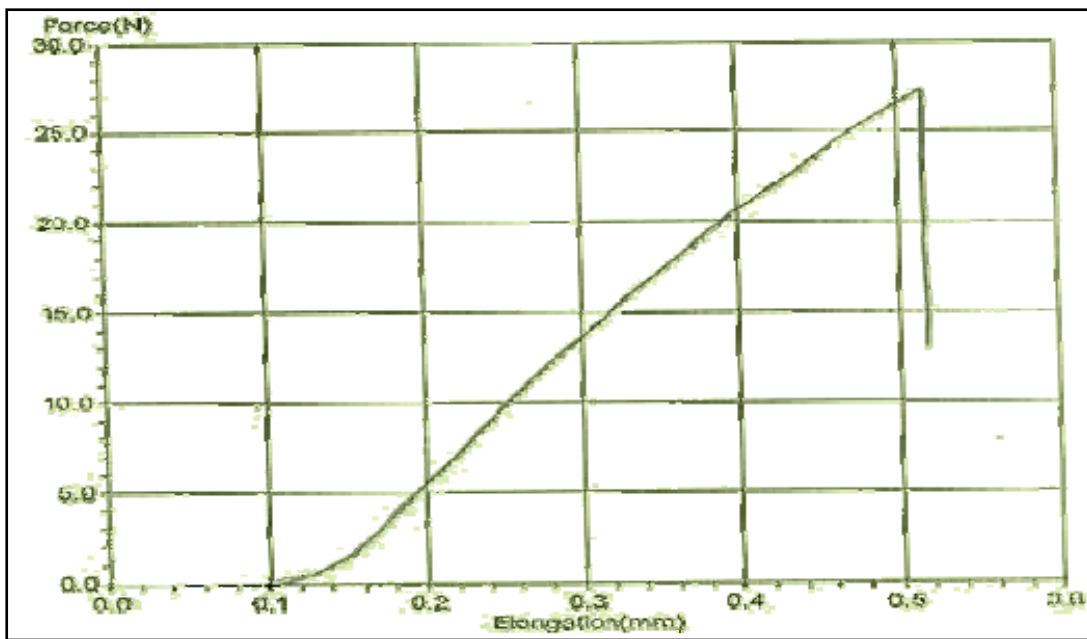


Fig.43. Tensile strength of PMMA+ glass composite

COMPARISON OF THE STUDIED
COMPOSITE SYSTEM

Thermal properties

Figure 44 illustrate that the thermal stability of PMMA/glass composite is higher than all studied system. It can be explained by the interaction between filler and polymer matrix. Hydrogen bonding and grafting of the Poly (methyl methacrylate) molecules onto the surface of the glass particles lead to decrease of the mobility chains and therefore scission of the polymer chains is inhabited. The Si – O – Si functional group may inhabit the thermal degradation of polymer matrix. Stabilization of the degradation products by the glass particles surface is also possible. The order of increasing thermal stability of various composite systems is:

PMMA < PMMA-activated carbon < PMMA-SiO₂ < PMMA-Na₂SO₄ <
PMMA –CaCO₃ < PMMA- clay < PMMA-ceramics < PMMA-glass

S.No.	Systems	Peak(C ⁰)
1	Pure PMMA	337.49
2	PMMA/Na ₂ SO ₄ composite	350.09
3	PMMA/ clay composite	378.02
4	PMMA/ activated carbon composite	345.40
5	PMMA/ CaCO ₃ composite	360.08
6	PMMA/ SiO ₂ composite	346.66
7	PMMA/ ceramics composite	443.58
8	PMMA/ glass composite	513.27

Table.2. Comparison of thermal stability of various composites system

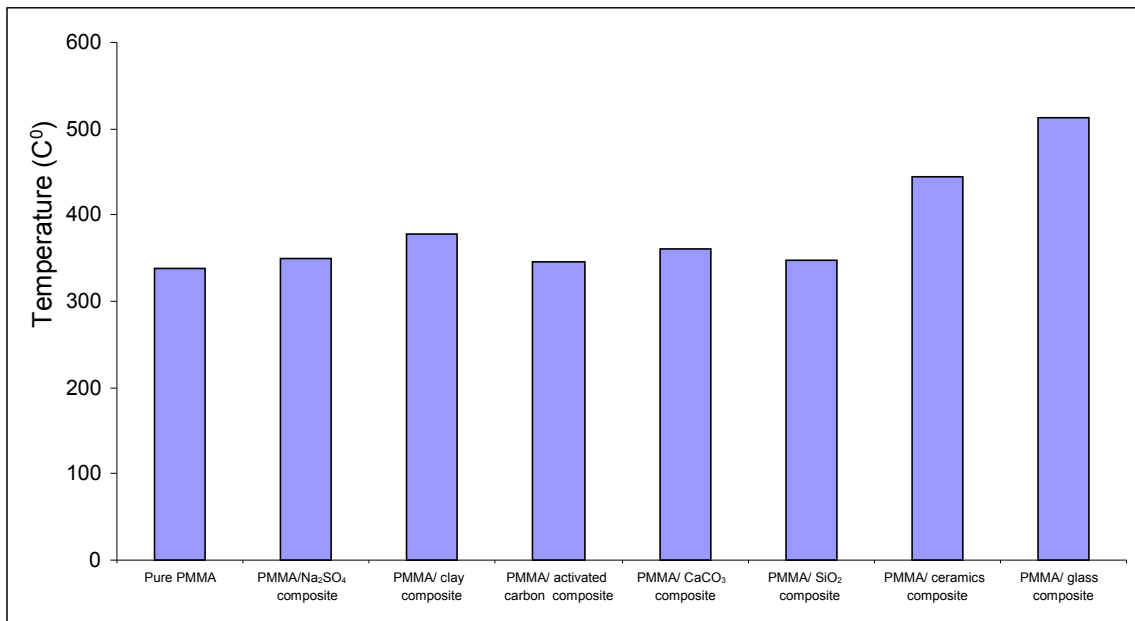


Fig.44. Comparison of thermal stability of various composites system

Mechanical properties

Tensile strength

The tensile strengths of PMMA/activated carbon is higher than other studied system as shown in figure 45, it is due to the incorporation of carbon particle into PMMA matrix having good reinforcing effect, which may originate from both the stiff carbon particle and carbon-induced increase in the degree of crystallinity of PMMA. The order of increasing tensile strength of various composite systems is:

PMMA < PMMA-Na₂SO₄ < PMMA-glass < PMMA- clay < PMMA-ceramics <

PMMA -CaCO₃ < PMMA-SiO₂ < PMMA-activated carbon

Elongation at break

The draw ability of PMMA/CaCO₃ and SiO₂ composites are more as compare to other systems as shown in figure 46. The addition of filler particles to the polymer matrix, the mobility of the polymer molecules increases. It can also be suggested that due to low adhesion and negligible intermixing of polymer and filler particles on the phase boundaries elongation at break of these system increase.

The order of increasing elongation at break of various composite systems is:

PMMA < PMMA-Na₂SO₄ < PMMA-activated carbon < PMMA- clay < PMMA-

ceramics < PMMA-glass < PMMA -CaCO₃ ≤ PMMA-SiO₂

S. No.	Systems	Force(N)
1	Pure PMMA	15
2	PMMA/Na ₂ SO ₄ composite	27
3	PMMA/ clay composite	37
4	PMMA/ activated carbon composite	50
5	PMMA/ CaCO ₃ composite	48
6	PMMA/ SiO ₂ composite	49
7	PMMA/ ceramics composite	40
8	PMMA/ glass composite	28

Table.3. Comparison of tensile strength of various composites system

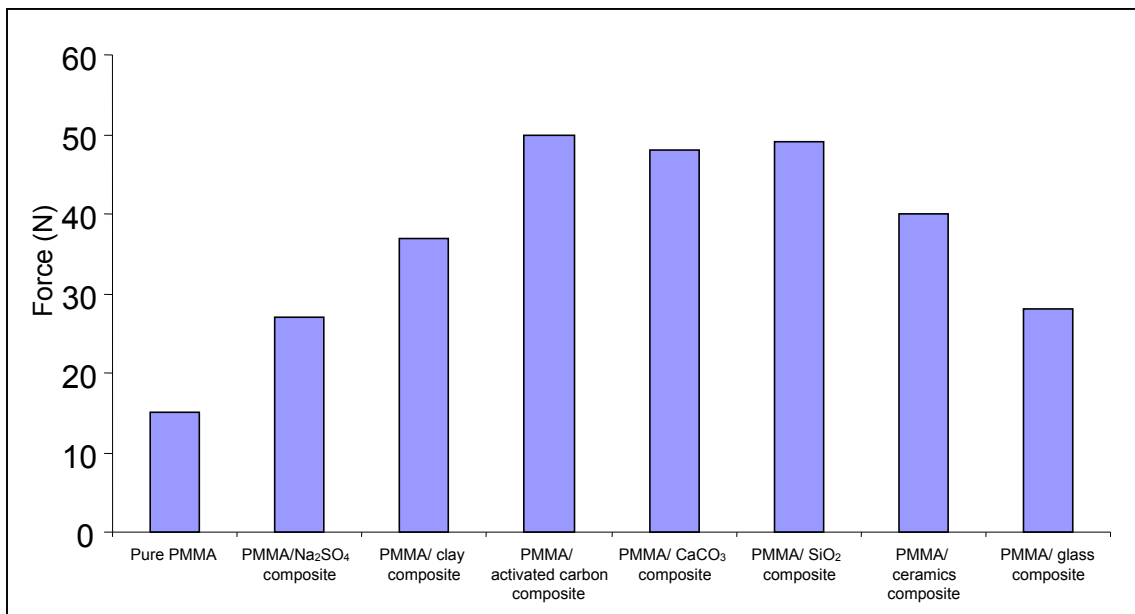


Fig.45. Comparison of tensile strength of various composites system

S. No.	Systems	Elongation (mm)
1	Pure PMMA	0.25
2	PMMA/Na ₂ SO ₄ composite	0.32
3	PMMA/ clay composite	0.43
4	PMMA/ activated carbon composite	0.42
5	PMMA/ CaCO ₃ composite	0.62
6	PMMA/ SiO ₂ composite	0.62
7	PMMA/ ceramics composite	0.52
8	PMMA/ glass composite	0.53

Table.4. Comparison of elongation at break of various composites system

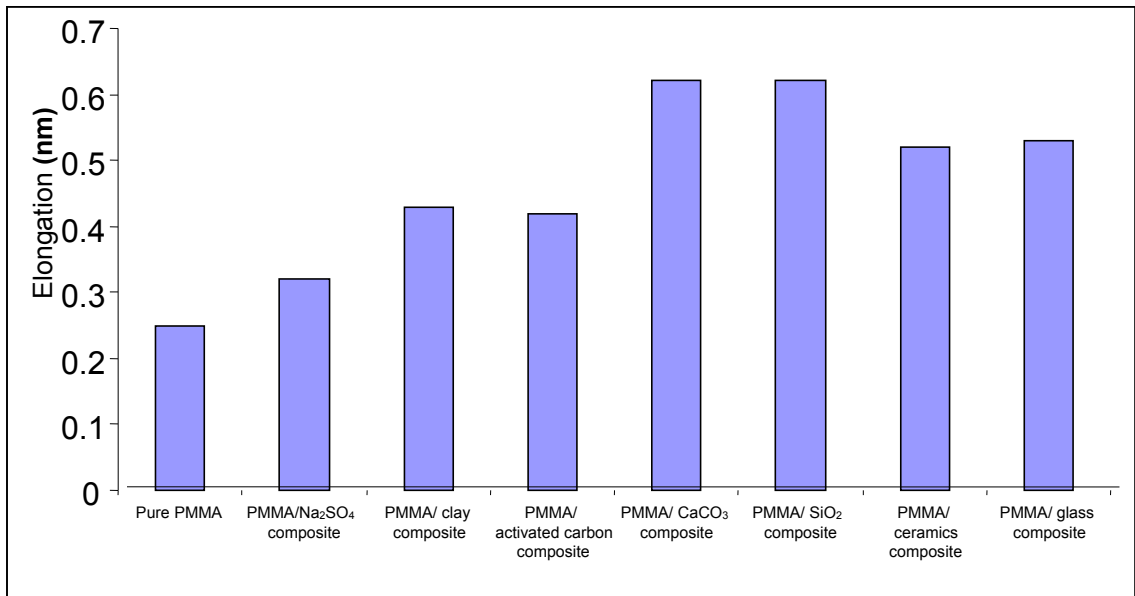


Fig.46. Comparison of elongation at break of various composites system

Conclusions

- The thesis has addressed the problems like thermal stability and tensile strength of polymer needed in practical industrial application. Emphasis is given on finding polymer composite which shows better properties as compare to its host polymer. The properties of these composites are characterized in view of finding the structure property correlation where ever possible. Thus the thesis presents the investigation of the thermal, mechanical and chemical properties and possible reason and mechanisms behind these. A comprehensive conclusion of the work is presented the following points.
- Solution casting technique was used for all types of polymer composite preparation
- Seven different types of polymer composites were prepared in which Na_2SO_4 , clay, CaCO_3 , activated carbon, SiO_2 , ceramics and glass were used as fillers and PMMA as the Matrix.
- SEM photograph shows that the filler particles are micrometer to nano meter size and almost equally dispersed in polymer matrix.
- EDX results confirmed the existence of the additives in studied systems in sufficient amount.
- The thermal properties of these composites were investigated by TG/DTA and DSC, the results shows that these composites have high thermal stability than plain PMMA.

- FTIR analysis shows the chemical nature of the studied polymer composite. The reduction in the absorption peaks in FTIR spectra were correlated to the presence of fillers particles
- Tensile testing were performed in order to investigate mechanical properties of these prepared polymer composites, The results shows that the tensile strength of the prepared composites are better as compare to the host polymer
- Thermal stability of PMMA/glass composite was found higher than all studied system. The order of increasing thermal stability of various composites was:

PMMA < PMMA-activated carbon < PMMA-SiO₂ < PMMA-Na₂SO₄ < PMMA -CaCO₃ < PMMA- clay < PMMA-ceramics < PMMA-glass

- The tensile strength of PMMA/activated carbon was found high with rest studied system. The order of increasing tensile strength of various composites was:

PMMA < PMMA-Na₂SO₄ < PMMA-glass < PMMA- clay < PMMA-ceramics < PMMA -CaCO₃ < PMMA-SiO₂ < PMMA-activated carbon

- Elongation at brick for PMMA/CaCO₃ and SiO₂ composites was found more as compare to other systems. The order of increasing elongation at break of various composites was:

PMMA < PMMA-Na₂SO₄ < PMMA-activated carbon < PMMA- clay < PMMA-ceramics < PMMA-glass < PMMA -CaCO₃ ≤ PMMA-SiO₂

REFERENCES

1. Reynaud E.; Jouen T.; Gaunthier C.; Vigier G.; Varlet J. *Polymer*, **2001**, 42, 8759.
2. Zhu J L.; Shen S N. *Pigments Technology, Second Ed, Chemical Industry Press, Beijing, 2002*
3. Hirth U. *Aluminum pigments for powder coating application, focus powder .Coat*, **2005**, 6, 2.
4. Liu H.; Ye H Q.; Zhang Y C. *Appl. surf. Sci.* **2007**, 253,7219.
5. Lewis G. J. *Biomed, Mater, Res.(Appl.Biomat.)* **1997**, 38,155.
6. Kenni S M.; Buggy M. *J.Mater. Sci., Mater.Med.*14,20.
7. Chujo Y.; Saegusa T.; **1992**. 100(1),11.*springer Berlin/Heidelberg*.
8. David I A.; Scherer G W. *Chem Mater.* **1995**, 7, 1957.
9. Tian D.; Dubios P.; Jérôme R. *J Polym Sci A, Polym Chem.* **1997**, 35,2295.
10. Melosh NA.; Lipic P.; Bates F S.; Wudl F.; Stucky G D.; Fredrickson G H.; Chmelka B F. *Macromolecules*, **1999**, 32, 4332.
11. Ogoshi T.; Itoh H.; Kim K M.; Chujo Y. *Macromolecules*, **2002**, 35,334.
12. Pyun J.; Matyjaszewski K.; Wu J.; Kim G M.; Chun S B.; Mather P T. *Polymer*, **2003**, 44,2739.
13. He W.; Pan C.; Lu T. *J. Appl. Polym. Sci.* **2001**, 80, 2455.
14. Huang Z.; Lin Z.; Cai Z.; Mai K. *Rubbers and Composite*, **2004**, 33, 343.
15. Lu Y.; McLellan J.; Xia Y. *Langmuir* **2004**, 20, 3464.
16. Chen M.; Zhou S.; You B.; Wu L. *Macromolecules*, **2005**, 38, 6411.
17. Li Z.; Zhu Y. *Appl. Surf. Sci* **2003**, 211, 315.

18. Avella M.; Errico M E.; Martelli S.; Martuscelli E. *Appl. Organomat. Chem.* **2001**, 15, 435.
19. Wu W.; He T.; Chen J.; Zhang X.; Chen Y. *Mater. Lett.* **2006**, 60, 2410.
20. Novak B M. *Adv. Mater.* **1993**, 5,422.
21. Mark J E. *Polym. Eng. Sci.* **1996**, 36, 2905.
22. Ahmad S.; Ahmad Sh.; Agnihorty S A. *J of power science*, **2005**, 140,151.
23. Zulfikar MA.; Mohammad A W.; Hilal N. *Desalination*, **2006**, 192,262.
24. Singh K.; Deshpande V.K. *Solid State ionics*, **1984**, 13,157.
25. Hofer H H.; Eysel W. *J Solid state chem.* **1981**, 36, 365.
26. Saito Y.; Kobayashi K.; Maruyama T. *Solid State Ionics*, **1984**, 14, 265.
27. Cavani F.; Trifiro F.; Vaccari A. *Catal.Today*, **1991**, 11, 173.
28. Srivastava S K.; Pramanik M.; Acharya H J. *Polym Sci.Part B: Polymer Phys.* **2006**, 44, 471
29. Lee W D.; Im S S.; Lim H M.; Kim K G. *Polymer*, **2006**, 47,1364
30. Yeh J M.; Liou S J.; Lai C Y.; Wu P C. *Chem. Mater.* **2001**,13,1133
31. Yeh J M.; Liou S J.; Lin C Y.;Cheng C Y.; Chang Y W. *Chem. Mater.***2002**, 14,154
32. Yeh J M.; Chen C L.; Chen Y C.; Ma C Y.; Lee K R.;Wei Y.;Li S X. *Polymer*, **2002**,43,2729
33. Reichert P.; Nitz H.; Klinke S.; Brandsch R.; Thomann R.; Mulhaupt R. *Macromol. Mter. Eng.* **2000**, 275, 8
34. Liu L M.; Qi Z M.; Zhu X G. *Appl. Polym. Sci.* **1999**,71,1133
35. Gilman J W. *Appl. Clay Sci.* **1999**,15,31
36. Zanetti M.; Kashiwagi T.; Falqui L.; Gamino G. *Chem. Mater*, **2002**, 14,881.

37. Alexandre M.; Dubois P. *Mater. Sci. Eng.* **2000**, 28, 1
38. Kim J W.; Kim S G.; Choi H J.; Jhon M S. *Macromol. Rapid Commun.* **1999**, 20, 450.
39. Cho M S.; Choi H J.; To K W. *Macromol. Rapid Commun.* **1998**, 19, 271.
40. N. Katsikis, F. Zahradnik, A. Helmschrott, H. Munstedt and A. Vital. *Polymer Degradation and Stability*, **2007**, 92, 1966.
41. Sellinger A T.; Martin A H.; Fitz-Gerald J M. *Thin Solid Films*, **2008**, 516, 6033.
42. Yuen S M.; Chi M C.; Chiang C L.; Chang J. A.; Huang S W.; Chen S.; Chuang C Y.; Yang C C.; Wei M H. *Composites, Part A*, **2007**, 38, 2527.
43. Shanmukaraj D.; Wang G X.; Murugan R.; Liu H K. *Journal of Physics and Chemistry of Solid*, **2008**, 69, 243.
44. Ye X.; Zhou Y.; Chen J.; Sun Y.; *Materials Chemistry and Physics*, **2007**, 106, 447.
45. Ding Y.; Gui Z.; Zhu J.; Hu Y.; Wang Z. *Materials Research Bulletin*, **2008**, 43, 3212.
46. Cai Y.; Huang F.; Eei Q.; Song L.; Hu Y.; Ye Y.; Xu Y.; Gao W. *Polymer Degradation and Stability*, **2008**, 93, 2180.
47. Fuan H.; Jintu F.; Sienting L. *Polymer testing*, **2008**, 27, 964.
48. Yanfeng L.; Bo Z.; Xiaobing P. *Composite Science and Technology*, **2008**, 68, 1954.
49. Raeve H D.; Cleemput J V.; Benoit. *Ann. Occup. Hyg.* **2001**, 45, 625.
50. Yang F, Nelson G I. *J. Appl Polymer Science*, **2004**, 91, 3844.
51. Goyal R. K.; Tiwari A N.; Mulik U P.; Negi Y S. *Composite Science and Technology*, **2007**, 67, 1802.

52. Qi D M.; Bao Y Z.; Huang Z M.; Weng Z X. *J. of applied Polymer Science*, **2006**, 99, 3425.
53. Aiping Z.; Zhehua S.; Aiyun C.; Feng Z.; Tianqing L. *Polymer Testing*, **2008**, 27, 540
54. Carrado K A. *J Appl. Clay Sci.* **2007**, 17, 1.
55. Reynaud E.; Jouen T.; Thair G C.; Vigier G.; Varlet J. *Polymer*, **2001**, 42, 8759.
56. Xu X.; Asher S A. *J. Am Chem, Soc.* **2004**, 126, 7940.
57. Xiaokam M.; Zhou B.; Deng Y.; Sheng Y.; Wang C.; Pan Y.; Wang Z. *J. and surface A: Physicochem. Eng. Aspects*, **2008**, 312, 190.
58. Meneghetti P.; Qutubuddin S, *Thermochimica Acta*, **2006**, 442 , 74.
59. Khan M S.; Shakoor A.; Nisar J. *Ionics*, **2010**, 16, 539.
60. Salahuddin N.; Shehata M *Polymer*, **2001**, 42, 8379.
61. Song X.; Wang X.; Wang H.; Zhong W.; Du Q. *Material Chemistry and Physics*, **2008**, 109, 143.
62. Shanmukakaraj D.; Wang G X.; Murugan R.; Liu H K. *Journal of Physics and Chemistry of solid*, **2008**, 69, 243.
63. Harrup M.; Wertsching A.; Jones M. *Energy and Environmental Sciences*, **2002**, 1, 1.
64. Ma Y.; Li N.; Yang C.; Yang X. *Colloids and Surfaces A: Physicochem. Eng. Aspects*, **2005**, 269 , 1.
65. Zhang N.; Xie J.; Varadan V K. *Smart Mater. Struct.* **2006**, 15,123
66. Tsai Y C.; Huang J D.; *Electrochemistry Communications*, **2006**, 8, 956.

67. Wu W T.; Shi L.; Zhu1 Q.; Wang Y.; Pang W.; Xu G.; Lu F. *Nanotechnology*, **2006**, 17, 1948.
68. Ishimori T.; Senna M. *Journal of Materials Science*, **1995**, 30, 488.
69. Zvonimir M.; Marko R.; Juraj S. *Polymer Degradation and stability*, **2009**, 94, 95.
70. Qian X. F.; Yin J.; Guo X. X.; Yang Y. F.; Zhu Z. K L. J. *Journal Of Materials Science Letters*, **2000**, 19, 2235.
71. Cora O. R.; Maria F H.; Lidia M. Q.; Marcelo D F. *European Polymer Journal*, **2008**, 44, 2749.
72. Kutsenko A. S.; Maloletov S. M.; Kuchmii S. Y.; Lyakhovetskii V. R.; Volkov V.I. *Theoretical and Experimental Chemistry*, **2002**, 38, 3.
73. Avella M.; Errico M. E.; Rimedio R. *Journal of Materials Science*, **2004**, 39, 6133.
74. Mirmohsenia A.; Wallace G G. *Polymer*, **2003**, 44, 3523.
75. Descamps M.; Hornez J C.; Leriche A. *Journal of European Ceramic Society*, **2009**, 29, 369.
76. Thomas P S.; Thomas S.; Bandyopadhyay S.; Wurm A.; Schick C. *Composite Science and Technology*, **2008**, 68, 3220.
77. Iwaseya M.; Watanabe M.; Yamaura K. *Journal of Materials Science*, **2005**, 40, 5695.
78. Xiaolin W.; Yihai W.; Pengli Z.; Rong S.; Shuhui Y.; Ruxu D. *Materials Letters*, **2011**, 65, 705.
79. Logakis E.; Pandis C.; Pissis P.; Pionteck J.; Pötschke P. *Composites Science and Technology*, 2011, 71(6), 854.

80. Jeffrey R. P.; Sun Hwa L.; Todd M. A.; Jinho A.; Meryl D. S.; Richard D. P.; Rodney S. R. *Carbon*, **2011**, 49(8), 2615.
81. Jun S K.; Shin J C.; Kwang S J.; Young C C.; Mun S J. *Carbon*, **2011**,49,2127.
82. Fa A Z.; Dong K L.; Thomas J. P. *Polymer*, **2009**, 50, 4768.
83. Charles M N.; Dan C.; Shengpei S.; Charles A. W. *Thermochimica Acta*, **2009**, 495, 63.
84. Yun H.; Xiaoyan M.; Xu W.; Xiao L. *Journal of Molecular Structure*, **2013**,1031, 30.
85. Yejin Lee.; Eunhee Kim.; Kijung Kim.; Byung H. Lee.; Soonja Choe. *Colloids and surfaces A: Physicochemical and Engineering Aspects*, **2012**, 396,195.
86. Akanksha Singh.; Sulabha K.; Kulkarni.; Chantal Khan-Malek. *Microelectronic Engineering*, **2011**, 8,(6), 939.
87. Mara Soares da Silva.; Raquel Viveiros. ; Mónica B.; Coelho. ; Ana Aguiar-Ricardo.; Teresa Casimiro. *Chemical Engineering Science*, **2012**, 68(1), 94.
88. Yuan-Li Huang.; Chen-Chi M.; Siu-Ming Yuen.; Chia-Yi Chuang.; Hsu-Chiang Kuan.; Chin-Lung Chiang.; Sheng-Yen Wu.; *Materials Chemistry and Physics*, **2011**,129(3)1214.
89. Eduard A.; Xiaoli Tan.; Zhiqun Lin. ; Nicola Bowler. ; Michael R. *Polymer*, **2011**,52(9),2016.
90. Yumi Kwon.; Hyungu Im.; Jooheon Kim.*Separation and Purification Technology*, **2011**, **78**(3)281.
91. Saladino M.L.; Motaung T.E.; Luyt A.S.; Spinella A.; Nasillo G.; Caponetti E. *Polymer Degradation and Stability* , **2012**, 97(3),452.

92. Qingqing Wang.; Xin Wang.; Xuejia Li.; Yibing Cai.; Qufu Wei.; *Applied Surface Science*, **2011**,258(1) 98.
93. Varela-Rizo H.; Montes de Oca G.; Rodriguez-Pastor I.; Monti M.; Terenzi A.; I. Martin-Gullon. *Composites Science and Technology*, **2012**, 72(2),218.
94. Telma Nogueira.; Rodrigo Botan.; Fernando Wypych. ; Liliane Lona.; *Part A: Applied Science and Manufacturing*, **2011**, 42(8) 1025.
95. Yang Zhao.; Jianhui Qiu.; Huixia Feng.; Min Zhang.; Lin Lei. ; Xueli Wu.; *Chemical Engineering Journal*, **2011**, 173(2)659.
96. Kristina B.; Vitalij S.; Hüseyin Ö.; Peter S.; Andreas S.; Luis A.S.A.; Karl S.; Stefan H.; Gerold A S.; *Science and Technology*, **2011**, 72 (1), 65.
97. Bhanvase B.A.; Pinjari D.V.; Gogate P.R.; Sonawane S.H.; Pandit A.B. *Chemical Engineering and Processing: Process Intensification*, **2011**, 50, (11–12)1160.
98. Mengjin Yang.; Zengfeng Di.; Jung-Kun Lee.; *Journal of Colloid and Interface Science*, **2012**, 368(1), 603.
99. Min-Kang Seo.; Soo-Jin Park.; *Materials Science and Engineering*,**2009**, 508(1–2) 28.
100. Hongpeng Liu.; Dan Yu.; Jian Wang.; Yongyuan Jiang.; Xiudong Sun.; *Optics & Laser Technology*, **2012**, 44(4) , 882.
101. Leg N T.; Koji O. *Macromolecules*, **2002**, 35, 7343.
102. Kuo S W.; Lin C l.; Chang F C. *Macromolecules*, **2002**, 35, 278.
103. Li D.; Brisson J. *Polymer*, **1998**, 39, 793.
104. Li D, Brisson J. *Polymer*, **1998**, 39, 801.
105. Rong M Z.; Zhang M Q.; Wang H B.; Zeng H M. *Appl. Surf. Sci.* **2000**, 200, 76.

106. Ash B J.; Siegel R W.; Schadler L S. *Macromolecule*, **2004**, 37, 1358.
107. Hirata, T.; Kashiwagi T.; Brown J E. *Macromolecule*, **1985**, 18, 1410.
108. Bai S.; Chen J K.; Huang Z P.; Yu Z Z. *J Matter. Sci. Lett.* **2000**, 19, 1587.
109. Choi B K.; Paric Y H. *Material science and engineering*, **2005**, 119, 177.
110. Yu Y H.; Lin C Yi.; Yeh J M, Lin W H. *Polymer*, **2003** ,44, 3553.
111. Ledoux R L.; White J L. *J Colloid interface Sci.* **1996**, 21 , 27.
112. Yanfeng Li.; Zhang B.; Xiaobing P. *J Science and Technology*, **2008**, 68, 1954.
113. Noh M W.; Lee D C. *Polym Bull.* **1999**, 42, 619.
114. He F A.; Zhang M L.; Yang F.; Chen L S.; Wu Q. *J Polym. Res.* **2006**, 13, 483.
115. Yang H.; Tian M.; Jia Q X.; shi J H.; Zhang L Q.; Lim S H.; Yu Z Z.; Y W Mai.
116. Zhang S H.; Zhang N H.; Huang C.; Ren K L.; Zhang Q M. *Adv. Mater*, **2005**, 17, 1897.
117. Alexandre M.; Dubois P. *Mater. Sci Eng.* **2000**, 28, 1
118. Wu W.; He T.; Chen J F.; Zhang X.; Chen Y. *J Materials Letters*, **2006**, 60, 2410.
119. Castrillo P D.; Olmos D.; Amador D R.; Gonzalez B J. *journal of Colloid and Interface science*, **2007**, 308, 318.
120. Ali M.; Zulfikar.; Wahab A. M.; Hilal N. *Desalination.* **2006**, 192 ,262.